UNIVERSITY OF SOUTHAMPTON

FACULTY OF MEDICINE

Clinical and Experimental Sciences Unit

Development of a global quantitative proteomics methodology and clinical applications in chronic diseases

by

Antigoni Manousopoulou, M.D.

Thesis for the degree of PhD by Published Works

July 2018

Abstract

Shotgun proteomics refers to the untargeted and unbiased analysis of the global proteome as this occurs in a biological system. The overarching aim of my research is to develop a proteomics methodology for the in-depth profiling of tissue and cell-lines and apply this novel methodology in mouse model and human samples in order to identify molecular mechanisms and novel therapeutic targets of obesity and obesity-related chronic diseases, including Alzheimer's disease and oesophageal adenocarcinoma.

The innovative quantitative proteomics methodology we developed for the global, untargeted proteomic profiling of cell lines and tissue has wide applications in different subject areas of biomedical research. Depending on the samples analysed and experimental design, this methodological approach can provide novel insight into physiological processes, the pathophysiology of disease, as well as identify novel therapeutic targets and disease markers.

Table of Contents

Author's declaration

I, Antigoni Manousopoulou declare that this thesis entitled "Development of a global quantitative proteomics methodology and clinical applications in chronic diseases" and the work presented in it are my own and has been generated by me as the result of my own original research.

I confirm that:

1. This work was done wholly or mainly while in candidature for a research degree at this University;
2. Where any part of this thesis has previously been submitted for a degree or any other qualification at this University or any other institution, this has been clearly stated;
3. Where I have consulted the published work of others, this is always clearly attributed;
4. Where I have quoted from the work of others, the source is always given. With the exception of such quotations, this thesis is entirely my own work;
5. I have acknowledged all main sources of help;
6. Where the thesis is based on work done by myself jointly with others, I have made clear exactly what was done by others and what I have contributed myself;
7. Parts of this work have been published as:
    - Manousopoulou A, Woo J, Woelk CH, Johnston HE, Singhania A, Hawkes C, Garbis SD, Carare RO. Are you also what your mother eats? Distinct proteomic portrait as a result of maternal high-fat diet in the cerebral cortex of the adult mouse. Int J Obes (Lond) 2015;39:1325-8.
    - Manousopoulou A, Koutmani Y, Karaliota S, Woelk CH, Manolakos ES, Karalis K, Garbis SD. Hypothalamus proteomics from mouse models with obesity and anorexia reveals therapeutic targets of appetite regulation. Nutr Diabetes 2016;6:e204.
    - Manousopoulou A, Saito S, Yamamoto Y, Al-Daghri NM, Ihara M, Carare RO, Garbis SD. Hemisphere Asymmetry of Response to

Pharmacologic Treatment in an Alzheimer's Disease Mouse Model. J Alzheimers Dis 2016;51:333-8.

- Manousopoulou A, Gatherer M, Smith C, Nicoll JAR, Woelk CH, Johnson M, Kalaria R, Attems J, Garbis SD, Carare RO. Systems proteomic analysis reveals that clusterin and tissue inhibitor of metalloproteinases 3 increase in leptomeningeal arteries affected by cerebral amyloid angiopathy. Neuropathol Appl Neurobiol 2017;43:492-504.
- Manousopoulou A, Hayden A, Mellone M, Garay-Baquero DJ, White CH, Noble F, Lopez M, Thomas GJ, Unerwood TJ, Garbis SD. Quantiative proteomic profiling of primary cancer-associated fibroblasts in oesophageal adenocarcinoma. Br J Cancer 2018;118:1200-7.

Signed:

Date: 02 July 2018

Acknowledgments

I would like to thank Dr. Spiro Garbis and Prof. Roxana Carare for believing in me and helping me become a better scientist and a better person. This work is dedicated to my parents, Anastasios and Eve, for nurturing my past with love and to my precious children, Sebastian Philip and Anastasia Eve, for giving meaning to my present and hope to my future.

List of Abbreviations

CID: Collision induced dissociation

ESI: Electrospray ionisation

GC-MS: Gas chromatography-mass spectrometry

HCD: Higher-energy collisional dissociation

HILIC: Hydrophilic interaction liquid chromatography

iTRAQ: isobaric tag for relative and absolute quantitation

LC-MS: Liquid chromatography-mass spectrometry

MALDI: Matrix assisted laser desorption ionization

MS: Mass spectrometry

MDLC: Multi-dimensional liquid chromatography

PI: isoelectric point

RP: Reversed phase

SAX: Strong anion exchange

SEC: Size exclusion chromatography

SCX: Strong cation exchange

SDS-PAGE: Sodium dodecyl sulphate polyacrylamide gel electrophoresis

SILAC: Stable isotope labelling using amino acids in cell culture

TMT: Tandem mass tag

TOF: Time of flight

Section 1: Introduction

1.1 Introduction on Proteomics

Shotgun proteomics refers to the untargeted and unbiased analysis of the global proteome as this occurs in a biological system. Shotgun proteomics has engaged the scientific community's interest as protein expression constitutes the functional end-point of a cell's genetic material and defines its phenotype. Therefore, studying the proteomic profile of a biological system within the context of a specific disease can provide insight into its pathophysiology. Furthermore, proteomics may also identify novel therapeutic targets and markers of diagnosis/prognosis and progression of disease. Additionally, examining proteome perturbations of a biological system after a particular intervention, for example pharmacologic treatment or nutritional/physical activity regiments can provide valuable information on the global, on- and off-target effects of the intervention to the system but also uncover novel markers of response to treatment.[1,2]

The global proteomic profiling of a biological system provides direct evidence of the expression levels of a particular protein, as opposed to the indirect evidence of a protein's levels derived from global transcriptomic (mRNA) analysis. It is well-established that mRNA expression levels do not always reflect the expression levels of the respective protein[3,4] and the correlation of the expression levels between mRNA and protein has been shown to be low.[5] Furthermore, transcription-level evidence cannot provide insight in the post-translational modifications of the respective protein.

Other analytical techniques used for the interrogation of proteins, for example ELISA measurements, immunohistochemistry and Western blotting, rely on the use of antibodies for the detection of *a priori* selected protein targets. In this reductionist science approach, the researcher forms a logical hypothesis based on current scientific knowledge and designs an experiment through the targeted analysis of specific proteins in order to confirm or disprove his working hypothesis. Even though the reductionist research approach has created a huge amount of knowledge and understanding in biomedical research, it also entails some important

limitations. Firstly, by focusing on a few proteins in a biological system the system-wide effects are largely ignored. This may thus create a “miss the forest for the trees” type of experimental bias, where too much focus is placed on a few selected protein targets whereas the holistic behaviour of the biological system is not examined. Another limitation of the reductionist approach is that since the formulation of the hypothesis is based on previous knowledge, the creation of entirely new and unanticipated knowledge is usually hampered. Yet another limitation is that functional aspects for any particular protein is also defined by its direct or indirect interaction(s) with other proteins constituting a biological system, a feature that is largely overlooked in reductionist experimental approaches.[6] For these reasons, a recently introduced research approach supports an untargeted profiling of the biological system as the initial step of biomedical research projects. In this type of systems biology scientific approach, one or several -omic experiments for the untargeted, global assessment of the biological system’s profile at the gene, transcript, non-coding RNA, proteome and metabolome level are performed. In a multi-omic approach, the biological system is profiled at multiple levels of biological organization and information ranging from DNA alterations to protein expression and metabolome differences can be combined for a more in-depth, multi-level interrogation of the system’s features.[7]

The main challenges of proteomics are still multifaceted. Proteins found in biological systems exhibit extensive diversity in their physico-chemical properties, including but not limited to their molecular weight, hydrophobic/hydrophilic character, dipole moment, innate protein-protein interactions, native concentration levels, topology, their induction from a post-translational modification event (i.e. phosphorylation status), their propensity to undergo oxidation and reduction, etc. These physicochemical properties have a direct effect on their ability to be detected with mass spectrometry.

Furthermore, the amino acid sequence of a given peptide that uniquely occurs in a protein directly affects its ability to ionize in the gas phase. For

example, if a peptide is composed of non-polar or non-acidic amino acids, it will be very difficult to analyse with the current mass spectrometry technologies.[8]

Another important limitation to current mass spectrometry techniques stems from the fact that only about 1% of the peptide ions introduced at the source get eventually detected. This fundamental drawback is due to a combination of factors including ion-optical design, limits to the degree of vacuum provided by the current pump systems, and detector ion-collection and electronics.[9] Also, the amino acid composition and charge state of a given target peptide may limit its fragmentation efficiency and thus hamper its amino-acid sequencing.[10] Other limitations include the current protein databases and their inability to deconvolute protein splice variants (induced by disease or viruses), and chemical covalent modifications or chemical adduct species.[11]

A shotgun proteomics approach in complex protein mixtures, such as those encountered in cell lines and tissue, includes: A. Protein extraction, B. Protein digestion, C. Label-based vs. label-free approach, D. Protein and peptide separation techniques, E. Liquid chromatography-mass spectrometry analysis, and F. Biostatistics and bioinformatics analysis.[12] Each of these steps will be discussed briefly in terms of the different approaches that exist along with their strengths and limitations. An overview of a typical proteomics pipeline is presented in **Appendix A**.

A. Protein extraction

Sample preparation is an important step in the proteomic analysis pipeline, as the effective extraction of proteins will dictate the depth of proteomic coverage. An optimal sample preparation protocol should reproducibly isolate the full complexity of a biological system's proteome without causing artificial, post-extraction alterations to the proteins and whilst removing non-specific contaminants (e.g. auto-digest peptides, fatty acids, phthalates, plastic polymers, DNA, RNA etc.) and artefacts (e.g. salt clusters, adduct species etc.). Isolating the full proteomic complement from a

biological system is an intrinsically difficult task because proteins vary widely in terms of molecular weight, charge state, conformational states, hydrophobic and hydrophilic character, post-translational modifications, sub-cellular distribution and complex formation with other macromolecules and enzymatic co-factors.[10] Samples collected for proteomic analysis should be stored in -80^{o}C freezers or in liquid nitrogen storage facilities (-196^{o}C) and transported/shipped between laboratories in dry ice (-78.5^{o}C) since enzymes maintain a small level of enzymatic activity even at -20^{o}C, thus causing protein degradation.

Specifically, for tissue analysis, a few important aspects of sample processing prior to long-term storage should be taken into consideration. Tissue specimens (derived from humans or animal models) should be thoroughly cleaned from blood contamination, as this can adversely affect the downstream analysis and final result. Blood contamination can affect the proteomic result for two main reasons: Firstly, because blood contains high-abundant blood proteins, such as albumin and a wide-array of low-abundant proteins derived from different cell types, tissues and organs. Contamination of tissue with high abundant blood proteins can mask the analysis of biologically relevant, low-abundant tissue proteins whereas contamination with low-abundant blood proteins can introduce noise in the expression levels of a protein at the tissue-level. Secondly, blood contains proteases that can cause decomposition of tissue proteins.

The total handling time between performing human tissue biopsy or animal model sacrifice and storing the respective tissue for proteomic analysis should ideally be kept consistent across samples and lasting for less than 15 minutes.[13] Consistency in tissue isolation is more feasible with mouse models but rather difficult in the isolation of human samples during surgery or post-mortem due to practical reasons. In this case, this information should be provided in the respective publication and inconsistency in sample collection and storage prior to proteomic analysis should be mentioned as a study limitation.

Biological specimens must be subjected to homogenisation as the initial pre-processing step. For cell lines, techniques used for sample homogenisation include benchtop homogenizing systems and probe-type sonication. Tissue samples can be disrupted by freezing them using liquid nitrogen and grinding them with a mortar and pestle or using a benchtop homogenizing system combined with specific sample tubes filled with ceramic beads. Tissue and cell line specimens are then dissolved in a solution that facilitates the solubilisation of proteins, for example triethylammonium bicarbonate (TEAB) buffer. This can be combined with an ionic surfactant (detergent) such as sodium dodecyl sulfate (SDS) or sodium deoxycholate (SDC) at concentrations less than 0.1% and 1% respectively, in order not to hinder enzymatic activity of trypsin in the respective downstream part of the protocol.[14] A cocktail of protease inhibitors can also be used at this step. However, caution must be given so as to minimise residual exposure for these proteases during the protein enzymolysis step.

During the tissue homogenisation steps, proteins can be briefly exposed to higher temperatures (e.g. during FastPrep and tip sonication). This increase in temperature can in turn activate proteases in the sample that may cause protein degradation. Special care should be taken to maintain the sample always on ice during all these steps. One further change that can occur to proteins during sample homogenisation is oxidation. Protein oxidation is usually an artefact during sample preparation, and this should be accounted for in the algorithm that matches spectra to peptides. Assessing the oxidative status of proteins in a biological system requires the use of specific chemical derivatization reagents (e.g. Daz-2, iodoacetamide, etc.) in order to stabilise protein oxidation as this occurs innately and allow its discrimination from that caused artificially during the sample handling process.

Other processes that can occur during the sample homogenization process may be the enzymatic cleavage of target proteins from the *in situ* presence of various proteases (i.e. serine proteases, zinc metalloproteases, collagenases, etc.). However, protease activity is minimised by keeping the

protein eluates on ice and by the inclusion of chaotropes and detergents, which denature the proteases thus hindering their enzymatic activity.

Samples are then centrifuged to eliminate contaminants and the supernatant is further analysed. Alternatively, after sample homogenisation, proteins can be precipitated using for example trichloroacetic acid (TCA) or chloroform-methanol (C-M). However, protein precipitation protocols have been reported to show non-reproducible results and a bias toward the precipitation of larger proteins while the smaller and hydrophilic proteins are poorly captured.[15]

B. Protein digestion

The two main techniques used for protein digestion are enzymatic and non-enzymatic (or chemical) digestion. The most commonly applied method for protein digestion involves proteases. There are many different proteases available, and each one has its own unique characteristics in terms of efficiency, specificity and optimal digestion conditions. Trypsin, a serine protease, is the most widely used enzyme in shotgun proteomics pipelines. Trypsin is relatively cheap and has high specificity, as it predominantly cleaves proteins at the carboxyl (or C-terminal) side of the amino acids lysine (Lys) and arginine (Arg), except when either of these two amino acids is followed by proline (Pro). However, large-scale proteomics studies suggest that trypsin cleaves even at the presence of proline.[16] Arg and Lys are abundant amino acid residues in the human proteome, and most often evenly distributed in a protein.[17] This results in tryptic peptides that have a length of approximately 14 amino acids on average with a minimum of two positive charges, an ideal situation for mass spectrometry analysis.[18]

Despite the numerous advantages of trypsin, the use of alternative proteases may be necessary in some cases, for example due to incompatible pH conditions or when Arg and Lys residues are not present or are present at high numbers in a protein. Alternative proteases include aspartic proteases (such as pepsin) that are active in low/acidic pH conditions and endoproteinases (including Arg-C, Glu-C, Lys-C, Asp-N) that provide high

cleavage specificity and efficiency and are thus used as an alternative to trypsin or sequentially/simultaneously combined with trypsin. The combined use of proteases can improve cleavage efficiency.[19,20]

Chemical digestion, an alternative method of protein digestion, can be achieved by treating the protein mixture with dilute solutions of acids (such as formic acid, acetic acid, hydrochloric acid) or with other types of chemicals (including cyanogen bromide, hydroxylamine and 2-nitro-5-thiocyanobenzoate). Chemical digestion usually produces larger peptides compared to enzymatic proteolysis that are suitable for middle-down proteomic approaches.[21,22] Middle-down proteomics, the analysis of larger peptides up to 15kDa as opposed to the analysis of smaller peptides up to 7kDa in a typical bottom-up proteomics experiment, require the use of ultra-high resolution platforms and longer duty cycles for the accurate assessment of their molecular weights. However, middle-down proteomics exhibits greater versatility in the analysis of peptides from a wide array of large proteins (>50 kDa) not amenable to top-down proteomics workflows, the mass spectrometry analysis of intact proteins. Middle down proteomics has been successfully used for antibody characterisation studies.[23]

C. Label-based vs. label-free proteomics

An important aspect of a shotgun proteomic experiment is being able to assess the relative expression levels of the identified proteins between sample groups (e.g. disease vs. control) when using data dependent acquisition approaches. In order to achieve this goal, there are two different approaches: the label-free and the label-based approach.

The chemical, label-based proteomics approach refers to the use of isobaric stable isotope reagents at the proteotypic peptide or protein level that impart improved ionization and fragmentation behaviour and multiplexed workflows. Commercially available kits that permit chemical label-based proteomic experimental designs include the Isotope Tags for Relative and Absolute Quantitation (iTRAQ) (Sciex, Inc., Toronto, Ontario, CA) and Tandem Mass Tags (TMT) (Thermo Pierce, Inc., Rockford, IL, USA). The kit suppliers also offer software tools that assist with data processing for the

relative quantitation of the labelled peptides or proteins. Isobaric tags, as the name implies, have the same molecular weight prior to the last fragmentation step of mass spectrometry analysis. Thus, labelled peptides of all samples included in the multiplex experiment can be mixed together post-labelling and analysed under the exact same conditions. This significantly reduces the instrument time required for analysis but also minimises bias stemming from analysing samples under different analytical conditions.

The main limitation of label-based proteomics, also referred to as isobaric tag-MS^2 pipelines, is peptide co-isolation or co-elution. Peptide co-isolation or co-elution refers to the parallel isolation of more than one precursor peptides and subsequent co-fragmentation due to their similarities in molecular weights and chromatographic retention time index stemming from homologous physico-chemical properties.[24] This process results in distorting the accuracy of relative peptide expression and compromises its precise identification. Efforts have been made to use the multi-notch MS^3 approach, whereby proteotypic product ions are further subjected to high-energy fragmentation and in the process eliminate peptide interference effects. Even though such an approach does indeed maximise accuracy of peptide relative quantitation, it requires the use of more specialized quadrupole-iontrap-Orbitrap (i.e. tribrid) platforms. Furthermore, the increased duty cycle time required to accumulate sufficient ion yield in the multi-notch MS^3 technique, significantly compromises sensitivity in the relative quantitation of lesser abundant proteins. Consequently, the resulting MS^3 derived proteomes lack both depth and breadth of coverage needed to gain important biological insight.[25] The effective use of the isobaric tag-MS^2 pipeline necessitates the use of good chromatographic technique so as to minimize peptide co-isolation effects in combination with using high-resolution tandem mass spectrometry systems with suitably high scan speeds to ensure sufficient chromatographic sampling.[26]

As a recent development, the use of the complement reporter ion approach (TMTc) to the isobaric tag-MS^2 pipeline substantially reduces the interference limitation to a higher degree achievable by the multi-notch MS^3

approach without compromising proteome coverage. The TMTc approach is based on the phenomenon whereby the TMT-isobaric labeled precursor peptides fragment to produce the MS^2 product ions that include the low *m/z* "reporter ions" in addition to residual non-fragmented precursor peptides that remain covalently bound to the mass balancing group of the TMT reagent, and referred to as complement TMT ions or TMTc. A key feature of these TMTc ions is that they encode for different experimental conditions analogously to the low *m/z* reporter ions do but with the added benefit that the *m/z* value of the TMTc ion varies in accordance to the *m/z* value of the intact peptide species. Consequently, accurate quantification can be inferred and corrected regardless if other peptides are co-isolated into the same product ion MS^2 spectrum. An additional advantage to the TMTc approach is that it could be used retroactively to existing datasets to verify and, if necessary correct, any inaccuracies of peptide relative quantitation.[27,28] The continuous improvements made to mass spectrometry hardware design in terms of higher resolution with faster scan speeds and chromatographic column design in combination with the developments of expanded multiplexing capabilities of isobaric reagents stand to maintain label-based approaches as the preferred quantitative proteomics approach.

The label-free proteomics approach refers to the qualitative analysis of each sample separately using LC-MS and assessment of the expression levels of a particular peptide between samples based on how many times the peptide was observed during mass spectrometry analysis (spectral counting). The main disadvantage of a label-free approach is that spectral counting is highly affected by sample handling and analytical conditions, which can in turn introduce analytical bias. To overcome this limitation, the same sample should be analysed multiple times (duplicate or triplicate analysis) to assess reproducibility of the findings. Therefore, the instrument time required for such type of analysis is significantly higher compared to a multiplexed, isobaric tag-based experiment that allows for the analysis of up to 11 samples simultaneously. By contrast to label-based methods, another fundamental limitation of label-free proteomics is its inability to quantify

peptides that exhibit a small, albeit significant, differential expression between biological or clinical replicates thus concealing important biochemical and molecular biology networks and pathways.[26,29]

D. Protein and peptide separation techniques

Protein separation can be performed using either gel-based techniques (i.e. SDS-PAGE) and/or liquid chromatography approaches (e.g. size exclusion chromatography). Gel electrophoresis for the initial separation of proteins followed by their in-gel digestion to generate their surrogate peptides prior to LC-MS analysis has some important limitations. Firstly, the separation of proteins using gel electrophoresis is not reproducible, especially when larger total protein amounts are applied (higher than 1 mg). This lack or reproducibility particularly holds true for the lower abundant proteins masked by the presence of the higher abundant proteins. Additionally, gel-based separation techniques lack the ability to efficiently capture proteins with molecular weights less than 10 kDa or higher than 200 kDa, or biologically important hydrophobic proteins typical associated with cell membranes. Also, highly acidic (pKa < 4) or highly alkaline (pKa > 10) proteins are poorly recovered with gel-based separation techniques. Another important limitation to gel-based techniques is their poor sensitivity of protein detection as the only mass spectrometry compatible staining reagent is Colloidal Coomasie Blue. Consequent to these important limitations, a broad spectrum of proteins that naturally occur in biological or clinical specimens are never observed with gel-based methods resulting in poor proteome coverage and a low degree of biological or biochemical inference that is essential to systems biology research and biomarker discovery.[10,30,31]

By contrast, the correct use of multi-dimensional liquid chromatography (MDLC) exploits the diverse physico-chemical properties found in proteins and peptides to maximise separation efficiency and thus making them more amenable to mass spectrometry. From this perspective, the science of liquid chromatography when hyphenated with mass spectrometry using the electrospray ionization source played a pivotal role

in the re-emergence of proteomics in biomedical research. A limitation of MDLC in shotgun proteomics is that it can generate many peptide fractions thus reducing analysis throughput, which is however offset by the extensive proteome coverage.

Liquid chromatography is an analytical chemistry technique that involves a pump in order to pass a sample mixture along with a pressurized liquid through a column filled with a stationary phase. Liquid chromatography allows the separation of a complex mixture of macromolecules, such as peptides, as these migrate at different speeds through the chromatographic column due to their differential degree of physico-chemical interaction with its stationary phase chemistry and its geometry. In other words, molecules are separated based on their differences in physicochemical properties that dictate the type of interaction with the stationary phase chemistry and geometry chosen for a particular analysis application.

MDLC constitutes an effective way to maximise separation efficiency and is well suited for reducing the intrinsic proteomic complexity of biological or clinical specimens. Such an approach makes sequential use of two or more columns with complimentary chromatographic behaviour that augment separation efficiency, a term referred to as chemical orthogonality.[32] A component to the MDLC approach includes the initial use of offline LC fractionation as the first dimension applied to the pooled sample of labelled peptides derived from all biological or clinical replicates. The offline chromatography can be performed in an HPLC system, using columns lengths ranging from 100mm to 300mm (as single or sequentially connected units), inner diameters (ID) ranging from 1mm to 7mm, particle sizes ranging from 3 – 5 μm and pore sizes ranging from 100 – 300 Å. Depending on these dimensions, the mobile phase flow rates span from 100 μL/min – 5 mL/min. From this initial offline peptide chromatographic step (1st dimension), a number of fractions is collected (usually 40-70) followed by their individual online chromatography (2nd dimension) with nano-capillary columns (0.05 – 0.075 mm ID), nanospray ionization and mass spectrometry (MS).

The use of the offline liquid chromatographic approach using larger ID columns as the 1st dimension, as opposed to smaller diameter columns commonly used in online two-dimensional liquid chromatographic approaches, permits the loading of higher protein amounts thanks to the higher chromatographic capacities available to these larger ID columns. This results in the collection of denser peptide fractions and therefore allow for the more sensitive online LC-MS analysis. Also, the manual collection of peptide fractions substantially reduces exposure of the online LC-MS system to salts, underivatized isobaric reagents, and other impurities. The collective attributes of the offline larger ID – online nano-capillary ID analysis strategy results to an increased proteome coverage as demonstrated in this thesis.

The most common types of liquid chromatography used for peptide separation are ion exchange (IEX), further categorized to strong anion (SAX) and strong cation exchange (SCX), reversed-phase (RP) and hydrophilic interaction liquid chromatography (HILIC). Ion exchange chromatography separates peptides based on their differences in charge state using an ion exchange mechanism. In the anion exchange chromatography the stationary phase is positively charged whereas in the cation exchange negatively charged. The use of increasing amounts of a counter-ion in the mobile phase such as ammonium hydroxide for anion exchange chromatography or formic acid for cation exchange chromatography allows the subsequent displacement and elution of the negatively or positively charged peptides, respectively. The peptide fractions from this type of chromatographic process contain high amounts of salts that may compromise the subsequent electrospray ionization process of the LC-MS analysis. Furthermore, a lower degree of chromatographic orthagonality is observed in IEX – RP combinations relative to HILIC – RP or RP-RP combinations. Such limitations associated with IEX have made its use less prevalent over the years.

In the RP chromatography, peptides are separated based on their hydrophobic/hydrophilic character. The stationary phase is comprised of carbon-chains (C4, C8 or C18 reflecting the number of carbons on the aliphatic chain) bonded to a silica particle substrate. As the percentage of

the organic mobile phase mixed with the aqueous mobile phase increases, peptides with a more hydrophobic character pass from the stationary phase to the mobile phase and are eluted. Therefore, in a RP type of chromatography, hydrophilic peptides are eluted first, followed by amphoteric peptides and finally hydrophobic peptides.

Similarly to RP, HILIC chromatography also separates peptides based on their hydrophobic/hydrophilic character although with the exact opposite trend, i.e. hydrophobic peptides are eluted first whereas hydrophilic peptides are eluted last. A potential limitation in the use of HILIC is the precipitation of larger and more hydrophilic peptides during the initial use of a high organic solvent content. This may be partially offset with fluorinated organic solvent substitutes. However, these solvents exhibit more health hazards to the chromatographic practitioner and are therefore avoided. Such a limitation is not observed with RP phase chromatographic applications and therefore constitutes a major advantage over the use of HILIC. Despite these limitations, the use of HILIC in combination with RP separation approaches is better suited for the analysis of specific post-tranlationally modified peptides such as phosphopeptides,[33] which was beyond the scope of the present thesis.

Gilar et al[34] examined different combinations of offline-online chromatography types providing maximum orthogonality in terms of peptide separation. SCX-RP, HILIC-RP and RP-RP combinations provided suitable orthogonality. The RP-RP (using significantly different pH in both separation dimensions, i.e. alkaline offline RP and acidic online RP chromatography) combination had the highest practical peak capacity of all two-dimensional systems examined. The on-going and increasing rate of technological advancements made to liquid chromatography makes it feasible to combine multiple chromatographic stationary phase chemistries (i.e. multiphasic columns); miniaturized geometries (nano-scale dimensions) and open tubular monolithic architectures that makes it possible to achieve a higher degree of separation efficiency at shorter chromatographic timelines and improved mass density.[35-37]

E. Mass spectrometry analysis

The constant technological improvements made to liquid chromatography make it increasingly possible to exploit and expand the analysis utility of the available ionization sources hyphenated with mass spectrometry.[38] A mass spectrometry system has three main components: an ion source, a mass analyser and a detector. Depending on the phase of the sample (solid, liquid) the ionization techniques vary. Two basic analytical approaches used in proteomics are: (I) the matrix-assisted laser desorption ionization time-of-flight mass spectrometry (MALDI-TOF-MS) and (II) liquid chromatography hyphenated with electrospray ionisation (ESI) and tandem mass spectrometry (LC-MS). Gas chromatography hyphenated with mass spectrometry (GC-MS) is primarily used for the analysis of thermally stable and volatile small molecules, most often for forensic substance identification, but not for peptide analysis.

MALDI and ESI are the only two ionization techniques able to generate ions without causing chemical decomposition of the analyte. MALDI is based on using a crystallisable organic substance (i.e. alpha cyano-cinnapinic acid) that can absorb at a specific wavelength in the UV spectrum (i.e. 190nm), referred as the “matrix”, which is mixed with a liquid solution containing protonated peptides derived from the proteolysis of target proteins in acidified water and acetonitrile. The matrix and peptide solution are deposited on a stainless-steel plate, referred to as the MALDI target, and allowed to air dry to form a homogeneous crystal spot. The spot is then irradiated with a UV laser (i.e. Gas Phase Nitrogen or Solid State Nyodium-Yag) under vacuum during which the matrix will absorb and transfer the UV energy to the embedded peptides. Exposure of the peptides to the UV energy increases their kinetic energy to a sufficient level for them to undergo desorption into the gaseous phase for subsequent mass spectrometry.[39,40]

Electrospray ionisation (ESI) refers to the application of a high voltage potential (i.e. 2000 – 5000 eV) to a liquid medium containing ionized macromolecules such as peptides in a mixture of acidified water and an organic solvent such as methanol or water and other additives. During this

process, the liquid undergoes droplet formation whose size decreases due to the vaporization of the solvent medium while at the same time the proximity of the contained protonated peptides increases. Eventually the ever-proximal protonated peptides will undergo electrostatic repulsion and expulsion into the gas phase and eventually mass spectrometry analysis.[41,42]

Both MALDI and ESI sources are classified as “soft” ion sources as the chemical integrity of the target analyte (i.e., peptides) remains predominately intact thus allowing their mass spectrometry analysis. However, the ESI ion source exhibits a substantially higher degree of versatility in the mass spectrometry analysis of a broad spectrum of peptides, and proteins along with their possible post-translational modifications.[43] Such a feature was not available with the other ionization techniques used in GC-MS methods, which cause extensive chemical decomposition to thermally labile bio-molecular compounds, such as peptides. In essence, the MALDI and ESI sources made it possible to apply mass spectrometry to molecular biology and biochemistry research. Such was the importance of the MALDI and ESI ion sources that Koichi Tanaka and John Fenn, inventors of MALDI and ESI techniques respectively, were awarded with the 2002 Nobel Prize in Chemistry.

The effective analysis of peptides and proteins requires the use of higher resolution mass spectrometry systems able to distinguish their mass-to-charge with high mass accuracy. This requirement in typically achieved by two basic mass spectrometry geometries, namely, the full-spectral acquisition systems that make use of multi-channel detectors available to Time-of-flight (TOF) platforms and their hybrid variants with single quadrupoles (QqTOF) or the mass scanning acquisition systems used in the ion trap-based geometries (3D Quadrupole ion traps, linear ion traps and Orbitrap based systems).

The main advantage of the Orbitrap geometry over the other geometries is its unsurpassed mass resolution, which offers, under optimum calibration conditions, the highest degree of mass accuracy. By comparison, the TOF based geometries offer better sensitivity with a broader linear

dynamic range and are therefore more ideally suited for targeted mass spectrometry applications. As such, the Orbitrap and TOF-based geometries exhibit a high degree of performance complementarity in terms of their use in non-targeted discovery and targeted absolute quantitative analysis workflows respectively.

Mass spectrometry is able to decipher the exact amino acid sequence of peptides (when using bottom-up proteomics methods) and proteins (when using top-down proteomics methods). In order to achieve this, the ion has to be first fragmented and then the mass/charge (m/z) ratio of the intact ion (precursor ion) and its fragment ions (product ions) are measured. Collision induced dissociation (CID), or collisionally activated dissociation (CAD), is a mass spectrometry technique that causes fragmentation of ions in the gaseous phase. Peptides undergo preferential fragmentation at the amide bond, constituting their least strong covalent bond. This results in the generation of the complementary b_n and y_n product ions whose masses are dependent on the type of amino acids comprising the peptide of interest from the N-terminus to the C-terminal end.

This fragmentation pattern allows the *de novo* interpretation of the amino acid sequence starting from the b_2 diagnostic product and then proceeding sequentially to the higher mass b-series ions. The mass differences between the b_n-series ions corresponds to the mass of the unknown amino acid that can qualitatively be determined from the high accuracy assessment of the mass difference.[44] The higher mass y-ion product species can be repeated in reverse (starting from the C-terminal end to the N-terminus) allowing the cross examination of the b-ion interpretation or even substituting the missing b-ions product ions or vice versa for those peptides observed with a poor signal to noise ratio. In general, established mass spectral interpretation rules are used to identify the b_n- and y_n- ion series and therefore the exact peptide sequence.[44] An example of an annotated peptide spectrum is presented in **Appendix B**.

Efforts are being made to automate this *de novo* sequencing process with the use of advanced algorithms that apply mass spectral interpretation

sub-routines (e.g. the Peaks software program). A complementary high-throughput approach use probability based algorithms, such as Mascot and Sequest, that compare the similarity of a given experimentally generated peptide product ion spectrum against those found in *in silico* digested protein databases.[45]

F. Biostatistics and bioinformatics analysis

Raw data files, containing the spectra of all analysed peptides, should be compared with a protein database of the studied species, *in silico* "digested" with the same method as the one used in the respective experiment (e.g. tryptic peptides). Spectra are then matched to peptides, and peptides are mapped to proteins. The most commonly used resource for proteome reference databases is the UniProt Knowledge Base (UniprotKB). The UniProtKB has two sections: the UniProtKB/Swiss-Prot, a manually annotated and reviewed database, and the UniProtKB/TrEMBL, an automatically annotated and not reviewed database of protein sequences. There are different algorithms, embedded in the respective software tools, that can be used in order to match the acquired spectra to peptides and these to proteins, such as Sequest, PEAKS, X!Tandem, Andromeda, Mascot Server, Comet etc. Peptides are characterized as unique or proteotypic if these occur uniquely in one specific protein and non-unique when these are common between several proteins. If an isobaric tag was used for peptide labelling, this should also be included in the search algorithm to examine the relative expression levels of each peptide between samples. Usually, reporter ion ratios of unique proteins only are used for the inference of the relative abundance levels between samples of the respective protein.

Once the spectra have been matched to peptides and these in turn to proteins, results should be analysed in order to identify differentially expressed proteins between studied groups (e.g. disease vs. control). In a label-based proteomic experiment, the relative expression levels of a protein between samples is calculated from the mean value of all reporter ion ratios of unique peptides (i.e. peptides that uniquely map to this specific protein as

opposed to non-unique peptides that map to multiple proteins). Reporter ion intensities from non-unique peptides are commonly excluded from the quantitation of a protein, since these map to more than one protein and can therefore introduce noise in the relative expression levels of a specific protein.

Protein reporter ion ratios are median normalised across all samples and then log_2transformed, in order to achieve a normal distribution of data points. Different statistical tests can be applied to identify differentially expressed proteins between sample groups, for example standard deviation cut-offs, permutation testing, linear modelling analysis, one-sample T-Test. Once the differentially expressed proteins between sample groups have been identified, *in silico* bioinformatics analysis can be performed in order to identify significantly over-represented biological processes, gene ontology terms, pathways and protein interaction networks. Some commonly used software tools used for bioinformatics analysis are DAVID (https://david.ncifcrf.gov), BiNGO (https://www.psb.ugent.be), STRING (https://string-db.org), Ingenuity Pathway Analysis (IPA) (Qiagen Bioinformatics, Hilden, Germany) and MetaCore (Clarivate Analytics, Philadelphia, PA, USA). A table briefly describing the type of bioinformatics analysis that can be performed with each one of these tools, as well as their strengths and limitations is presented in **Appendix C**.

The overarching aim of my research was to develop a proteomics methodology for the in-depth profiling of tissue and cell-line specimens and apply this novel methodology in mouse model and human samples affected by three different types of chronic disease, namely obesity, Alzheimer's disease and cancer.

The specific methodological objectives of my research were to:

- Develop a refined protocol for tissue/cell-line homogenisation and protein extraction
- Identify the most effective combination of offline and online liquid chromatographic chemistries in order to maximise proteomic coverage
- Create a mass spectrometry method for data acquisition that increases protein identifications in cell-line and tissue samples

1.2 Obesity: a modern pandemic

Obesity is a modern pandemic and a major public health burden in both developed and developing countries.[46] Obesity, defined as excessive body fat accumulation, is an endocrine disorder that increases the risk of other co-morbidities and reduces life expectancy.[47,48] The most commonly used index to define obesity is the body mass index (BMI).[49] BMI is an anthropometric measurement that is calculated by dividing a person's weight by the squared meters of their height (normal range: 18-25 kg/m^2). Overweight is defined by a BMI between 25 and 30 kg/m^2, obesity by a BMI between 30 and 35 kg/m^2, and morbid obesity by a BMI over 35 kg/m^2. According to the WHO, in 2008 35% of adults over 20 years were overweight and another 12% were obese worldwide.[50] The global prevalence of obesity has increased since 1980.[51] A study by Finkelstein et al[52] estimated that obesity prevalence will increase by 33% whereas morbid obesity prevalence by 130% within the next two decades. The United Kingdom has the highest rates of obesity in western Europe, with 28% of the population classified as obese in 2014, whereas for the same year, over two-thirds of males and 60% of females were overweight or obese.[53] Medical care costs attributed to obesity-related diseases in 2008 were estimated to be $147 billion in the United States, whereas in the UK obesity is costing the healthcare system approximately £5.1 billion a year.[54]

Obesity is a multifactorial disease, most commonly attributed to the increased consumption of highly processed, energy-dense and nutrient-void food in combination with a sedentary lifestyle.[55,56] Environmental pollutants, including various classes of chemicals in air pollution, water pollution, food, household cleaning agents, personal hygiene products, cosmetics etc., may also play a role in this modern pandemic [57,58] whereas genetic factors are only considered to have a very small contribution to the incidence of obesity.[59]

Addressing the obesity epidemic is a major public health challenge. Targeting individual perceptions and lifestyle choices is one venue of reducing the rates of obesity in a population, however changing the

obesogenic environment through political initiatives and economic incentives has the potential of being more effective.

Obesity is associated with an increased risk of various chronic diseases, including type II diabetes mellitus[60], cardiovascular disease[61], dementia[62,63] and cancer.[64] Insulin resistance, the pathological state of cells not responding normally to the hormonal stimulus of insulin, could play an important role as a mechanistic link between obesity and the development of chronic diseases.[65]

1.3 Maternal obesity & foetal programming

Women of reproductive age have also been affected by the global obesity epidemic. On a global scale, over 20% of young women are estimated to be obese.[66] Rates of obesity during pregnancy are also high, both due to a high number of women with obesity becoming pregnant but also because of excess weight gain during pregnancy.[67,68]

Obesity during pregnancy adversely affects equally the health of the mother and the offspring. Prenatal complications due to maternal obesity include increased risk of pre-eclampsia, thromboembolism, gestational diabetes and miscarriage.[69] Furthermore, maternal obesity can negatively affect the placental physiology, the embryonic and foetal growth, as well as incur post-partum complications.[68-70]

David Barker first suggested that *in utero* exposure to adverse nutritional conditions is linked to an increased risk of later-life disease, a process described as foetal or developmental programming.[71] Foetal exposure to obesity during pregnancy can increase the offspring's long-term risk for several diseases, including asthma, cardiovascular disease, type II diabetes mellitus, and premature death in the adult offspring.[72] A recent systematic review found that children born to mothers with overweight/obesity prior to pregnancy were at high risk of autism spectrum disorders [OR=1.36; 95% CI 1.08 to 1.70; I^2=60.5], developmental delay [OR=1.58; 95% CI 1.39 TO 1.79; I^2=75.8], attention deficit hyperactivity

disorder [OR=1.62; 95% CI 1.62; 95% CI 1.08 to 1.70; I^2=70.15] and emotional/behavioural problems [OR=1.42; 95% CI 1.26 to 1.59; I^2=87.74].[73]

Four possible underlying mechanisms linking maternal obesity with adverse neurodevelopmental outcome in the offspring have been suggested[74]:

1. Insulin/glucose dysregulation and leptin signalling in the developing brain;
2. Inflammation and oxidative stress;
3. Dysregulation of serotonergic and dopaminergic signalling in the reward system;
4. Changes in brain derived neurotrophic factor (BDNF) - mediated synaptic plasticity

The increased number of children born to mothers with obesity makes it important to clarify a potential association between early exposure to obesity and adverse neurodevelopmental outcomes in the adult offspring. Therefore, the aim of the first paper was to decipher the role of maternal obesity on the proteomic profile of the adult offspring's cerebral cortex.

1.4 First publication

OPEN

International Journal of Obesity (2015) **39,** 1325–1328

www.nature.com/ijo

SHORT COMMUNICATION

Are you also what your mother eats? Distinct proteomic portrait as a result of maternal high-fat diet in the cerebral cortex of the adult mouse

A Manousopoulou[1,2], J Woo[2], CH Woelk[2], HE Johnston[1,3], A Singhania[2], C Hawkes[2], SD Garbis[1,2,3,4] and RO Carare[2,4]

Epidemiological studies suggest an association between maternal obesity and adverse neurodevelopmental outcomes in offspring. Our aim was to compare the global proteomic portrait in the cerebral cortex between mice born to mothers on a high-fat or control diet who themselves were fed a high-fat or control diet. Male mice born to dams fed a control (C) or high-fat (H) diet 4 weeks before conception and during gestation, and lactation were assigned to either C or H diet at weaning. Mice were killed at 19 weeks and their cerebral cortices were analysed using a two-dimensional liquid chromatography-mass spectrometry methodology. In total, 6 695 proteins were identified ($q < 0.01$), 10% of which were modulated in at least one of the groups relative to controls. *In silico* analysis revealed that mice clustered based on the diet of the mother and not their own diet and that maternal high-fat diet was significantly associated with response to hypoxia/oxidative stress and apoptosis in the cerebral cortex of the adult offspring. Maternal high-fat diet resulted in distinct endophenotypic changes of the adult offspring cerebral cortex independent of its current diet. The identified proteins could represent novel therapeutic targets for the prevention of neuropathological features resulting from maternal obesity.

International Journal of Obesity (2015) **39,** 1325–1328; doi:10.1038/ijo.2015.35

INTRODUCTION

Females of reproductive age have not been exempted from the obesity epidemic.[1] Since the 'Barker' theory arose 22 years ago,[2] accumulating evidence corroborates that fetal adaptations to nutritionally compromised intrauterine environments (for example, malnutrition, obesity) may result in later-life adverse health consequences, a process defined as developmental programming.[3,4] Epidemiological studies have found an association between maternal obesity and neuropathological features in the offspring such as cognitive problems in childhood, eating disorders in adolescence and psychotic episodes in adulthood.[5]

High-fat diet-induced obesity in rodents has been extensively used as an *in vivo* model to study the effects of obesity on various organ systems.[6] To our best knowledge, global tissue proteomics has not been previously applied to assess the effects of maternal obesity on brain regions of the adult offspring. Our aim was to examine and compare the endophenotypic portrait of male adult mouse cerebral cortices whose mothers during pregnancy/lactation and themselves after weaning were exposed to a high-fat or control diet.

MATERIALS AND METHODS

Proven C57b1/6 dams were fed a control (C) (21% kcal fat, 17% kcal protein, 63% kcal carbohydrate, $n = 4$) or high-fat (H) chow diet (45% kcal fat, 20% kcal protein, 35% kcal carbohydrate; Special Diet Services, United Kingdom, $n = 4$) 4 weeks before conception and during gestation and lactation. At weaning, 4-week-old male offspring ($n = 24$) were assigned to C or H, generating four groups (CC, CH, HC, HH, $n = 6$ for each) (Figure 1a).

Nineteen week-old mice were anaesthetised, perfused intracardially with phosphate-buffered saline, brains removed, dissected for frontoparietal cortices and snap frozen. Experimental procedures were approved by the Institutional Animal Care and Use Committee at the University of Southampton and the Home Office.[7]

Specimens were dissolved in 0.5 M triethylammonium bicarbonate, 0.05% sodium dodecyl sulfate and homogenised using the FastPrep system (Savant Bio, Illkirch, France) followed by pulsed probe sonication (Misonix, Farmingdale, NY, USA). Lysates were centrifuged (16 000 *g*, 10 min, 4 °C) and supernatants were measured for protein content using the bicinchoninic acid assay (Thermo Pierce, Rockford, IL, USA) per manufacturer's instructions. Three individual protein extracts were pooled (33.3 μg from each lysate giving 100 μg final protein content) to form two biological replicates for each of the four conditions and subjected to reduction, alkylation, trypsin proteolysis and Isobaric tags for relative and absolute quantitation (iTRAQ) labelling per supplier's specifications (ABSciex, San Hose, CA, USA). Only biological replicates were included in the study design as the technical reproducibility of the iTRAQ proteomics method used has been reported by the authors.[8,9] Labelled peptides were pooled and

[1]Centre for Proteomic Research, Institute for Life Sciences, University of Southampton, Southampton, UK; [2]Clinical and Experimental Sciences, University of Southampton, Southampton, UK and [3]Cancer Sciences, University of Southampton, Southampton, UK. Correspondence: Dr SD Garbis, Cancer Sciences and Clinical and Experimental Sciences, Institute for Life Sciences – Centre for Proteome Research, Faculty of Medicine, University of Southampton, Southampton SO16 6YD, UK or Dr RO Carare, Clinical and Experimental Sciences, Faculty of Medicine, University of Southampton, LD 66 Southampton General Hospital, Southampton SO16 6YD, UK.
E-mail: S.D.Garbis@soton.ac.uk or R.O.Carare@soton.ac.uk
[4]SDG and ROC jointly led the study and are co-senior authors.
Received 18 August 2014; revised 9 December 2014; accepted 6 January 2015; accepted article preview online 23 March 2015; advance online publication, 21 April 2015

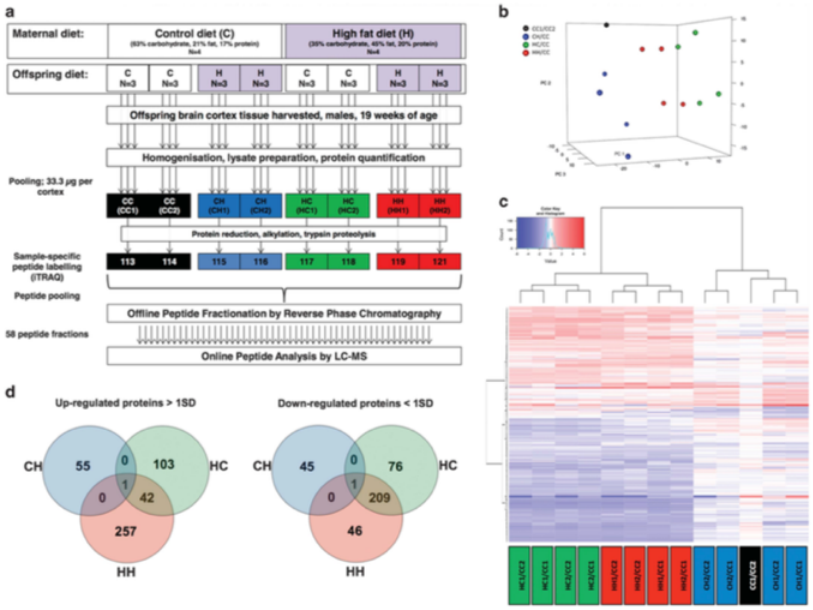

Figure 1. (**a**) Proteomics workflow and labelling scheme, (**b**) Principal component analysis of the iTRAQ ratios of all analysed proteins in the cerebral cortex showing clustering of mice based on the maternal diet and not their current diet, that is, blue dots (CH/CC) clustering separately from red (HH/CC) and green dots (HC/CC) along principal component 1. The sample division along principal component 2 results from dividing each sample by a different control, that is, CC1 (dots in the top) or CC2 (dots in the bottom). (**c**) Venn diagrams of commonly up- and downregulated proteins in CH, HC and HH mice compared with controls (CC). (**d**) Hierarchical clustering analysis of modulated proteins: the HC and HH groups have a similar proteomic portrait, which was different from that of CH mice.

fractionated with high-PH reverse phase chromatography using the Waters, XBridge C_8 column (150 × 3 mm, 3.5 µm particle) with the UltiMate HPLC (LC Packings, Amsterdam, NL, USA) (Supplementary Methods 1).[9] Each resulting fraction was liquid chromatography-mass spectrometry analysed with low-pH reverse phase capillary chromatography (PepMap C_{18}, 75 µm ID × 50 cm length, 100 Å pore, 3.5 µm particle) and nanospray ionisation FT-MS (Ultimate 3000 UHPLC - LTQ-Velos Pro Orbitrap Elite, Thermo Scientific, Bremen, DE, USA) (Figure 1a) (Supplementary Methods 2).[8,9]

The unprocessed raw files were submitted to Proteome Discoverer 1.4 for target decoy searching with SequestHT for tryptic peptides, allowing two missed cleavages, 10 ppm tolerance, minimum peptide length 6 and 2 maximum variable (1 equal) modifications: oxidation (M), deamidation (N, Q), phosphorylation (S, T, Y), iTRAQ 8plex (Y). Methythio (C) and iTRAQ (K and N-teminus) were set as fixed modifications. Fragment ion mass tolerances were 0.02 Da and 0.5 Da for the higher energy collisional induced dissociation and collision induced dissociation spectra, respectively. False discovery rate (FDR) was estimated with the Percolator at ⩽0.01 and validation set at q-value < 0.01. Reporter ions extracted within 20 ppm and rejected if any channels were absent. Quantification ratios were median-normalised and $\log_2$ transformed. A protein was considered modulated in one group relative to controls when its $\log_2$ ratio was above or below ± 1 s.d. across all biological replicates. Proteomics data were deposited to the ProteomeXchange Consortium via the PRIDE partner repository (data set identifier PXD001540).

Principal component analysis using reporter ion ratios of the study proteome and heatmap construction of reproducibly modulated proteins were generated using BioConductor-R (version 2.15.1) and g-plots in R (version 3.0.2). MetaCore (GeneGo, St Joseph, MI, USA) and BiNGO were applied to identify prebuilt processed networks and gene ontology terms overrepresented in the modulated proteome. FDR corrected P-values < 0.05 were considered significant.

RESULTS

The proteomic analysis resulted in the identification of 18 543 peptides surrogate to 6695 unique proteins (Supplementary Table 1). The average coefficient variation for the iTRAQ ratios of all proteins profiled across biological replicates was determined to be 16%, 12% and 13% for the CH, HC and HH groups, respectively. Analogous coefficient variation values between biological replicates were reported by the authors using similar proteomics methodologies.[8,9] Principal component analysis of the analysed proteome showed clustering of mice perinatally exposed to high-

fat diet irrespective of their current diet (Figure 1b). A total of 662 proteins (Supplementary Table 2) were found modulated in at least one of the three groups. Their hierarchical clustering revealed that the cerebral cortex of mice whose mothers were on high-fat diet, regardless their own diet, shared a very similar endophenotypic portrait, which was distinct from that of mice whose mothers were on control diet (Figure 1c).

Of the modulated proteins, 251 were common in the HC and HH groups (Figure 1d and Supplementary Table 3). MetaCore analysis showed that response to hypoxia/oxidative stress (FDR corrected *P*-value = 1.45E-02) and the apoptosis/endoplasmic reticulum stress pathway (FDR corrected *P*-value = 3.53E-02) were significantly overrepresented processes only in the cerebral cortices of mice perinatally exposed to high-fat diet (Figure 2). Induction of apoptosis by oxidative stress was cross-referenced with BiNGO (Supplementary Figure 1). By contrast these functions were not significantly enriched in CH mice.

DISCUSSION

Our study constitutes the most comprehensive proteomic profiling of the mouse cerebral cortex to date. The results provide novel evidence of an association between maternal high-fat diet with endophenotypic alterations in the cerebral cortex of the adult offspring. Epigenetic DNA methylation patterns may be a possible mechanism by which this 'nutritional imprinting' was established,[10] but deciphering this was beyond the scope of this study.

In silico interpretation of proteins commonly modulated in the cerebral cortex of mice perinatally exposed to high-fat diet revealed a significant overrepresentation of response to hypoxia/oxidative stress and apoptosis/endoplasmic reticulum stress (Figure 2), both suggestive of a progression to a neurodegenerative phenotype.

The analysed enzymes associated with response to hypoxia/oxidative stress were peroxiredoxin-1, peroxiredoxin-2, peroxiredoxin-4, superoxide dismutase (Mn) mitochondrial, glutathione peroxidase 1, glutathione S-transferase omega 1, thioredoxin reductase 1 cytoplasmic and xanthine dehydrogenase/oxidase. The downregulation of these reactive oxygen species (ROS) scavenging proteins could suggest increased oxidative stress in the cerebral cortex of adult mice as a result of maternal obesity.

It has been previously reported that maternal high-fat diet leads to increased oxidative stress in brain regions of the adult offspring by measuring levels of 3-nitrotyrosine and protein carboxylation, providing thus an indirect cue to oxidative stress.[11] The oxidative metabolism of fatty acids typically generates ROS, that cause the covalent modification of intracellular nucleophiles such as mitochondrial DNA and proteins, including those involved in redox processing.[12] The accumulation of oxidative damage products in the cytoplasm of neurons precedes the deposition of Aβ in cerebral amyloid angiopathy and Alzheimer's disease.[13] The ROS-mediated covalent modification of Aβ, among other proteins, may also have a role to its reduced clearance.[14]

Global cerebral ischaemia/reperfusion (I/R) is a useful model on the effects of increased oxidative stress in brain regions. I/R leads to increased free radical production and oxidative stress, which in turn can cause neuronal apoptosis.[15] Through the I/R model, it has been found that by reducing oxidative stress neuronal damage in the brain could be prevented.[16] As neuronal apoptosis is an irreversible process, ameliorating oxidative stress could reduce the risk of neurodegenerative disease. A recent study showed the neuroprotective effects of β-myrcene, a natural product derived from thyme and parsley, in mice following I/R.[17] In this study, β-myrcene treatment concomitantly with the induction of I/R reduced oxidative stress and prevented neurodegeneration via the induction of ROS-scavenging enzymes such as glutathione peroxidase and superoxide dismutase.

Another study showed that pre-treatment of Swiss albino mice with S-allyl cysteine, a phytochemical in garlic, prevented the cognitive and behavioural impairment of streptozotocin-induced experimental dementia. This effect was attributed to the induction of ROS-scavenging proteins, including glutathione peroxidase.[18] Similar trends have been observed for fruit-derived polyphenols. Despite their low systemic bioavailability and slow reactivity in the direct sequestration of ROS species, polyphenols trigger cellular and molecular mechanisms, in part through the induction of ROS-scavenging enzymes, that result in reduced neuronal oxidative damage and cognitive decline.[19] Denny Joseph *et al.*[20] highlighted the efficiency of combining fish oil and quercetin, a compound

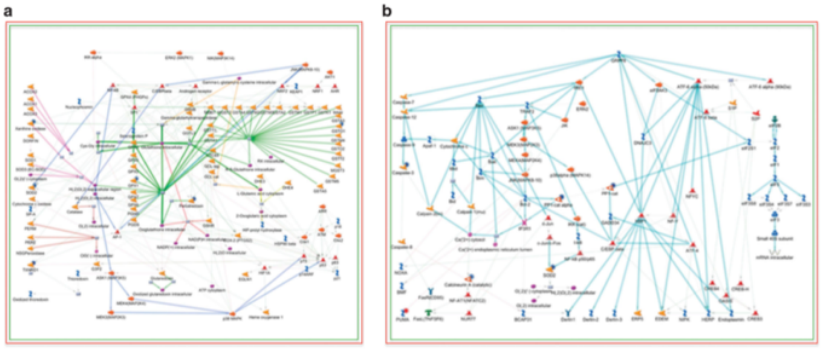

Figure 2. Process Network Analysis using MetaCore: significant enrichment for (**a**) response to hypoxia/oxidative stress (FDR corrected *P*-value = 3.53E-02) and (**b**) apoptosis/endoplasmic reticulum stress pathway (FDR corrected *P*-value = 1.45E-02) in the cerebral cortex of the adult offspring as a result of maternal high-fat diet. Analysed proteins are denoted with a circle (red = upregulation, blue = downregulation).

found in red onions, in lowering oxidative stress in rat brain and thus protecting against neurodegeneration.

Study limitations include the non-validated mass spectrometry analysis results using alternative approaches (for example, immunohistochemistry), the lack of functional assays and protein oxidation status assessment. These constitute objectives for prospective studies. In conclusion, our study demonstrated that maternal obesity resulted in distinct proteomic portraits, suggesting a neurogenerative phenotype in the adult offspring cerebral cortex.

CONFLICT OF INTEREST

The authors declare no conflict of interest.

ACKNOWLEDGEMENTS

This study was funded by the BBSRC, Rosetrees Trust and the Wessex Cancer Trust and Medical Research, United Kingdom. We are indebted to Mr Roger Allsopp, Mr Derek Coates and Hope for Guernsey for their enthusiasm, fund raising and vision in establishing the proteomics infrastructure at the University of Southampton—Cancer Sciences/Institute for Life Sciences. We thank Dr X Zhang and Dr D Ankrett for the use of the high-performance liquid chromatography system. We would also like to acknowledge the PRIDE Team for their support.

REFERENCES

1 Flegal KM, Carroll MD, Ogden CL, Curtin LR. Prevalence and trends in obesity among US adults, 1999–2008. *JAMA* 2010; **303**: 235–241.
2 Barker DJ. The fetal origins of diseases of old age. *Eur J Clin Nutr* 1992; **46**: S3–S9.
3 Iozzo P, Holmes M, Schmidt MV, Cirulli F, Guzzardi MA, Berry A *et al.* Developmental ORIgins of Healthy and Unhealthy AgeiNg: the role of maternal obesity-introduction to DORIAN. *Obes Facts* 2014; **7**: 130–151.
4 Gluckman PD, Hanson MA, Cooper C, Thornburg KL. Effect of in utero and early-life conditions on adult health and disease. *N Engl J Med* 2008; **359**: 61–73.
5 Van Lieshout RJ, Taylor VH, Boyle MH. Pre-pregnancy and pregnancy obesity and neurodevelopmental outcomes in offspring: a systematic review. *Obes Rev* 2011; **12**: e548–e559.
6 Zambrano E, Nathanielsz PW. Mechanisms by which maternal obesity programs offspring for obesity: evidence from animal studies. *Nutr Rev* 2013; **71**: S42–S54.
7 Hawkes CA, Gentleman SM, Nicoll JA, Carare RO. Prenatal high-fat diet alters the cerebrovasculature and clearance of β-amyloid in adult offspring. *J Pathol* 2014; **235**: 619–631.
8 Papachristou EK, Roumeliotis TI, Chrysagi A, Trigoni C, Charvalos E, Townsend PA *et al.* The shotgun proteomic study of the human ThinPrep cervical smear using iTRAQ mass-tagging and 2D LC-FT-Orbitrap-MS: the detection of the human papillomavirus at the protein level. *J Proteome Res* 2013; **12**: 2078–2089.
9 Al-Daghri NM, Al-Attas OS, Johnston HE, Singhania A, Alokail MS, Alkharfy KM *et al.* Whole serum 3D LC-nESI-FTMS quantitative proteomics reveals sexual dimorphism in the Milieu Intérieur of overweight and obese adults. *J Proteome Res* 2014; **13**: 5094–5105.
10 Soubry A, Murphy SK, Wang F, Huang Z, Vidal AC, Fuemmeler BF *et al.* Newborns of obese parents have altered DNA methylation patterns at imprinted genes. *Int J Obes (Lond)* 2015; **39**: 650–657.
11 White CL, Pistell PJ, Purpera MN, Gupta S, Fernandez-Kim SO, Hise TL *et al.* Effects of high fat diet on Morris maze performance, oxidative stress, and inflammation in rats: contributions of maternal diet. *Neurobiol Dis* 2009; **35**: 3–13.
12 Jacobs AT, Marnett LJ. Systems analysis of protein modification and cellular responses induced by electrophile stress. *Acc Chem Res* 2010; **43**: 673–683.
13 Carare RO, Hawkes CA, Jeffrey M, Kalaria RN, Weller RO. Review: cerebral amyloid angiopathy, prion angiopathy, CADASIL and the spectrum of protein elimination failure angiopathies (PEFA) in neurodegenerative disease with a focus on therapy. *Neuropathol Appl Neurobiol* 2013; **39**: 593–611.
14 Butterfield DA, Bader Lange ML, Sultana R. Involvements of the lipid peroxidation product, HNE, in the pathogenesis and progression of Alzheimer's disease. *Biochim Biophys Acta* 2010; **1801**: 924–929.
15 Heo JW, Han SW, Lee SK. Free radicals as triggers of brain edema formation after stroke. *Free Radic Biol Med* 2005; **39**: 51–70.
16 Oztanir MN, Ciftci O, Cetin A, Aladag MA. Hesperidin attenuates oxidative and neuronal damage caused by global cerebral ischemia/reperfusion in a C57BL/J6 mouse model. *Neurol Sci* 2014; **35**: 1393–1399.
17 Ciftci O, Oztanir MN, Cetin A. Neuroprotective effects of β-myrcene following global cerebral ischemia/reperfusion-mediated oxidative and neuronal damage in a C57BL/J6 mouse. *Neurochem Res* 2014; **39**: 1717–1723.
18 Javed H, Khan MM, Khan A, Vaibhav K, Ahmad A, Khuwaja G *et al.* S-allyl cysteine attenuates oxidative stress associated cognitive impairment and neurodegeneration in mouse model of streptozotocin-induced experimental dementia of Alzheimer's type. *Brain Res* 2011; **1389**: 133–142.
19 Singh M, Arseneault M, Sanderson T, Murthy V, Ramassamy C. Challenges for research on polyphenols from foods in Alzheimer's disease: bioavailability, metabolism, and cellular and molecular mechanisms. *J Agric Food Chem* 2008; **56**: 4855–4873.
20 Denny Joseph KM, Muralidhara. Enhanced neuroprotective effect of fish oil in combination with quercetin against 3-nitropropionic acid induced oxidative stress in rat brain. *Prog Neuropsychopharmacol Biol Psychiatry* 2013; **40**: 83–92.

Supplementary Information accompanies this paper on International Journal of Obesity website (http://www.nature.com/ijo)

1.5 Commentary on first publication

The main finding of the first publication is that exposure to maternal obesity creates a “nutritional imprinting” in the cerebral cortex of the adult offspring, suggestive of a neurodegenerative phenotype, that is independent of its own diet. One possible mechanism that could mediate the observed association is epigenetic changes established in the brain of the offspring *in utero* and persisting until adulthood.

To examine whether this holds true, the epigenetic modifications, e.g. DNA methylation status and histone modification, of the adult offspring cerebral cortex could be examined in future studies. This study findings could be functionally validated by examining the cognitive function and memory of the adult mice *in utero* exposed to maternal obesity using a variety of tests (e.g. novel object recognition, Morris water maze etc.).

It would also be interesting to investigate whether this effect of “nutritional imprinting” can be extended to more than one generation, i.e. examine the effects of obesity in the grandmother to the brain proteomic profile of the grandchild. Furthermore, a future study could also examine whether supplementation with whole food extracts (e.g. green coffee, cocoa, blueberry) to pregnant mice on a high-fat diet can reduce the risk of a neurodegenerative phenotype in the adult offspring.

In order to avoid introducing experimental variability due to sexual dimorphism, only male offspring were included in the present study. It would be interesting to perform the same study for female offspring and assess potential sex-specific effects of maternal obesity to the offspring’s brain.

One study limitation was the sample pooling strategy used (n=6 mice per experimental condition; n=3 samples pooled to form two biological replicates of pooled samples per experimental condition) to include all four experimental conditions (mother/offspring diet: N/N, HF/N, N/HF, HF/HF; N=normal diet, HF=high-fat diet) in an eight-plex design. Sample pooling does not allow the assessment of biological variability and entails the risk of an outlier affecting the protein expression levels within the group of pooled samples. Furthermore, due to the sample pooling used, this study did not

have sufficient statistical power, since only two biological replicates of pooled samples were assessed per experimental group. Another study limitation is that the entire cerebral cortex was analysed, which could have resulted in non-specific findings compared to examining specific parts of the cerebral cortex (e.g. neocortex, allocortex etc).

1.6 Hypothalamus: central appetite control

The hypothalamus is a brain region that controls circadian rhythms, sleep, fatigue, body temperature, hunger, thirst and attachment behaviours.[75] The hypothalamus is comprised of anatomically distinct regions and nuclei.[76] The anatomical regions of the hypothalamus are defined as anterior, tuberal and posterior. The anterior region contains the medial preoptic, supraoptic, paraventricular, anterior hypothalamic and suprachiasmatic nuclei. The tuberal region contains the dorsomedial hypothalamic, ventromedial, arcuate, lateral and lateral tuberal nuclei. The posterior region contains the mammillary, posterior, lateral and tuberomammillary nuclei. A schematic overview of the hypothalamic nuclei is provided in **Appendix D**.

Supporting evidence gathered over the past century suggests that body fat accumulation could also partly stem from the central nervous system.[76-80] The participation of hypothalamic regions in the regulation of energy balance was identified in the 1940s and 1950s from degeneration studies: lesions in the lateral hypothalamus reduced food intake whereas destruction of the hypothalamic dorsomedial, paraventricular and ventromedial nuclei was associated with hyperphagia.[81-85]

Even though these approaches appear crude by today's research standards, they were nevertheless crucial in identifying the hypothalamus as an important regulator of food intake and energy balance. A breakthrough came in the 1990s when the gene encoding leptin was discovered. Leptin is a hormone primarily produced by adipose cells that participates in the regulation of energy homeostasis by inhibiting hunger.[86]

Following this discovery, receptors for leptin were found to be localized on hypothalamic structures, including these implicated in regulating energy homeostasis by degeneration studies.[87] However, the leptin receptors were predominantly identified in a tuberal hypothalamic structure, the arcuate nucleus.[88] Leptin was shown to activate the pro-opiomelanocortin neurons leading to increased energy expenditure and suppressed food intake while simultaneously suppressing the activity of the orexigenic agouti-related

protein - neuropeptide Y neurons.[89] Reducing central orexigenic signals is an attractive therapeutic approach in addressing the current obesity epidemic. Therefore, the aim of the second publication was to examine the proteomic profile of mice with obesity in order to identify novel therapeutic targets of appetite regulation.

1.7 Second publication

OPEN

Citation: Nutrition & Diabetes (2016) **6**, e204; doi:10.1038/nutd.2016.10

www.nature.com/nutd

ORIGINAL ARTICLE

Hypothalamus proteomics from mouse models with obesity and anorexia reveals therapeutic targets of appetite regulation

A Manousopoulou[1,7], Y Koutmani[2,7], S Karaliota[2], CH Woelk[1], ES Manolakos[3,4], K Karalis[2,4,8] and SD Garbis[1,5,6,8]

OBJECTIVE: This study examined the proteomic profile of the hypothalamus in mice exposed to a high-fat diet (HFD) or with the anorexia of acute illness. This comparison could provide insight on the effects of these two opposite states of energy balance on appetite regulation.
METHODS: Four to six-week-old male C56BL/6J mice were fed a normal (control 1 group; $n = 7$) or a HFD (HFD group; $n = 10$) for 8 weeks. The control 2 ($n = 7$) and lipopolysaccharide (LPS) groups ($n = 10$) were fed a normal diet for 8 weeks before receiving an injection of saline and LPS, respectively. Hypothalamic regions were analysed using a quantitative proteomics method based on a combination of techniques including iTRAQ stable isotope labeling, orthogonal two-dimensional liquid chromatography hyphenated with nanospray ionization and high-resolution mass spectrometry. Key proteins were validated with quantitative PCR.
RESULTS: Quantitative proteomics of the hypothalamous regions profiled a total of 9249 protein groups ($q < 0.05$). Of these, 7718 protein groups were profiled with a minimum of two unique peptides for each. Hierachical clustering of the differentiated proteome revealed distinct proteomic signatures for the hypothalamus under the HFD and LPS nutritional conditions. Literature research with in silico bioinformatics interpretation of the differentiated proteome identified key biological relevant proteins and implicated pathways. Furthermore, the study identified potential pharmacologic targets. In the LPS groups, the anorexigen pro-opiomelanocortin was downregulated. In mice with obesity, nuclear factor-κB, glycine receptor subunit alpha-4 (GlyR) and neuropeptide Y levels were elevated, whereas serotonin receptor 1B levels decreased.
CONCLUSIONS: High-precision quantitative proteomics revealed that under acute systemic inflammation in the hypothalamus as a response to LPS, homeostatic mechanisms mediating loss of appetite take effect. Conversely, under chronic inflammation in the hypothalamus as a response to HFD, mechanisms mediating a sustained 'perpetual cycle' of appetite enhancement were observed. The GlyR protein may constitute a novel treatment target for the reduction of central orexigenic signals in obesity.

Nutrition & Diabetes (2016) **6,** e204; doi:10.1038/nutd.2016.10; published online 25 April 2016

INTRODUCTION

Overweight and obesity as a result of positive energy balance constitute major public health burdens with significant economic and social implications.[1] The hypothalamus is the key brain site for the regulation of food intake and energy balance in mammals. Under physiological conditions, a variety of peripheral signals regulate appetite and adjust energy intake to match energy consumption requirements.[2] Systemic acute inflammatory signals can cause profound anorexia by disrupting the physiological regulation of appetite in the hypothalamus.[3] Conversely, emerging evidence suggests that hypothalamic 'inflammatory' activation as a result of a high-fat diet (HFD) and obesity can disturb anorexigenic and thermogenic signals and promote abnormal body weight control.[4] Deciphering the molecular events of these two contradictory observations in a global and directly comparative way allows for a more causal understanding on the relations between diet, inflammatory signals and appetite regulation. Provided that nutritional intervention protocols are likely to interfere with multiple pathways inside the cell, a system-wide interrogation of the host response using non-targeted quantitative proteomics was warranted.[5]

The aim of this study was to compare the global proteomic profile of the hypothalamus in mice exposed to a HFD or with anorexia of acute illness. We hypothesise that such a comparison can shed new insight on the effects of these two opposite states of energy balance on appetite regulation.

MATERIALS AND METHODS

Animal model

Studies were conducted in male mice on C56BL/6J background. Mice were bred and maintained at regular housing temperatures (23 °C) and 12-h light/dark cycle starting at 0700 hours. Animals had *ad libitum* access to water and food and were weighed at weekly intervals. Four to six-week-old mice ($n = 34$) were randomly divided into four groups: the control 1 (C1) group ($n = 7$), the HFD group ($n = 10$), the control 2 (C2) group ($n = 7$) and the lipopolysaccharide (LPS) group ($n = 10$). Mice in the C1 group were fed a control diet (4.5% fat, 34% starch, 5.0% sugar and 22.0% protein), whereas the HFD group was fed a HFD (24% fat, 41% carbohydrate, and 24% protein; Research diets D12451 formula) for 8 weeks after which they were anaesthetised and perfused intracardially with phosphate-buffered saline. A diet containing 24% fat (45% kcal fat) was selected because it efficiently induces obesity and better simulates

[1]Clinical and Experimental Sciences Unit, University of Southampton, Southampton, UK; [2]Centre of Basic Research, Biomedical Research Foundation of the Academy of Athens, Greece; [3]Information Technologies in Medicine and Biology, Department of Informatics and Telecommunications, University of Athens, Athens, Greece; [4]Wyss Institute of Biological Inspired Engineering, Boston, MA, USA; [5]Institute for Life Sciences, University of Southampton, Southampton, UK and [6]Cancer Sciences and CES Unit, University of Southampton, Southampton, UK. Correspondence: Dr K Karalis, Wyss Institute of Biological Inspired Engineering, Boston, MA, USA or Dr SD Garbis, Cancer Sciences and CES Units, University of Southampton, University Road, Southampton SO171BJ, UK.
E-mail: Katia.Karalis@wyss.harvard.edu or S.D.Garbis@soton.ac.uk
[7]These authors contributed equally to this work.
[8]SDG and KK jointly led the study and are co-senior authors.
Received 10 July 2015; revised 25 January 2016; accepted 1 March 2016

a human HFD as opposed to a more extreme 60% kcal fat diet.[6,7] Mice in the C2 and LPS groups were fed a control diet for 8 weeks. After this period, mice in the C2 group received an intraperitoneal injection of 0.3 ml saline, whereas in the LPS group received an intraperitoneal injection of LPS (*Escherichia coli* O111:B4 (Sigma No. L-2630)) at a dose of 120 μg per mouse dissolved in 0.3 ml saline. Mice in the C2 and LPS groups were killed 18 h after the injection as described above. As protein expression in the hypothalamus is known to be under circadian regulation,[8] mice were killed at 0700 hours. Experimental procedures were approved by the Institutional Animal Care and Use Committee at the Centre of Basic Research, Biomedical Research Foundation of the Academy of Athens.

Determination of insulin resistance by HOMA-IR

HOMA-IR analysis was used to assess insulin resistance in HFD-fed mice. After overnight fasting, values for homeostasis model assessment of insulin resistance (HOMA-IR) were calculated from the values of fasting serum glucose (mg dl^{-1}) and fasting serum insulin (μU ml^{-1}) by using the following formula: HOMA-IR = fasting glucose value (mg dl^{-1}) × fasting insulin value (μU ml^{-1})/405. Low HOMA-IR values indicate high insulin sensitivity, whereas high HOMA-IR values indicate low insulin sensitivity (insulin resistance). Fasting glucose concentrations were measured using a hand-held glucometer (Biorad, Hercules, CA, USA), whereas serum insulin levels were quantified by ELISA (Mercodia, Uppsala, Sweden).

Quantitative proteomics sample processing

Hypothalamic regions were removed and snap frozen at − 80 °C. Specimens were dissolved in 0.5 M triethylammonium bicarbonate, 0.05% sodium dodecyl sulphate, homogenised using the Fast Prep system (Savant Bio, Cedex, France) followed by pulsed probe sonication (Misonix, Farmingdale, NY, USA). Lysates were centrifuged (16 000 *g*, 10 min, 4 °C) and supernatants were measured for protein content using infra-red spectroscopy (Merck Millipore, Darmstadt, Germany). For the quantitative proteomic analysis, the hypothalamic regions from three mice were used for the C1 and C2 groups and from six mice for the HFD and LPS groups ($n = 18$ in total). Three individual protein extracts were pooled (33.3 μg from each lysate giving 100 μg final protein content) to form one sample for the C1 and C2 groups and two biological replicates for the HFD and LPS groups. Lysates were then reduced, alkylated and subjected to trypsin proteolysis. Peptides were labelled using six of the eight-plex iTRAQ reagent kit (113 = C1, 114 = C2, 115 = HFD1, 116 = HFD2, 117 = LPS1, 118 = LPS2) and analysed using high-precision two-dimensional liquid chromatography with nanospray ionization tandem mass spectrometry as reported previously by the authors[9–12] (Figure 1a) (Supplementary Methods 1).

Database searching

Unprocessed raw files were submitted to Proteome Discoverer 1.4 for target decoy searching against the UniProtKB/TrEMBL mus musculus database comprised of 57 475 entries (release date 03 September 2014), allowing for up to two missed cleavages, a precursor mass tolerance of 10 ppm, a minimum peptide length of six and a maximum of two variable (one equal) modifications of; iTRAQ 8-plex (Y), oxidation (M), deamidation (N, Q) or phosphorylation (S, T, Y). Methylthio (C) and iTRAQ (K, N terminus) were set as fixed modifications. Reporter ion ratios from unique peptides only were taken into consideration for the quantitation of the respective protein. Quantification ratios were median-normalised and log2 transformed. Proteins were grouped using the protein grouping inference algorithm in the Proteome Discoverer 1.4 application (Supplementary Methods 2). A protein was considered modulated in the HFD or LPS group relative to control when its log2 ratio was above or below ± 1 s.d. across both biological replicates.[13] In adherence to the Paris Publication Guidelines for the analysis and documentation of peptide and protein identifications (http://www.mcponline.org/site/misc/ParisReport_Final.xhtml) and the recently published guidelines for high-confidence protein identification by Omenn *et al.*,[14] only proteins identified with at least two unique peptides were further subjected to bioinformatics analysis. Proteins of biological relevance, two of which were identified with one unique peptide, were validated using targeted quantitative PCR. Proteomics data were deposited to the ProteomeXchange Consortium via the PRIDE partner repository with the dataset identifier PXD003475.

Bioinformatics analysis

Heatmap construction of differentially expressed proteins in the HFD and LPS groups compared with their respective control was generated using Cluster 3.0 (http://bonsai.hgc.jp/~mdehoon/software/cluster/software.htm) and Java Treeview (http://jtreeview.sourceforge.net). MetaCore (GeneGo, St Joseph, MI, USA) and BiNGO were applied to differentially expressed proteins analysed with at least two unique peptides to identify over-represented processes in the modulated proteome of each group compared with their respective control. FDR-corrected *P*-values < 0.05 were considered significant.

Total RNA isolation and cDNA synthesis

For the quantitative PCR analysis the hypothalamic regions from four mice were utilised per group (C1, C2, HFD, LPS) ($n = 16$ in total). Total RNA from mouse hypothalamus was extracted using an RNA Isolation Kit (Qiagen, Hilden, Germany) according to the manufacturer's instructions. RNA concentration and purity were determined by NanoDrop 2000c Spectrophotometer (Thermo Scientific, Waltham, MA, USA). Ribosomal RNA band integrity was evaluated by conventional 1% agarose gel electrophoresis and the Agilent Bioanalyzer with the RNA 6000 Nano Kit (Agilent, Santa Clara, CA, USA).

For complementary DNA (cDNA) synthesis, 300 ng total RNA from each sample was reverse transcribed into cDNA using M-MLV Reverse Transcriptase (Thermo Scientific) according to the manufacturer's instructions. All the cDNA samples were stored at − 20 °C until quantitative PCR analyses.

Quantification of mRNA

Quantification of mRNA was performed for the following proteins: NFκ-B, neuropeptide Y (NPY), 5-hydroxytryptamine (serotonin) receptor 1B, glycine receptor alpha-4 subunit, pro-opiomelanocortin. The PCR mixture contained 1 μl diluted cDNA, 10 μM gene-specific primer (forward and reverse mixed together) and 10 μl of 2 × Fast SYBR Green Master Mix (Roche Diagnostics, Rotkreuz, Switzerland) in a total volume of 20 μl. Amplification was performed in 96-well optical reaction plates (Roche Diagnostics) on LightCycler 480 (Roche Diagnostics) using the following programme: 94 °C for 3 min to activate polymerase, 40 cycles at 94 °C for 20 s, 60 °C for 20 s and 72 °C for 20 s; melting curve analysis was performed after every run by heating up to 95 °C to monitor presence of unspecific products. Two negative controls were included in each assay run, with water instead of template. Three replicate measurements for each sample were performed. Primers were designed and checked with Primer Quest Tool (IDT) and NCBI primer BLAST tool and synthesised by Macrogen (Seoul, South Korea). Primer sequences are listed in Supplementary Table 1.

Quantitative PCR data analysis

The mRNA expression of genes in the hypothalamus of LPS-treated and HFD-fed mice was calculated relative to the expression in their respective control mice, according to the delta–delta Ct method ($2 - \Delta\Delta Ct$) using the most and least stable reference genes found, as well as the most commonly used glyceraldehyde-3-phosphate dehydrogenase and beta-actin.

RESULTS

Mice fed a HFD weighed significantly more than those fed a control diet (Supplementary Figure 1A). Furthermore, they were insulin resistant with significantly higher HOMA-IR values (Supplementary Figure 1B). The proteomic analysis of the hypothalamic regions resulted in the profiling of 9249 protein groups ($q < 0.05$) (Supplementary Tables 2 and 3), of which 7718 were identified with at least two unique peptides. Among the proteins identified with at least two unique peptides, 201 were upregulated in the HFD and 193 in the LPS groups compared with their respective control, of which 30 were common between the two conditions. Furthermore, 169 proteins were downregulated in the HFD and 194 in the LPS groups, of which 18 were common between the two conditions (Figure 1b, Supplementary Tables 4–6). The R^2 value between biological replicates was 0.69 and 0.89 for the differentially expressed proteins of the HFD and LPS groups, respectively. Hierarchical clustering of the differentiated proteome revealed a

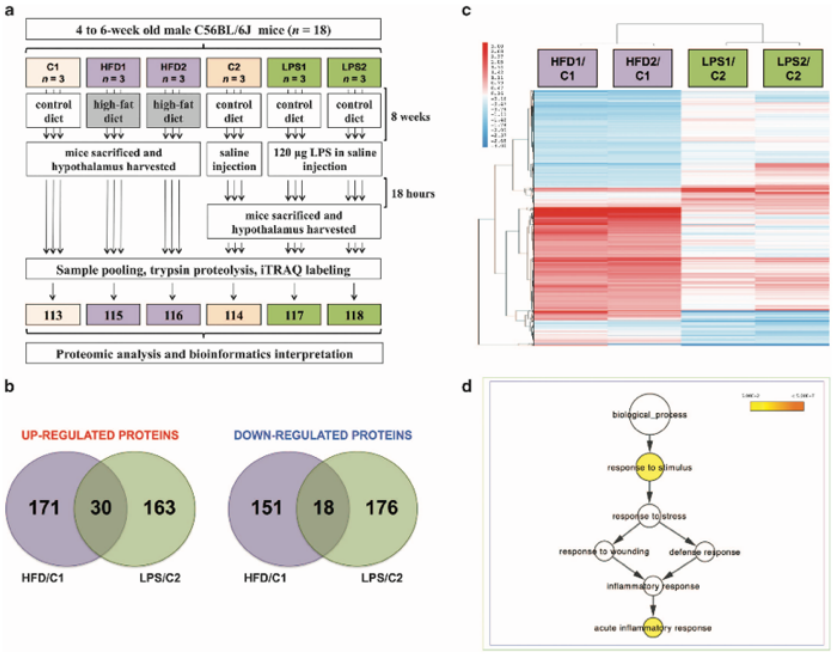

Figure 1. (**a**) Overview of the proteomics pipeline (**b**) Venn diagram description of the differentiated proteins between the HFD and LPS groups relative to their respective controls. (**c**) Hierarchical clustering analysis of modulated proteins: the HFD and LPS groups have a distinct endophenotypic portrait in the hypothalamus. (**d**) Gene ontology analysis using BiNGO of the commonly modulated proteins in the HFD and LPS conditions compared with their respective control showed a significant enrichment for acute inflammatory response. Coloured nodes representing GO terms correspond to those that were significant according to the *P*-value colour scale, whereas white nodes were not significant. The size of the node reflects the number of proteins that mapped to the corresponding GO term.

distinct proteomic signatures of the hypothalamus under the HFD and LPS (Figure 1c) nutritional conditions.

Gene ontology analysis using BiNGO of the 48 commonly modulated proteins showed a significant enrichment for acute inflammatory response (Figure 1d). In the hypothalamus of the LPS-exposed mice *protein folding and maturation_posttranslational processing of neuroendocrine peptides* (FDR-corrected *P*-value = 1.2E-6) (Figure 2a) and *apoptosis and survival_caspase cascade* (FDR-corrected *P*-value = 1.8E-2) (Figure 2b) were significantly enriched.

In the differentially expressed proteins of the HFD groups, *inflammation_IL-6 signalling* (FDR-corrected *P*-value = 6.5E-6) (Figure 3a), *inflammation_kallikrein-kinin system* (FDR-corrected *P*-value = 9.3E-6), and *inflammation_protein C signalling* (FDR-corrected *P-value* = 9.2E-3) were significantly over-represented. A nodal protein in all three inflammatory pathways was NF-κB, analysed to increase in the HFD groups compared with control (Figure 1c). Gene ontology analysis using BiNGO confirmed that both acute and chronic inflammatory responses were significantly over-represented in the modulated proteome of the hypothalamus in HFD-fed mice compared with control (Figure 3b).

Of potential biomedical interest to be discussed, nuclear factor-κB (NF-κB), pro-NPY and glycine receptor alpha-4 subunit levels increased, whereas serotonin receptor 1B levels were reduced in the HFD groups relative to control. In the LPS groups compared with control, pro-opiomelanocortin was profiled to be down-regulated. The relative quantitation of these proteins at the mRNA level was validated using quantitative PCR (Figure 4).

DISCUSSION

Molecular perturbations in the hypothalamus as a result of obesity have been studied primarily at the transcriptome but not the proteome level.[15,16] This study compared the global proteomic profile of the mouse hypothalamus between two experimental groups in opposite states of energy balance, that is, mice with increased caloric intake through a HFD, versus mice with severely compromised food intake due to acute systemic inflammation. Acute inflammatory response was significantly enriched in the commonly modulated proteins of both groups (Figure 1d), in agreement with a number of studies indicating the altered 'inflammatory' state in these experimental models.[3,17]

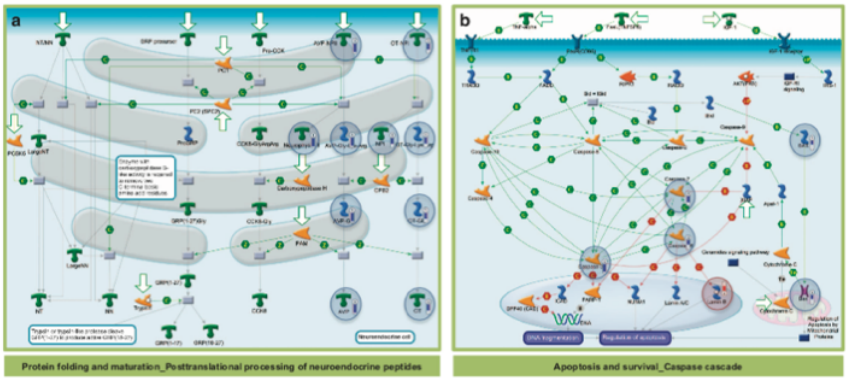

Figure 2. *In silico* analysis using MetaCore showed that (**a**) protein folding and maturation_posttranslational processing of neuroendocrine peptides (FDR-corrected *P*-value = 1.2E-6) and (**b**) apoptosis and survival_caspase cascade (FDR-corrected *P*-value = 1.8E-2) were significantly enriched in the differentially expressed proteins of the LPS groups compared with control. Analysed proteins are denoted with a circle (red = upregulation, blue = downregulation).

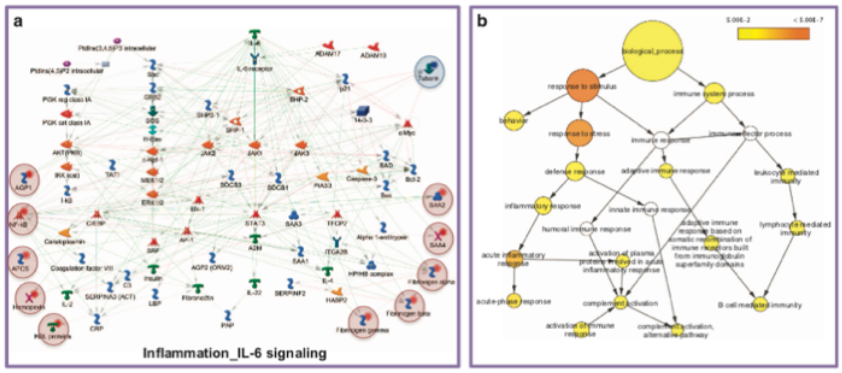

Figure 3. (**a**) *In silico* analysis using MetaCore showed that inflammation_IL-6 signalling was significantly enriched in the differentially expressed proteins of the HFD groups compared with control (FDR-corrected *P*-value = 6.5E-6). Analysed proteins are denoted with a circle (red = upregulation, blue = downregulation). (**b**) Gene ontology analysis using BiNGO confirmed that acute and chronic inflammatory responses are significantly enriched in the differentially expressed hypothalamic proteins of HFD-fed mice compared with control. Coloured nodes representing GO terms correspond to those that were significant according to the *P*-value colour scale, whereas white nodes were not significant. The size of the node reflects the number of proteins that mapped to the corresponding GO term.

It is well established that LPS induces anorexia in mouse models.[18] Our results showed that the acute systemic inflammatory response caused by LPS treatment specifically decreased pro-opiomelanocortin (Figure 4) and the related ACTH and alpha-MSH peptides with well-shown anorexigenic effects (Figure 2a). This paradoxical downregulation of anorexigenic signals possibly highlights the presence of a negative feedback loop, aiming to re-establish homoeostasis. Furthermore, hypothalamic sampling was done 18 h after LPS administration, as the mice were recovering from the endotoxin effects, as the administered LPS dose was at a medium range. Along this theme, reduced expression levels of caspase isoforms 3, 6 and 7 in the hypothalamus of LPS-treated mice was observed (Figure 2b). This finding suggests control of apoptotic processes and protection of neurons during re-establishment of homoeostasis, supporting the theory that inflammatory and homoeostatic control mechanisms may antagonise in a time- and immune activation phase-dependent manner.[19]

In the modulated proteome of the HFD groups, a number of inflammatory pathways, including the IL-6 pathway (Figure 3a), kallikrein-kinin system and protein C signalling, were significantly enriched, reflecting a more pronounced, chronic inflammatory response, also evident in the gene ontology analysis (Figure 3b).

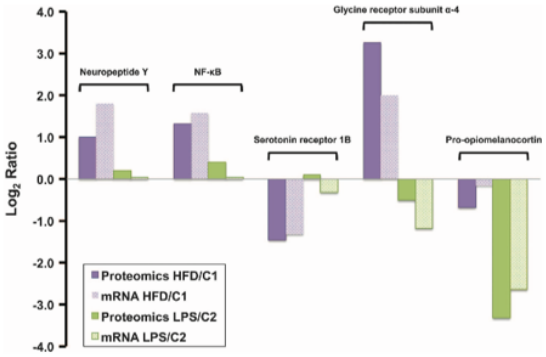

Figure 4. Validation of key proteomic findings using qPCR: NF-κB, pro-neuropeptide Y and glycine receptor alpha-4 subunit levels increased, whereas serotonin receptor 1B levels were reduced in the HFD groups relative to control. In the LPS groups compared with control, pro-opiomelanocortin was profiled to be downregulated.

Upregulation of pro-inflammatory mediators in the hypothalamus is a hallmark of obesity and constitutes a major component of insulin resistance pathogenesis.[20] The exact mechanisms mediating this phenotype remain a subject of intense investigation with endoplasmic reticulum stress, oxidative stress or direct activation of inflammatory-related transcription factors among the implicated processes.

A central node in the hypothalamic inflammatory processes was NF-κB, found to be upregulated as a result of HFD (Figure 4). NF-κB, an important mediator of metabolic inflammation, is enriched in hypothalamic neurons but normally remains inactive.[21] Over-nutrition alone, even before the onset of obesity, activates hypothalamic NF-κB partly through increased endoplasmic reticulum stress.[21] Furthermore, activation of hypothalamic NF-κB interrupts central insulin and leptin signalling and actions, whereas local suppression in the mediobasal hypothalamus, or more specifically in hypothalamic Agouti-related peptide neurons, significantly protects against obesity and glucose intolerance.[21]

NPY was profiled to increase in the hypothalamus of HFD-fed mice compared with control (Figure 4). Central administration of NPY, a well-established orexigenic peptide in the hypothalamus,[22] has been found to increase food intake and body weight, with chronic administration leading to development of obesity.[23,24] Furthermore, NPY overexpression in the dorsomedial hypothalamus induces hyperphagia and obesity,[25,26] whereas knockdown of NPY improves these changes.[27,28] A recent study showed that dorsomedial hypothalamus NPY knockdown rats on HFD had normal food intake, body weight and glucose tolerance/insulin sensitivity indexes as observed in lean control rats.[28] These authors suggest that dorsomedial hypothalamus NPY could be a potential therapeutic target for obesity and diabetes.

In the hypothalamus of HFD-fed mice compared with control, levels of serotonin receptor 1B (5-hydroxytryptamin receptor 1B; 5-HT1BR), a key modulator of energy homeostasis and a therapeutic target for obesity, were analysed to decrease (Figure 4). Serotonin reduces the activity of the orexigenic AgRP/NPY neurons via the 5-HT1BR in mice (or 5-HT1DBR in humans).[29] Studies have shown that mice lacking the 5-HT1BR develop hyperphagia, resulting in body weight increase.[30] In addition, administration of CP-94,253, a highly selective 5-HT1BR agonist, significantly decreases food intake[31] and potentiates the anorectic effects of pro-opiomelanocortin.

GlyR was analysed to be upregulated in the hypothalamus of mice with obesity compared with control (Figure 4). Although glycine is a well-established inhibitory neurotransmitter in the spinal cord and brain stem,[32] studies examining the function of glycine receptors in higher brain structures including the hypothalamus are limited. A study by Karnani *et al.*[33] showed that glycine receptor agonists exert a hyperpolarizing action on mature hypocretin/orexin (hcrt/orx) neurons in the hypothalamus, important regulators of arousal and reward seeking behaviour. To the best of our knowledge, our study is the first to identify an increase of GlyR levels in the hypothalamus of mice exposed to HFD. GlyR receptor antagonists, could be tested for their efficacy to reduce central orexigenic signals in obesity.

CONCLUSION

High-precision quantitative proteomics revealed that under acute systemic inflammation in the hypothalamus as a response to LPS, homeostatic mechanisms mediating loss of appetite take effect. Conversely, under chronic inflammation in the hypothalamus as a response to HFD, mechanisms mediating a sustained 'perpetual cycle' of appetite enhancement were observed. The combinatorial protein level modulation of the NF-κB, 5-HT1BR, GlyR and pro-NPY provides strong evidence for the enhancement of orexigenic signals as a response to HFD. Our study is the first to identify an increase of GlyR levels in the hypothalamus of mice exposed to HFD. Antagonists for this receptor could be tested for their efficacy to reduce central orexigenic signals in obesity.

CONFLICT OF INTEREST

The authors declare no conflict of interest.

ACKNOWLEDGEMENTS

This work has been partially supported by research grant 03ED306, implemented within the framework of the 'Program of Human Research Manpower Reinforcement' (PENED) co-financed by the Greek General Secretariat of Research and Technology and EU funds, and by EU FP7 grant TranSMed (Ref. number 245928). We are indebted to Mr Roger Allsopp, Mr Derek Coates and Hope for Guernsey for their fund raising and vision in establishing the clinical mass spectrometry infrastructure at the University of Southampton. We are grateful to the support of King Saud University, Deanship of Scientific Research Chair, Prince Mutaib Bin Abdullah Chair for Biomarkers of Osteoporosis, College of Science, as well as the Visiting Professor Program of King Saud University, Riyadh, Saudi Arabia. This work was also co-funded by the European Regional Development Fund and the Republic of Cyprus through

the Research Promotion Foundation (Projects NEKYP/0311/17 and YGEIA/BIOS/0311 (BIE/07)). The research leading to these results has also received funding from the European Union's Seventh Framework Programme FP7/2007-2013 under grant agreement n° 245928 (TRANSMED).

REFERENCES

1 Agborsangaya CB, Ngwakongnwi E, Lahtinen M, Cooke T, Johnson JA. Multimorbidity prevalence in the general population: the role of obesity in chronic disease clustering. *BMC Public Health* 2013; **13**: 1161.
2 Schwartz MW, Woods SC, Porte Jr D, Seeley RJ, Baskin DG. Central nervous system control of food intake. *Nature* 2000; **404**: 661–671.
3 Hart BL. Biological basis of the behavior of sick animals. *Neurosci Biobehav Rev* 1988; **12**: 123–137.
4 Thaler JP, Schwartz MW. Minireview: Inflammation and obesity pathogenesis: the hypothalamus heats up. *Endocrinology* 2010; **151**: 4109–4115.
5 Moresco JJ, Dong MQ, Yates JR 3rd. Quantitative mass spectrometry as a tool for nutritional proteomics. *Am J Clin Nutr* 2008; **88**: 597–604.
6 Ghibaudi L, Cook J, Farley C, van Heek M, Hwa JJ. Fat intake affects adiposity, comorbidity factors, and energy metabolism of sprague-dawley rats. *Obes Res* 2002; **10**: 956–963.
7 Johnston SL, Souter DM, Tolkamp BJ, Gordon IJ, Illius AW, Kyriazakis I *et al.* Intake compensates for resting metabolic rate variation in female C57BL/6J mice fed high-fat diets. *Obesity (Silver Spring)* 2007; **15**: 600–606.
8 Nicolaides NC, Charmandari E, Chrousos GP, Kino T. Circadian endocrine rhythms: the hypothalamic-pituitary-adrenal axis and its actions. *Ann N Y Acad Sci* 2014; **1318**: 71–80.
9 White CH, Johnston HE, Moesker B, Manousopoulou A, Margolis DM, Richman DD *et al.* Mixed effects of suberoylanilide hydroxamic acid (SAHA) on the host transcriptome and proteome and their implications for HIV reactivation from latency. *Antiviral Res* 2015; **123**: 78–85.
10 Delehouzé C, Godl K, Loaëc N, Bruyère C, Desban N, Oumata N *et al.* CDK/CK1 inhibitors roscovitine and CR8 downregulate amplified MYCN in neuroblastoma cells. *Oncogene* 2014; **33**: 5675–5687.
11 Papachristou EK, Roumeliotis TI, Chrysagi A, Trigoni C, Charvalos E, Townsend PA *et al.* The shotgun proteomic study of the human ThinPrep cervical smear using iTRAQ mass-tagging and 2D LC-FT-Orbitrap-MS: the detection of the human papillomavirus at the protein level. *J Proteome Res* 2013; **12**: 2078–2089.
12 Hanley CJ, Noble F, Ward M, Bullock M, Drifka C, Mellone M *et al.* A subset of myofibroblastic cancer-associated fibroblasts regulate collagen fiber elongation, which is prognostic in multiple cancers. *Oncotarget* 2016; **7**: 6159–6174.
13 Manousopoulou A, Woo J, Woelk CH, Johnston HE, Singhania A, Hawkes C *et al.* Are you also what your mother eats? Distinct proteomic portrait as a result of maternal high-fat diet in the cerebral cortex of the adult mouse. *Int J Obes (Lond)* 2015; **39**: 1325–1328.
14 Omenn GS, Lane L, Lundberg EK, Beavis RC, Nesvizhskii AI, Deutsch EW. Metrics for the Human Proteome Project 2015: progress on the human proteome and guidelines for high-confidence proteins identification. *J Proteome Res* 2015; **14**: 3452–3460.
15 Paternain L, Batlle MA, De la Garza AL, Milagro FI, Martínez JA, Campión J. Transcriptomic and epigenetic changes in the hypothalamus are involved in an increased susceptibility to a high-fat-sucrose diet in prenatally stressed female rats. *Neuroendocrinology* 2012; **96**: 249–260.
16 Jovanovic Z, Tung YC, Lam BY, O'Rahilly S, Yeo GS. Identification of the global transcriptomic response of the hypothalamic arcuate nucleus to fasting and leptin. *J Neuroendocrinol* 2010; **22**: 915–925.
17 Kälin S, Heppner FL, Bechmann I, Prinz M, Tschöp MH, Yi CX. Hypothalamic innate immune reaction in obesity. *Nat Rev Endocrinol* 2015; **11**: 339–351.
18 Larson SJ, Collins SM, Weingarten HP. Dissociation of temperature changes and anorexia after experimental colitis and LPS administration in rats. *Am J Physiol* 1996; **271**: R967–R972.
19 Okin D, Medzhitov R. Evolution of inflammatory diseases. *Curr Biol* 2012; **22**: R733–R740.
20 de Git KC, Adan RA. Leptin resistance in diet-induced obesity: the role of hypothalamic inflammation. *Obes Rev* 2015; **16**: 207–224.
21 Zhang X, Zhang G, Zhang H, Karin M, Bai H, Cai D. Hypothalamic IKKβ/NF-κB and ER stress link overnutrition to energy imbalance and obesity. *Cell* 2008; **135**: 61–73.
22 Bi S, Kim YJ, Zheng F. Dorsomedial hypothalamic NPY and energy balance control. *Neuropeptides* 2012; **46**: 309–314.
23 Clark JT, Kalra PS, Crowley WR, Kalra SP. Neuropeptide Y and human pancreatic polypeptide stimulate feeding behavior in rats. *Endocrinology* 1984; **115**: 427–429.
24 Zarjevski N, Cusin I, Vettor R, Rohner-Jeanrenaud F, Jeanrenaud B. Chronic intracerebroventricular neuropeptide-Y administration to normal rats mimics hormonal and metabolic changes of obesity. *Endocrinology* 1993; **133**: 1753–1758.
25 Bi S, Ladenheim EE, Schwartz GJ, Moran TH. A role for NPY overexpression in the dorsomedial hypothalamus in hyperphagia and obesity of OLETF rats. *Am J Physiol Regul Integr Comp Physiol* 2001; **281**: R254–R260.
26 Schroeder M, Zagoory-Sharon O, Shbiro L, Marco A, Hyun J, Moran TH *et al.* Development of obesity in the Otsuka Long-Evans Tokushima Fatty rat. *Am J Physiol Regul Integr Comp Physiol* 2009; **297**: R1749–R1760.
27 Yang L, Scott KA, Hyun J, Tamashiro KL, Tray N, Moran TH *et al.* Role of dorsomedial hypothalamic neuropeptide Y in modulating food intake and energy balance. *J Neurosci* 2009; **29**: 179–190.
28 Kim YJ, Bi S. Knockdown of neuropeptide Y in the dorsomedial hypothalamus reverses high-fat diet-induced obesity and impaired glucose tolerance in rats. *Am J Physiol Regul Integr Comp Physiol* 2016; **310**: R134–R142.
29 Kennett GA, Dourish CT, Curzon G. 5-HT1B agonists induce anorexia at a postsynaptic site. *Eur J Pharmacol* 1987; **141**: 429–435.
30 Bouwknecht JA, van der Gugten J, Hijzen TH, Maes RA, Hen R, Olivier B. Male and female 5-HT(1B) receptor knockout mice have higher body weights than wild-types. *Physiol Behav* 2001; **74**: 507–516.
31 Lee MD, Kennett GA, Dourish CT, Clifton PG. 5-HT1B receptors modulate components of satiety in the rat: behavioural and pharmacological analyses of the selective serotonin1B agonist CP- 94,253. *Psychopharmacology* 2002; **164**: 49–60.
32 Gold MR, Martin AR. Characteristics of inhibitory post-synaptic currents in brainstem neurons of the lamprey. *J Physiol* 1983; **342**: 85–98.
33 Karnani MM, Venner A, Jensen LT, Fugger L, Burdakov D. Direct and indirect control of orexin/hypocretin neurons by glycine receptors. *J Physiol* 2011; **589**: 639–651.

Supplementary Information accompanies this paper on the Nutrition & Diabetes website (http://www.nature.com/nutd)

1.8 Commentary on second publication

The main finding of the second publication is that a vicious circle of increased appetite signals is observed in the hypothalamus of mice with obesity, partly attributed to chronic inflammation. We also identified proteins that are differentially expressed in obesity vs. control and can be further examined as potential therapeutic targets for obesity. We selected some of the identified differentially expressed proteins for further validation based on bibliographic evidence of their association with appetite regulation. Furthermore, we requested that these proteins are localized in the extracellular compartment or membrane in order for them to be more suitable as therapeutic targets. Glycine-receptor subunit α-4 can be further examined as a potential therapeutic target for the reduction of appetite signals in obesity.

The standard operating procedure used to isolate the hypothalamus is presented in **Appendix E**. Similarly to the first publication, we only analysed male mice in order to reduce sex-dependent variability. It would be interesting to perform the study in female mice in order to compare with the results of the present study and identify potential sex-specific effects of obesity on the proteomic profile of the hypothalamus.

One study limitation is that the entire hypothalamus was subjected to proteomic analysis, as opposed to a more specific region or nucleus of relevance to appetite regulation, e.g. arcuate nucleus. Furthermore, samples were pooled, a limitation that was also discussed within the context of the first publication.

1.9 Alzheimer's disease

In parallel with my work on obesity, I also became interested in exploring the suitability of our developed proteomics methodology in examining other types of chronic disease, such as Alzheimer's disease. I became interested in Alzheimer's disease mainly because there are currently no effective treatment options to reverse or at least delay the progression of this disease.

Dementia is a clinical term used to describe a decline in memory and cognitive ability that is severe enough to compromise an individual's ability to perform daily activities. Dementia is a relatively common disease of older age and an important public health burden.

Alzheimer's disease (AD) is the most prevalent form of dementia, since two-thirds of dementia cases in people aged 65 years and over are classified as AD.[90] According to the World Alzheimer Report 2015, approximately 47 million people worldwide live with dementia, and this prevalence is projected to increase to 75 million by 2030 and 132 million people by 2050.[72]

The annual healthcare cost of AD in the US is approximately $ 172 billion.[91] In the UK, the combined direct and indirect cost of dementia to the UK society is estimated to be £26 billion.[92]

AD is characterized by neurodegeneration that leads to progressive impairment of cognitive functions, including comprehension, language, memory, attention, judgement, and reasoning.[93] AD is invariably progressive and patients eventually develop severe cognitive decline. Currently, there is no treatment for AD and the need arises for the discovery of novel therapeutic targets. The aim of the third publication was to examine the hemisphere-specific global proteome changes following pharmacologic treatment in a transgenic mouse model of Alzheimer's disease.

1.10 Third publication

Journal of Alzheimer's Disease 51 (2016) 333–338
DOI 10.3233/JAD-151078
IOS Press

Short Communication

Hemisphere Asymmetry of Response to Pharmacologic Treatment in an Alzheimer's Disease Mouse Model

Antigoni Manousopoulou[a,b], Satoshi Saito[c], Yumi Yamamoto[c], Nasser M. Al-Daghri[d,e], Masafumi Ihara[f], Roxana O. Carare[b,1] and Spiros D. Garbis[a,b,g,1,*]
[a]*Institute for Life Sciences, University of Southampton, UK*
[b]*Clinical and Experimental Sciences, Faculty of Medicine, University of Southampton, UK*
[c]*Department of Regenerative Medicine and Tissue Engineering, National Cerebral and Cardiovascular Center, Japan*
[d]*Biomarkers Research Program, Department of Biochemistry College of Science, King Saud University, KSA*
[e]*Prince Mutaib Chair for Biomarkers of Osteoporosis, Department of Biochemistry King Saud University, KSA*
[f]*Department of Neurology, National Cerebral and Cardiovascular Center, Japan*
[g]*Cancer Sciences, Faculty of Medicine, University of Southampton, UK*

Accepted 7 December 2015

Abstract. The aim of this study was to examine hemisphere asymmetry of response to pharmacologic treatment in an Alzheimer's disease mouse model using cilostazol as a chemical stimulus. Eight-month-old mice were assigned to vehicle or cilostazol treatment for three months and hemispheres were analyzed using quantitative proteomics. Bioinformatics interpretation showed that following treatment, aggregation of blood platelets significantly decreased in the right hemisphere whereas neurodegeneration significantly decreased and synaptic transmission increased in the left hemisphere only. Our study provides novel evidence on cerebral laterality of pharmacologic activity, with important implications in deciphering regional pharmacodynamic effects of existing drugs thus uncovering novel hemisphere-specific therapeutic targets.

Keywords: Alzheimer's disease, cilostazol, hemisphere asymmetry, mass spectrometry pharmacology, pharmacodynamics, pharmacoproteomics

INTRODUCTION

Structural asymmetry in the human brain was first described by Broca in the 19th century [1]. Brain asymmetries have also been described in other mammals, including mice [2]. The asymmetry between cerebral hemispheres encompasses functional and neurochemical aspects [3]. Data from gene expression studies in humans demonstrated lateralization of gene transcription involved in synaptic transmission and neuronal electrophysiology [4].

Cerebral laterality has been implicated in the pathophysiology of Alzheimer's disease [5]. However, whether therapeutic agents used for Alzheimer's disease exert hemisphere-specific pharmacologic effects has yet to be elucidated.

Pharmacoproteomics, as a subdiscipline of proteomics, examines how a pharmacologic agent

[1]ROC and SDG jointly led the study and are co-corresponding senior authors.

*Correspondence to: Spiros D. Garbis, PhD, Cancer Sciences and CES Units, Faculty of Medicine, University of Southampton, Southampton, UK. Tel.: +44 2380 48 20 02; Fax: +44 2381 20 51 52; E-mail: S.D.Garbis@soton.ac.uk.

perturbs a system of proteins that map to canonical or novel biological pathways. Such a discourse provides a more unbiased and holistic approach to understanding pharmacologic on-target or off-target effects at the protein level [6–9].

We have shown that treatment with cilostazol, a cyclic nucleotide phosphodiesterase III inhibitor, prevented cognitive decline as a result of amyloid-β (Aβ) deposition in the brain of Tg-SwDI mice [10]. Our hypothesis was that pharmacologic treatment of Alzheimer's disease exerts hemisphere asymmetry.

MATERIALS AND METHODS

Transgenic mouse model

To ensure reproducibility of the pharmacologic treatment and subsequent proteomic analysis the experiment was performed in duplicate. For experiments A and B, male, eight-month-old, homozygous Tg-SwDI mice ($n = 6$ per experiment, $n = 12$ in total) on a pure C57BL/6 background were obtained from Jackson Laboratories. These mice express low levels of human Swedish/Dutch/Iowa mutant AβPP in neurons under the control of the mouse Thy1.2 promoter. Mice were randomly assigned to two groups and fed with pelleted chow containing 0.3% cilostazol ($n = 3$ per experiment, $n = 6$ in total) or standard pelleted chow only ($n = 3$ per experiment, $n = 6$ in total) for 3 months. Cilostazol was supplied by Otsuka Pharmaceutical Co. Ltd.

A previous study reported that in rats treated with 0.1% cilostazol, the plasma cilostazol concentration was approximately 1 μM [11]. Based on the *in vitro* IC_{50} value, this concentration is estimated to sufficiently inhibit phosphodiesterase III activity [12]. Additionally, studies have shown that treatment with 0.1-0.3% cilostazol in rats positively affected vascular function [12, 13]. Based on this evidence, a 0.3% cilostazol treatment was used in the present study.

Mice were perfused intracardially with phosphate buffer saline, cerebral hemispheres removed and snap frozen in liquid nitrogen. All experimental procedures were approved by the Institutional Animal Care and Use Committee at the National Cerebral and Cardiovascular Center, Japan.

Proteomic analysis

For experiments A and B, respectively, cerebral hemispheres were suspended in dissolution buffer (0.5 M triethylammonium bicarbonate, 0.05% sodium dodecyl sulfate) and homogenized using the FastPrep system (Savant Bio, Cedex, Fr) followed by pulsed probe sonication (Misonix, Farmingdale, NY, USA). Lysates were subjected to centrifugation (16,000 g, 10 min, 4°C) and supernatants measured for protein content using the Direct Detect™ system (Merck Millipore, Darmstadt, Germany). For experiments A and B separately, protein extracts were pooled from each hemisphere of the three vehicle treated mice (33.3 μg from each lysate giving 100 μg final protein content). Left and right hemispheres of cilostazol treated mice were individually analyzed (100 μg from each lysate). All samples were subjected to reduction, alkylation, trypsin proteolysis, eight-plex iTRAQ labeling and two-dimensional liquid chromatography, tandem mass spectrometry analysis as described previously [8, 14, 15] (Fig. 1A).

Unprocessed raw files were submitted to Proteome Discoverer 1.4 for target decoy searching with SequestHT [8, 14]. Quantification ratios were median-normalized and $\log_2$ transformed. After treatment, a protein was considered differentially expressed in the left compared to the right hemisphere relative to its respective control when its two-group *T*-Test *p-value* across both experiments was equal to or below 0.05.

Principal component analysis (using the iTRAQ ratios of all analyzed proteins for experiments A and B) was performed using BioConductor-R (version 2.15.1) and g-plots in R (version 3.1.2). Heatmap construction of differentially expressed proteins between the two hemispheres was generated using Gene Cluster (version 3.0) and Java Treeview (version 1.1.6r4). Ingenuity Pathway Analysis (Qiagen, Venlo, Netherlands) was applied to identify canonical pathways and biological processes enriched in the differentially expressed proteins between right and left cerebral hemispheres. An lactivation z-score$| \geq 2.0$ and a *p-value* ≤ 0.05 were considered significant.

RESULTS

A total of 9,116 proteins were quantitatively analyzed in experiment A ($p < 0.05$) and another 7,418 proteins in experiment B ($p < 0.05$), of which 6,137 were reproducibly profiled in both experiments. The average coefficient variation (CV) for the iTRAQ ratios of all proteins profiled across biological replicates was determined to be 24% and 23% for the right and left hemispheres, respectively, of cilostazol treated mice compared to control in experiment A

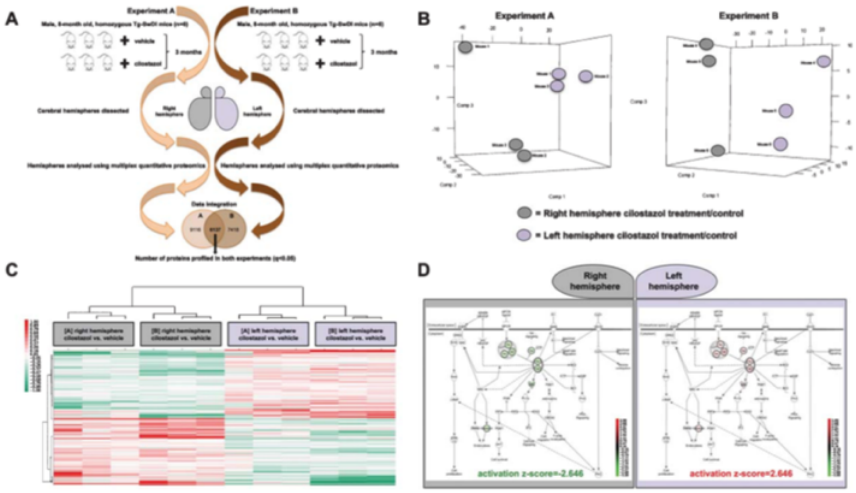

Fig. 1. A) Experimental workflow. B) Principal component analysis for each experiment showed separate clustering for the right and left hemispheres of cilostazol treated mice compared to controls suggesting hemisphere asymmetry of pharmacologic response to cilostazol treatment. C) Hierarchical clustering analysis of differentially expressed proteins between the right and left hemispheres in both experiments visualized in heatmap format. D) Canonical pathway analysis of differentially expressed proteins between right and left hemisphere following cilostazol treatment showed that the G beta-gamma (Gβγ) signaling pathway significantly decreased in the right ($p = 1.16E-2$; activation z-score = –2.646) whereas it significantly increased in the left hemisphere of cilostazol treated mice ($p = 1.16E-2$; activation z-score = 2.646).

and 15% and 16% for the right and left hemispheres, respectively, of cilostazol treated mice compared to control in experiment B. Analogous CV values between biological replicates were reported by the authors using similar proteomic methodologies [14, 15]. Principal component analysis of the reporter ion ratios of proteins profiled in each experiment showed that the right hemispheres clustered separately from the left hemispheres of cilostazol treated mice (Fig. 1B). Following treatment with cilostazol, 765 proteins were differentially expressed between the right and left cerebral hemispheres across both proteomic experiments ($p \leq 0.05$) (Fig. 1C) (Supplementary Table 1).

Bioinformatics interpretation of proteomic results

Ingenuity Pathway Analysis (IPA) using the average reporter ion ratios across both experiments of differentially expressed proteins between right and left hemisphere following cilostazol treatment showed that the G beta-gamma (Gβγ) signaling pathway significantly decreased in the right hemisphere of cilostazol treated mice ($p = 1.16E-2$; activation z-score = –2.646) whereas it significantly increased in the left hemisphere of cilostazol treated mice ($p = 1.16E-2$; activation z-score = 2.646) (Fig. 1D).

IPA also showed that aggregation of blood platelets significantly decreased in the right hemisphere only of cilostazol treated mice ($p = 3.98E-3$; activation z-score = –2.231) (Fig. 2A) whereas neurodegeneration significantly decreased ($p = 7.7E-6$; activation z-score = –2.071) (Fig. 2B) and synaptic transmission significantly increased ($p = 8.62E-6$; activation z-score = 2.028) (Fig. 2C) specifically in the left hemisphere of cilostazol treated mice.

DISCUSSION

This study provided novel protein level evidence on the hemisphere-specific pharmacologic effects of cilostazol, a drug that has been reported to ameliorate the symptoms of Alzheimer's disease [16]. This observation may have important implications for an ongoing clinical trial assessing the efficacy of cilostazol in mild cognitive impairment (COMCID

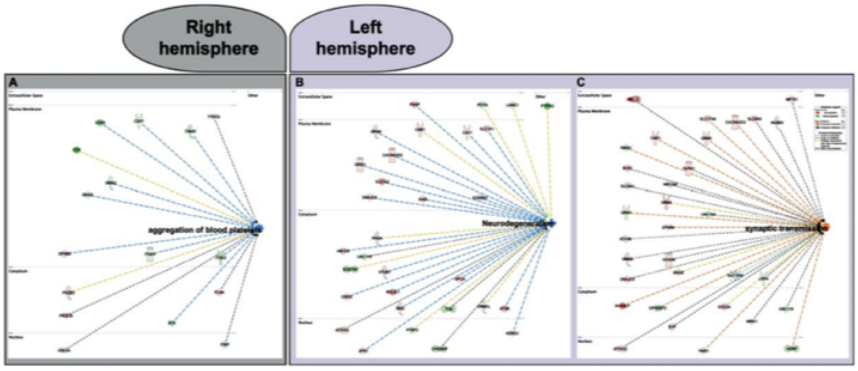

Fig. 2. Bioinformatics interpretation of the results showed that (A) aggregation of blood platelets significantly decreased in the right hemisphere ($p = 3.98E\text{-}3$; activation z-score=–2.231) whereas (B) neurodegeneration significantly decreased ($p = 7.7E\text{-}6$; activation z-score = –2.071) and (C) synaptic transmission significantly increased ($p = 8.62E\text{-}6$; activation z-score = 2.028) in the left hemisphere of cilostazol treated mice.

trial, ClinicalTrials.gov identifier: NCT02491268) but may also be extended to other pharmacologic agents.

There are only few studies examining cerebral laterality in the pathophysiology of Alzheimer's disease. Douaud et al. [17] suggested that neurodegenerative pathology may develop asymmetrically in humans, with left hemisphere atrophy being an important predictor of progression from mild cognitive impairment to Alzheimer's disease. Singh et al. [5] have found that atrophy of the cerebral cortex occurred earlier and progressed faster in the left compared to the right hemisphere in patients with Alzheimer's disease. Their findings confirmed previous observations by Chetelat et al. [18] on left lateralization of temporal changes occurring during mild cognitive impairment to Alzheimer's disease transition. Thompson et al. [19] examined the dynamics of grey matter loss in Alzheimer's disease and concluded that shifting deficits were asymmetric and predominantly occurring in the left compared to the right hemisphere.

Our results showed that cilostazol asymmetrically affected the two hemispheres of a transgenic Alzheimer's disease mouse model. In the right hemisphere, aggregation of blood platelets was found to significantly decrease following cilostazol treatment (Fig. 2A). Cerebral amyloid angiopathy (CAA), characterized by the deposition of amyloid-beta in the walls of cerebral arteries plays an important role in the pathogenesis of Alzheimer's disease. Recent evidence suggests that platelet activation may also contribute to the development of CAA [20, 21]. Targeting blood platelets has been examined as a new venue for the treatment of Alzheimer's disease and cilostazol is a well-established antiplatelet agent currently used for the secondary prevention of cerebral infarction [22, 23].

In the left hemisphere, cilostazol decreased neurodegeneration (Fig. 2B) and increased synaptic transmission (Fig. 2C), both suggestive of an improvement to the neurodegenerative phenotype. Furthermore, Gβγ signaling was asymmetrically increased in the left and decreased in the right cerebral hemisphere following cilostazol treatment (Fig. 1D). G-protein coupled receptors are highly diverse membrane proteins that participate in the transduction of external signals to various subcellular compartments via trimetric G-proteins. G-protein signaling in the central nervous system has been implicated in nuclear gene expression and cytoskeletal reorganization, processes that significantly contribute to synaptic plasticity and memory [24]. To further investigate whether these processes were on- or off-target effects of cilostazol was beyond the scope of the present proof-of-concept study.

In conclusion, our pharmacoproteomic study provides novel endophenotypic evidence on the hemisphere-specific pharmacologic effects of cilostazol. Future studies should account for hemisphere laterality with important implications in deciphering regional pharmacodynamic effects of

existing drugs thus uncovering new hemisphere-specific therapeutic targets.

Some limitations of the present study include the non-validated proteomic findings using an alternative technique (e.g., immunohistochemistry). Furthermore, sub-regions of the cerebral hemispheres (e.g., hippocampus, cortex, cerebellum) were not studied separately to identify regional asymmetric patterns of pharmacologic response to treatment. These constitute objectives in future studies.

ACKNOWLEDGMENTS

We are indebted to Mr. Roger Allsopp, Mr. Derek Coates, and Hope for Guernsey for their fund raising and vision in establishing a clinical mass spectrometry laboratory at the University of Southampton. This study was funded by the BBSRC, Rosetrees Trust and the Wessex Cancer Trust and Medical Research, UK. The authors are grateful to the support of King Saud University, Deanship of Scientific Research Chair, Prince Mutaib Bin Abdullah Chair for Biomarkers of Osteoporosis, College of Science, as well as the Visiting Professor Program of King Saud University, Riyadh, Saudi Arabia.

Authors' disclosures available online (http://j-alz.com/manuscript-disclosures/15-1078).

SUPPLEMENTARY MATERIAL

The supplementary material is available in the electronic version of this article: http://dx.doi.org/10.3233/JAD-151078.

REFERENCES

[1] Broca MP (1861) Remarques sur le siège de la faculté du langage articulé, suivies d'une observation d'aphémie (perte de la parole). *Bull Soc Anatomique* **6**, 330-357.

[2] Sun T, Walsh CA (2006) Molecular approaches to brain asymmetry and handedness. *Nat Rev Neurosci* **7**, 655-662.

[3] Toga AW, Thompson PM (2003) Mapping brain asymmetry. *Nat Rev Neurosci* **4**, 37-48.

[4] Karlebach G, Francks C (2015) Lateralization of gene expression in human language cortex. *Cortex* **67**, 30-36.

[5] Singh V, Chertkow H, Lerch JP, Evans AC, Dorr AE, Kabani NJ (2006) Spatial patterns of cortical thinning in mild cognitive impairment and Alzheimer's disease. *Brain* **129**, 2885-2893.

[6] D'Alessandro A, Zolla L (2010) Pharmacoproteomics: A chess game on a protein field. *Drug Discov Today* **15**, 1015-1023.

[7] Roumeliotis TI, Halabalaki M, Alexi X, Ankrett D, Giannopoulou EG, Skaltsounis AL, Sayan BS, Alexis MN, Townsend PA, Garbis SD (2013) Pharmacoproteomic study of the natural product Ebenfuran III in DU-145 prostate cancer cells: The quantitative and temporal interrogation of chemically induced cell death at the protein level. *J Proteome Res* **12**, 1591-1603.

[8] White CH, Johnston HE, Moesker B, Manousopoulou A, Margolis DM, Richman DD, Spina CA, Garbis SD, Woelk CH, Beliakova-Bethell N (2015) Mixed effects of suberoylanilide hydroxamic acid (SAHA) on the host transcriptome and proteome and their implications for HIV reactivation from latency. *Antiviral Res* **123**, 78-85.

[9] Delehouzé C, Godl K, Loaëc N, Bruyère C, Desban N, Oumata N, Galons H, Roumeliotis TI, Giannopoulou EG, Grenet J, Twitchell D, Lahti J, Mouchet N, Galibert MD, Garbis SD, Meijer L (2014) CDK/CK1 inhibitors roscovitine and CR8 downregulate amplified MYCN in neuroblastoma cells. *Oncogene* **33**, 5675-5687.

[10] Maki T, Okamoto Y, Carare RO, Hase Y, Hattori Y, Hawkes CA, Saito S, Yamamoto Y, Terasaki Y, Ishibashi-Ueda H, Taguchi A, Takahashi R, Miyakawa, Kalaria RN, Lo EH, Arai K, Ihara M (2014) Phosphodiesterase III inhibitor promotes drainage of cerebrovascular β-amyloid. *Ann Clin Transl Neurol* **1**, 519-533.

[11] Miyamoto N, Tanaka R, Shimura H, Watanabe T, Mori H, Onodera M, Mochizuki H, Hattori N, Urabe T (2010) Phosphodiesterase III inhibition promotes differentiation and survival of oligodendrocyte progenitors and enhances regeneration of ischemic white matter lesions in the adult mammalian brain. *J Cereb Blood Flow Metab* **30**, 299-310.

[12] Oyama N, Yagita Y, Kawamura M, Sugiyama Y, Terasaki Y, Omura-Matsuoka E, Sasaki T, Kitagawa K (2011) Cilostazol, not aspirin, reduces ischemic brain injury via endothelial protection in spontaneously hypertensive rats. *Stroke* **42**, 2571-2577.

[13] Fujita Y, Lin JX, Takahashi R, Tomimoto H (2008) Cilostazol alleviates cerebral small-vessel pathology and white-matter lesions in stroke-prone spontaneously hypertensive rats. *Brain Res* **1203**, 170-176.

[14] Manousopoulou A, Woo J, Woelk CH, Johnston HE, Singhania A, Hawkes C, Garbis SD, Carare RO (2015) Are you also what your mother eats? Distinct proteomic portrait as a result of maternal high-fat diet in the cerebral cortex of the adult mouse. *Int J Obes (Lond)* **39**, 1325-1328.

[15] Papachristou EK, Roumeliotis TI, Chrysagi A, Trigoni C, Charvalos E, Townsend PA, Pavlakis K, Garbis SD (2013) The shotgun proteomic study of the human ThinPrep cervical smear using iTRAQ mass-tagging and 2D LC-FT-Orbitrap-MS: The detection of the human papillomavirus at the protein level. *J Proteome Res* **12**, 2078-2089.

[16] Ihara M, Nishino M, Taguchi A, Yamamoto Y, Hattori Y, Saito S, Takahashi Y, Tsuji M, Kasahara Y, Takata Y, Okada M (2014) Cilostazol add-on therapy in patients with mild dementia receiving donepezil: A retrospective study. *PloS One* **9**, e89516.

[17] Douaud G, Menke RA, Gass A, Monsch AU, Rao A, Whitcher B, Zamboni G, Matthews PM, Sollberger M, Smith S (2013) Brain microstructure reveals early abnormalities more than two years prior to clinical progression from mild cognitive impairment to Alzheimer's disease. *J Neurosci* **33**, 2147-2155.

[18] Chételat G, Desgranges B, De La Sayette V, Viader F, Eustache F, Baron JC (2002) Mapping gray matter loss with voxel-based morphometry in mild cognitive impairment. *Neuroreport* **13**, 1939-1943.

[19] Thompson PM, Hayashi KM, de Zubicaray G, Janke AL, Rose SE, Semple. J, Herman D, Hong MS, Dittmer SS,

Doddrell DM, Toga AW (2003) Dynamics of gray matter loss in Alzheimer's disease. *J Neurosci* **23**, 994-1005.

[20] Jarre A, Gowert NS, Donner L, Münzer P, Klier M, Borst O, Schaller M, Lang F, Korth C, Elvers M (2014) Pre-activated blood platelets and a pro-thrombotic phenotype in APP23 mice modeling Alzheimer's disease. *Cell Signal* **26**, 2040-2050.

[21] Kniewallner KM, Ehrlich D, Kiefer A, Marksteiner J, Humpel C (2015) Platelets in the Alzheimer's disease brain: Do they play a role in cerebral amyloid angiopathy? *Curr Neurovasc Res* **12**, 4-14.

[22] Shi L, Pu J, Xu L, Malaguit J, Zhang J, Chen S (2014) The efficacy and safety of cilostazol for the secondary prevention of ischemic stroke in acute and chronic phases in Asian population–an updated meta-analysis. *BMC Neurol* **14**, 251.

[23] Shinohara Y, Katayama Y, Uchiyama S, Yamaguchi T, Handa S, Matsuoka K, Ohashi Y, Tanahashi N, Yamamoto H, Genka C, Kitagawa Y, Kusuoka H, Nishimaru K, Tsushima M, Koretsune Y, Sawada T, Hamada C (2010) *CSPS 2 group*, Cilostazol for prevention of secondary stroke (CSPS 2): An aspirin-controlled, double-blind, randomised non-inferiority trial. *Lancet Neurol* **9**, 959-968, pp.

[24] El Far O, Betz H (2002) G-protein-coupled receptors for neurotransmitter amino acids: C-terminal tails, crowded signalosomes. *Biochem J* **365**, 329-336.

1.11 Commentary on third publication

The main finding of the third publication is that a systemically administered drug, cilostazol, exerts hemisphere-specific effects in an AD mouse model. The hemisphere specificity of the drug action could be possibly attributed to the hemisphere asymmetry that has been experimentally observed in the development and progression of AD.[94-96]

Another finding was that cilostazol treatment decreased Gβγ signalling activity in the right hemisphere whereas this was increased in the left hemisphere. Gβγ receptors belong to the broader G-protein coupled receptors (GPCRs) family. GPCR signalling in the brain has been implicated in cytoskeletal reorganization, a biological process that affects memory and synaptic plasticity. Cyclic nucleotide phosphodiesterases control the intracellular levels of cyclic second messengers as well as their degradation. cAMP participate as a downstream mediator of the GPCR initiated signalling cascade. Cilostazol, a cyclic phosphodiesterase 3 inhibitor that reduces the intracellular levels of cAMP, can thus affect the GPCR signalling pathway directly, by reducing the levels of the downstream cAMP mediator or indirectly through a positive or negative feedback loop between cAMP levels and GPCR activation/deactivation.[97,98]

A few study limitations include the pooling strategy used for the control mice and the small number of animals studied (n=6 control mice; n=6 Tg-SwDI mice). These results have to be validated in larger *in vivo* animal model studies.

1.12 Cerebral amyloid angiopathy (CAA)

AD is characterized by the accumulation of hyper-phosphorylated tau protein in neurons as neurofibrillary tangles and the deposition of amyloid-beta (Aβ) peptides in the brain parenchyma and the walls of cerebral arteries and capillaries as cerebral amyloid angiopathy (CAA).[99] Aβ is a 36-43 amino-acid long peptide derived from the amyloid precursor protein (APP), a transmembrane glycoprotein with an undetermined function. APP is cleaved by β- and γ- secretases to produce Aβ.[100] Aβ is a soluble peptide, but it is converted into an insoluble form and fibrils as a result of Aβ concentration levels, various tissue factors and pH.[101] In AD, soluble and insoluble forms of Aβ co-exist.

AD is diagnosed in post-mortem brains by the distribution and number of neurofibrillary alterations, including neurofibrillary tangles, neuritic amyloid plaques and neuropil threads, and by the presence of plaques comprised of insoluble Aβ.[102,103] However, studies have shown that in particular three pathological features correlate with clinical dementia: a) increased brain levels of soluble Aβ, b) distribution and number of neurofibrillary changes and c) the severity of CAA.

There are three main mechanism of Aβ elimination from the brain: 1. enzymatic degradation in the brain parenchyma by proteases, including insulin-degrading enzyme and neprilysin, 2. Absorption of Aβ-apolipoprotein complexes in the blood through low-density lipoprotein receptor (LRP)-1 and -2 that are present on the blood brain barrier and 3. Intramural periarterial drainage (IPAD) along capillary and artery walls. Certain familial forms of AD are caused by over-production of Aβ due to mutations in the APP gene. In sporadic AD, decreased elimination of Aβ, also attributed to ageing, has been identified as the main mechanism leading to Aβ accumulation in the brain. IPAD is approximately six-fold slower compared to Aβ elimination to blood via LRP, but IPAD appears to compensate when the LRP mechanism fails and when levels of neprilysin in the brain are decreased.[104]

The aim of the fourth publication was to identify novel therapeutic targets of AD, by studying the global proteomic profile of post-mortem, human leptomeningeal arteries affected with cerebral amyloid angiopathy.

1.13 Fourth publication

Neuropathology and Applied Neurobiology (2017), **43**, 492–504 doi: 10.1111/nan.12342

Systems proteomic analysis reveals that clusterin and tissue inhibitor of metalloproteinases 3 increase in leptomeningeal arteries affected by cerebral amyloid angiopathy

A. Manousopoulou*·†, M. Gatherer*, C. Smith‡, J. A. R. Nicoll*, C. H. Woelk*, M. Johnson§, R. Kalaria§, J. Attems§, S. D. Garbis*·†·¶·[1] and R. O. Carare*·[1]

**Clinical and Experimental Sciences Unit, Faculty of Medicine, †Institute for Life Sciences, University of Southampton, Southampton, ‡Pathology Department, University of Edinburgh, Edinburgh, §Institute of Neuroscience, Newcastle University, Newcastle upon Tyne, and ¶Cancer Sciences Unit, Faculty of Medicine, University of Southampton, Southampton, UK*

A. Manousopoulou, M. Gatherer, C. Smith, J. A. R. Nicoll, C. H. Woelk, M. Johnson, R. Kalaria, J. Attems, S. D. Garbis and R. O. Carare (2017) *Neuropathology and Applied Neurobiology* **43**, 492–504
Systems proteomic analysis reveals that clusterin and tissue inhibitor of metalloproteinases 3 increase in leptomeningeal arteries affected by cerebral amyloid angiopathy

Aims: Amyloid beta (Aβ) accumulation in the walls of leptomeningeal arteries as cerebral amyloid angiopathy (CAA) is a major feature of Alzheimer's disease. In this study, we used global quantitative proteomic analysis to examine the hypothesis that the leptomeningeal arteries derived from patients with CAA have a distinct endophenotypic profile compared to those from young and elderly controls. **Methods**: Freshly dissected leptomeningeal arteries from the Newcastle Brain Tissue Resource and Edinburgh Sudden Death Brain Bank from seven elderly (82.9 ± 7.5 years) females with severe capillary and arterial CAA, as well as seven elderly (88.3 ± 8.6 years) and five young (45.4 ± 3.9 years) females without CAA were used in this study. Arteries from four patients with CAA, two young and two elderly controls were individually analysed using quantitative proteomics. Key proteomic findings were then validated using immunohistochemistry. **Results**: Bioinformatics interpretation of the results showed a significant enrichment of the immune response/classical complement and extracellular matrix remodelling pathways ($P < 0.05$) in arteries affected by CAA *vs.* those from young and elderly controls. Clusterin (apolipoprotein J) and tissue inhibitor of metalloproteinases-3 (TIMP3), validated using immunohistochemistry, were shown to co-localize with Aβ and to be up-regulated in leptomeningeal arteries from CAA patients compared to young and elderly controls. **Conclusions**: Global proteomic profiling of brain leptomeningeal arteries revealed that clusterin and TIMP3 increase in leptomeningeal arteries affected by CAA. We propose that clusterin and TIMP3 could facilitate perivascular clearance and may serve as novel candidate therapeutic targets for CAA.

Keywords: clusterin, complement pathway, extracellular matrix remodelling, leptomeningeal arteries, proteomics, TIMP3

Correspondence: Roxana O. Carare, Experimental Sciences Unit, Faculty of Medicine, Southampton General Hospital, Academic Block, MP806, Clinical Neurosciences, Tremona Road, Southampton SO16 6YD UK. Tel: +447909518498. Fax: +442381 206085; E-mail: R.O.Carare@soton.ac.uk

[1]SDG and ROC jointly led the study and are co-senior authors.

Introduction

The deposition of amyloid-β (Aβ) peptides in the walls of cerebral arteries as cerebral amyloid angiopathy (CAA) is a major feature of Alzheimer's disease and may contribute to cognitive decline [1,2]. CAA

predominantly affects the leptomeningeal and cortical arteries especially in the occipital lobe, while capillaries are less frequently and veins rarely involved [3–5]. In the majority of cases there is no overproduction of Aβ in the vessel wall, suggesting that the deposition of Aβ in the walls of cerebral arteries is a result of a failure of elimination of neuronally derived Aβ [6]. Increasing age and possession of at least one apolipoprotein ε4 (APOE4) allele are risk factors for CAA and both have been suggested to impair cerebral Aβ clearance systems, thereby reducing Aβ elimination from the brain [7–10]. We have demonstrated that Aβ and other solutes are eliminated along the basement membranes of capillaries and arteries, effectively the lymphatic drainage of the brain [11]. Experimental work involving intraparenchymal injections of tracers demonstrated that the biochemical structure and morphology of the basement membranes of capillaries and arteries change with age and with possession of APOE4 genotype, resulting in failure of efficient clearance of Aβ [12–14]. The exact targets for the facilitation of perivascular clearance of Aβ are not clear.

Proteomics allows the in-depth and global assessment of gene products at the protein level as they occur in a variety of biological specimens, including cell lines, tissue, blood and proximal fluids. The advanced use of liquid chromatography combined with mass spectrometry permits the identification of thousands of proteins with ultra-high precision and sensitivity, not available by any other analytical approach. Using stable isotope isobaric reagents allow such proteomes to be profiled in parallel across multiple biological or clinical states under identical analytical conditions, a feature referred to as the multiplex advantage [15–23]. For example, such a strategy allows the comparison of a given *in vitro* or *in vivo* model under a given homeostatic state (that is physiological condition) relative to a perturbation state (that is pathological condition or exposure to a stimulus) under exactly the same experimental conditions.

This study employed isobaric quantitative proteomic analysis of fresh frozen human leptomeningeal arteries from young and elderly subjects and patients with CAA to test the hypothesis that leptomeningeal arteries derived from patients with CAA have a unique endophenotypic profile compared to those from young and elderly controls.

Materials and methods

Isolation of human leptomeningeal arteries

Human fresh frozen *post mortem* leptomeningeal arteries from the Newcastle Brain Tissue Resource and MRC Sudden Death Brain & Tissue Bank (Edinburgh) were used for this study. CAA cases were diagnosed *post mortem* by JA, according to published criteria including the neuritic Braak stages [24], Thal amyloid phases [25], CERAD scores [26], NIA-AA scores [27] and McKeith criteria [28] and showed varying degrees of Alzheimer's disease pathology. For CAA we used a recently developed staging system, which assesses meningeal and parenchymal CAA separately and also scores capillary CAA [1,2]. All CAA cases had severe CAA as they showed widespread circumferential Aβ in meningeal and cortical arterial vessels as well as Aβ depositions in capillary walls. None of the cases was diagnosed with CAA during their lifetime. The cases from the MRC Sudden Death Brain & Tissue Bank (Edinburgh) had no neurological disease during life and no significant neuropathological changes *post mortem*. We excluded cases with arteriolosclerosis/lipohyalinosis from this cohort. Samples were collected and prepared in accordance with the National Research Ethics Service-approved protocols. Leptomeningeal arteries in the occipital regions were removed from the frozen coronal slices from brains of young females (45.4 ± 3.9 years; $n = 5$), elderly females without CAA (88.3 ± 8.6 years; $n = 7$) and females with severe CAA (82.6 ± 7.5 years; $n = 7$) (Table 1). Only female subjects were included in the present study as it has been shown that sex-dependent differences exist in CAA [29–31]. The frozen coronal slices were placed at −20°C overnight to acclimatize from the −70°C storage prior to dissection in a cold cabinet at −12°C. Arteries were identified based on their morphology of a vessel and they were distinguished from veins by the thicker wall and leptomeningeal sheet as they penetrate the cortex. The abundant presence of vascular smooth muscle actin confirmed they were arteries. Selected vessels were eased with a micro-scalpel from the meningeal surface of the gyri and sulci, removed and placed in precooled tubes to avoid thawing. These specimens were then snap frozen at −80°C.

Table 1. Details of *post mortem* samples

Sample #	*Study group*	*Age (years)*	*Used in proteomic analysis*	*Braak stage*	*Thal amyloid phase*	*Post mortem delay (h)*	*Cause of death*	*Duration of dementia (years)*	*CAA inflammation/vasculitis*
1	Young control	51	Yes	0	Not applicable	81	Metastatic carcinoma	0	Not applicable
2	Young control	46	Yes	0	Not applicable	49	Myocardial infarction: coronary artery thrombosis: coronary artery atherosclerosis	0	Not applicable
3	Young control	45	No	0	Not applicable	93	Coronary artery atherosclerosis	0	Not applicable
4	Young control	40	No	0	Not applicable	77	Bronchial asthma	0	Not applicable
5	Young control	45	No	0	Not applicable	40	Suspension by ligature	0	Not applicable
6	Elderly control	79	Yes	IV	3	9	Old age, dementia with Parkinson's disease	9	Mild, some vessels with perivascular infiltrate
7	Elderly control	88	Yes	III	0	22	Aspiration pneumonia: total anterior circulation stroke	Not available	Not remarkable
8	Elderly control	74	No	III	1	53	Heart failure and lung cancer	Not available	Not remarkable
9	Elderly control	94	No	II	1	15	Left ventricle failure: ischaemic heart disease	Not available	Not remarkable
10	Elderly control	95	No	III	0	66	Ischaemic bowel disease (inoperable)	Not available	Not remarkable
11	Elderly control	96	No	II	3	114	Stroke and left ventricular failure	2 (mild)	Not remarkable
12	Elderly control	92	No	VI	5	74	Pneumonia	>2	Not remarkable
13	CAA case	93	Yes	VI	5	53	Stroke, general deterioration	13	Mild, some vessels with perivascular infiltrate
14	CAA case	73	Yes	IV	5	47	Frontal lobe dementia	1.3	Not remarkable
15	CAA case	76	Yes	VI	3	37	not applicable	8	Not remarkable
16	CAA case	87	Yes	VI	5	54	Aspiration pneumonia secondary to stroke	8	Not remarkable
17	CAA case	86	No	VI	5	47	not applicable	6	Not remarkable
18	CAA case	77	No	VI	2	63	Aspiration pneumonia	14	Not remarkable
19	CAA case	88	No	VI	5	84	Bronchopneumonia	15	Not remarkable

CAA, cerebral amyloid angiopathy.

Quantitative proteomic analysis on human leptomeningeal arteries

For the proteomic analysis, samples from two young and two elderly subjects and four patients with CAA were randomly selected from the cohort (Table 1). The justification for this number of CAA cases was to compensate for their innate tissue heterogeneity and to ensure a statistical power of over 0.7, factoring in a representative 30% measurement error and a fold change >1.5 between replicate observations, as reported in a recent simulation study [32]. Samples were dissolved in dissolution buffer (0.5 M triethylammonium bicarbonate/0.05% sodium dodecyl sulphate), homogenized using the FastPrep system (Savant Bio, Cedex, Fr) and then subjected to pulsed probe sonication (Misonix, Farmingdale, NY, USA). Lysates were centrifuged (16 000 *g*, 10 min, 4°C) and supernatants were measured for protein content using the Direct Detect™ Spectroscopy system (Merck Millipore, Darmstadt, Germany) according to the manufacturer's instructions. From each lysate volume (adjusted to the highest volume of 40 µl) containing 100 µg final protein content was subjected to reduction, alkylation, trypsin proteolysis and eight-plex isobaric tag for relative and absolute quantitation (iTRAQ AbSciex, San Hose, CA, USA) labelling per supplier's specifications (ABSciex, San Hose, CA, USA). Labelled peptides were pooled and fractionated with high-pH reversed-phase (RP) chromatography using the Waters, XBridge C8 column (150 × 3 mm, 3.5 µm particle) with the Shimadzu LC-20AD HPLC (Shimadzu, Kyoto, Japan). Each resulting fraction was LC-MS analysed with low-pH RP capillary chromatography (PepMap C18, 50 µm ID × 50 cm L, 100 Å pore, 3.5 µm particle) and nanospray ionization FT-MS (Ultimate 3000 UHPLC – LTQ-Velos Pro Orbitrap Elite, Thermo Scientific, Bremen, DE) as reported previously [19,20,23] (Figure 1**a**).

Unprocessed raw files were submitted to Proteome Discoverer 1.4 for target decoy searching with SequestHT for tryptic peptides as reported by the authors [19,20,23]. Quantification ratios were normalized on the median value and log2 transformed. A protein was considered modulated in leptomeningeal arteries from elderly subjects *vs.* young controls or those affected by CAA type 1 relative to these from young and elderly controls when its log2 ratio was above or below ±1 SD across all analysed samples per category as reported previously [23].

Hierarchical clustering analysis visualized in heatmap format was generated using Gene Cluster (version 3.0) and Java Treeview (version 1.1.6r4). MetaCore (GeneGo, St. Joseph, MI, USA) and DAVID (http://david.abcc.ncifcrf.gov) were applied to identify prebuilt processed networks and gene ontology terms over-represented in the modulated proteome. False discovery rate (FDR) and Fisher's exact corrected *P*-values ≤0.05 were considered significant.

Immunohistochemistry

The immunochemistry validation of key proteomic findings was performed in all 19 subjects (young female controls: $n = 5$, elderly female controls: $n = 7$, females with CAA type 1: $n = 7$). Three sections of occipital cortex from each of the cases were immunostained. After dewaxing in xylene and rehydration through graded alcohols, antigen retrieval was performed by immersing slides in citrate buffer, microwaving on medium power for 25 min and subsequently cooling. This was followed by incubation in pepsin for 5 min (1 mg/ml 0.2 M HCl). The tissue was blocked in 3% H_2O_2 and 15% goat serum. Occipital cortex from each of the cases was incubated in clusterin (Abcam: Cambridge, UK, ab42673, rabbit polyclonal, dilution 1:500), or tissue inhibitor of metalloproteinases 3 (TIMP3) (Abcam, Ab93637, rabbit polyclonal, dilution 1:100) overnight at 4°C followed by biotinylated goat anti-rabbit antibodies (Vector BA1000 dilution 1:200) and ABC peroxidase enzyme complex (Vector PK4000, dilution 1:500). Reaction was detected using diaminobenzidine with glucose oxidase enhancement. Images were captured an Olympus: Southend-on-Sea, Essex, UK, BX51 microscope fitted with Olympus CC-12 colour microscope camera.

Double immunofluorescence was performed for Aβ and TIMP3. Prior to the antigen retrieval previously described, pre-treatment was required which consisted of 5 min in formic acid at 37°C. Tissue was blocked in 15% goat serum followed by incubation in primary antibodies overnight at 4°C. Aβ was detected using mouse monoclonal anti-Aβ IgG2b Clone 4G8, antibody (BioLegend: London, UK, 800701; dilution 1:100). The secondary antibody for Aβ was goat anti-mouse IgG2b, AlexaFluor 647 (A-21242), and for TIMP 3 and clusterin was goat anti-rabbit IgG AlexaFluor 594 (A-27096). These were obtained from Thermo Fisher Scientific and dilution 1:200. Images were captured and

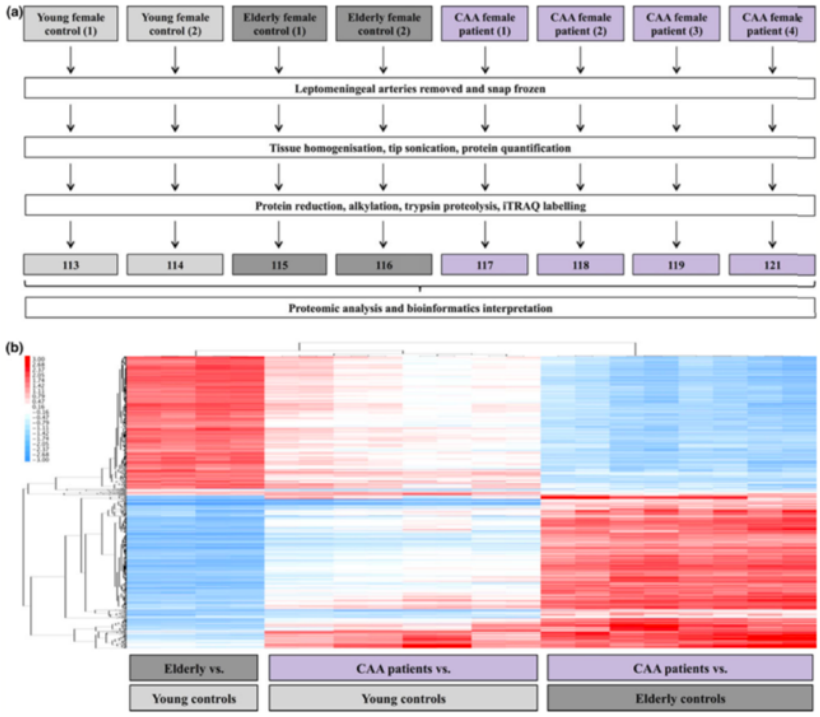

Figure 1. (a) Experimental pipeline of proteomics experiment. (b) Heatmap of differentially expressed proteins in leptomeningeal arteries of elderly controls compared to young controls, cerebral amyloid angiopathy (CAA) patients compared to young controls and CAA patients compared to elderly controls.

examined with a Leica SP8 confocal microscope. The specificity of the immunohistochemistry staining was confirmed by omitting the primary antibody.

Results

Quantitative proteomic analysis

The proteomic analysis resulted in the profiling of 5957 proteins (peptide FDR confidence ≥ 99%) (Table S1). A total of 1364 proteins were differentially expressed in arteries from elderly relative to young subjects (Table S2), 280 in arteries from CAA cases relative to young controls (Table S3) and another 983 in arteries from CAA cases relative to elderly controls (Table S4). The hierarchical clustering analysis of differentially expressed proteins between groups revealed that leptomeningeal arteries derived from CAA patients compared to those from young and elderly controls had a distinct proteomic profile from arteries derived from elderly compared to young subjects (Figure 1b).

In silico bioinformatics analysis showed that the *immune response/classical complement pathway* (P = 5.0E-11; 5.007E-2; 1.168E-10 in elderly *vs.* young controls;

CAA *vs.* young controls; CAA *vs.* elderly controls respectively) (Figure 2) and *extracellular matrix remodelling* (P = 3.3E-8; 6.349E-6; 2.317E-8 in elderly *vs.* young controls; CAA *vs.* young controls; CAA *vs.* elderly controls respectively) (Figure 3) were significantly over-represented processes. For both pathways, the expression levels of most proteins were found to decrease in arteries from elderly *vs.* young controls, whereas they increased in arteries from CAA patients compared to young and elderly controls.

The expression of clusterin (apolipoprotein J) and TIMP3 from the immune response/classical complement and the extracellular matrix remodelling pathways, respectively, were up-regulated in arteries from patients with CAA compared to both young and elderly controls [clusterin: iTRAQ mean log2 ratio (SD) = 2.30 (0.45) and 2.87 (0.44) in CAA *vs.* young and CAA *vs.* elderly controls respectively] [TIMP3: iTRAQ mean log2 ratio (SD) = 1.63 (0.89) and 2.48 (0.90) in CAA *vs.* young and CAA *vs.* elderly controls respectively].

Immunohistochemistry

Clusterin was found to co-localize with Aβ in the occipital cortex of CAA cases, but not in the young or elderly controls (Figure 4). The pattern of expression for the immunocytochemistry of TIMP3 was weak in arteries from young controls, increased in elderly controls and was strong in CAA patients (Figure 5). TIMP3 and clusterin were found to co-localize with Aβ in the leptomeningeal vessels of the occipital cortex from CAA cases (Figure 6).

Discussion

Our study showed that the global endophenotypic profile of leptomeningeal arteries from elderly female patients with severe CAA was different from that of age-matched and young controls. The immune response/classical complement and extracellular matrix remodelling pathways were significantly enriched in the differentially expressed proteome of arteries between patients with CAA compared to young and elderly controls. Most proteins participating in these pathways were up-regulated in leptomeningeal arteries from patients with CAA compared to these from controls, possibly reflecting a pro-inflammatory response in arteries affected by CAA, which could have in turn triggered tissue remodelling processes. The inflammatory profile of CAA is well characterized [33,34] and previous studies have described an increased activation of the complement system in cerebral amyloid plaques as well as deposition of complement components in CAA affected cerebral arteries [35–37]. Extracellular matrix components can influence the deposition of Aβ thus contributing to Alzheimer's disease progression [38,39]. Conversely, Aβ accumulation damages the

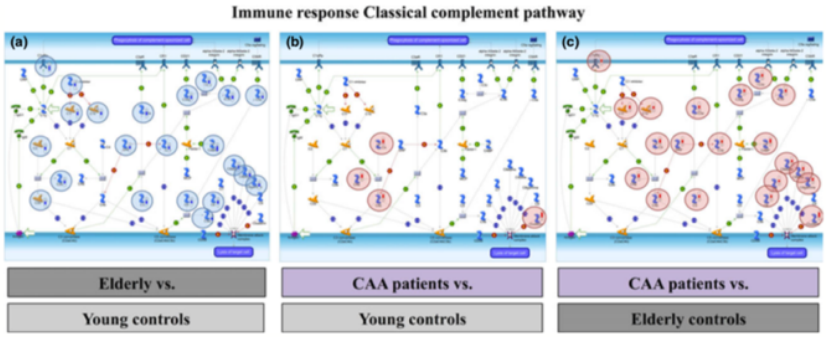

Figure 2. The immune response/classical complement pathway was significantly enriched in the differentially expressed proteome of leptomeningeal arteries from elderly *vs.* young controls (P = 5.0E-11) (**a**), CAA patients compared to young controls (P = 5.007E-2) (**b**) and cerebral amyloid angiopathy patients compared to elderly controls (P = 1.168E-10) (**c**).

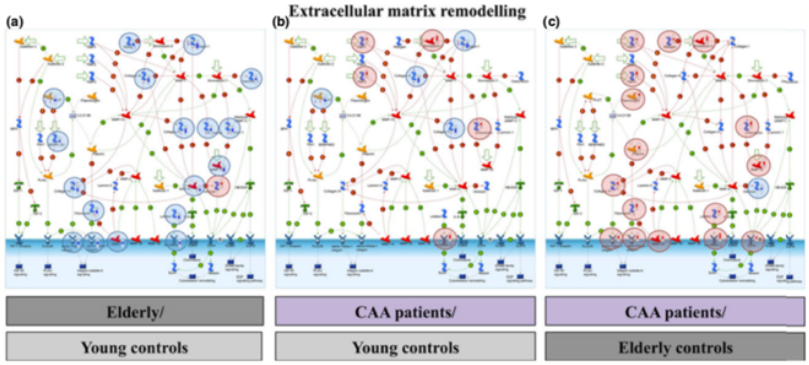

Figure 3. The extracellular matrix remodelling pathway was significantly enriched in the differentially expressed proteome of leptomeningeal arteries from elderly compared to young controls (P = 3.3E-8) (**a**), cerebral amyloid angiopathy (CAA) patients compared to young controls (P = 6.349E-6) (**b**) and CAA patients compared to elderly controls (P = 2.317E-8) (**c**).

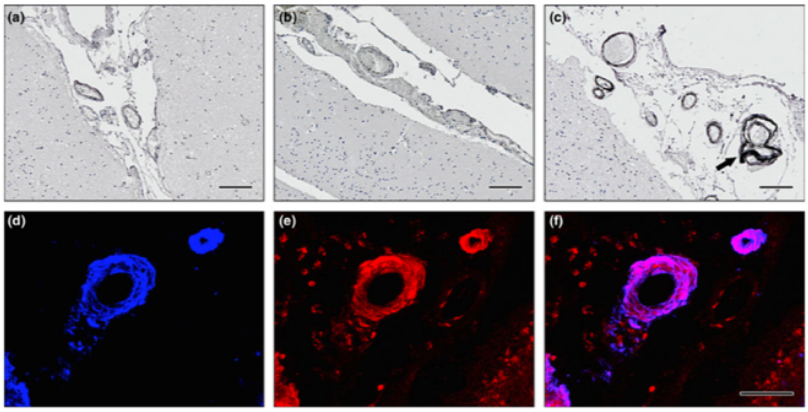

Figure 4. Immunohistochemistry of clusterin. DAB with haematoxylin counterstain in (**a**) young and (**b**) elderly controls and (**c**) cerebral amyloid angiopathy (CAA). The intensity of immunostaining of clusterin is increased in the leptomeningeal vessels present in the sulci in elderly control cases compared to young cases and in CAA compared to elderly control cases. Immunofluorescence for Aβ and clusterin in leptomeningeal arteries in CAA (**d**–**e**). Aβ immunofluorescence (blue) in (**d**) is present in the whole thickness of the arterial wall in a concentric manner; clusterin immunofluorescence (red) in (**e**) is also present throughout the thickness of the arterial wall; co-localization (pink) of Aβ and clusterin occupies most of the thickness of the arterial walls in (**f**). Scale bars: (**a**–**c**) = 100 μm/(**d**–**f**) = 50 μm.

integrity of existing extracellular matrix, which affects brain microvascular functions during the early stages of Alzheimer's disease [40–42].

The study results show that clusterin co-localizes with Aβ within the walls of leptomeningeal arteries and its expression levels increase in leptomeningeal

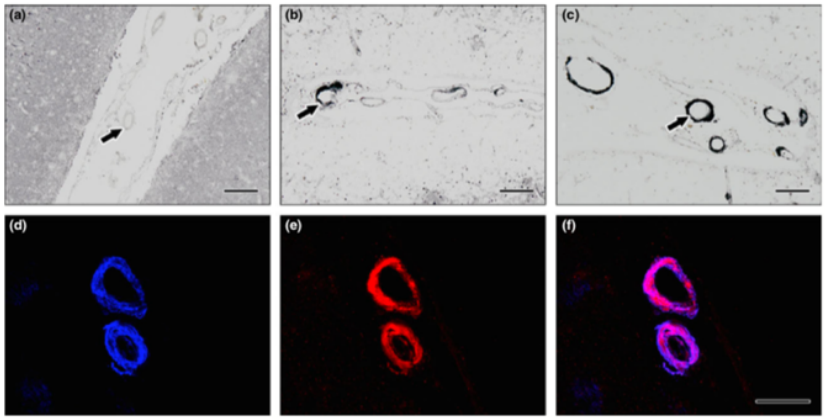

Figure 5. Immunohistochemistry of tissue inhibitor of metalloproteinases 3 (TIMP3) in leptomeningeal arteries. DAB with haematoxylin counterstain in (**a**) young and (**b**) elderly controls and (**c**) cerebral amyloid angiopathy (CAA). The intensity of immunostaining of TIMP3 is increased in the leptomeningeal vessels present in the sulci of elderly control cases compared to young and in CAA cases compared to elderly. Immunofluorescence for Aβ and TIMP3 in leptomeningeal arteries in CAA (**d**–**e**). Aβ immunofluorescence (blue) in (**d**) is present in the whole thickness of the arterial wall in a concentric manner; TIMP3 immunofluorescence (red) in (**e**) is also present throughout the thickness of the arterial wall; co-localization (pink) of Aβ and TIMP3 occupies most of the thickness of the arterial walls, especially concentrated in the tunica media, with less in the endothelium and outer layers of the wall (**f**). Scale bars: (**a**–**c**) = 100 μm/(**d**–**f**) = 50 μm.

arteries from patients with CAA compared to those from young and elderly controls. Clusterin (apolipoprotein J or ApoJ) is a disulphide-linked heterodimeric glycoprotein that activates microglia, initiating an inflammatory cascade [43]. Genome-wide association studies of sporadic Alzheimer's disease, in which Aβ accumulates both in cortical plaques and CAA, have highlighted the importance of common genetic variations in the gene encoding clusterin [44]. Experimental work suggests that clusterin regulates Aβ fibril formation [45] and plays a major role in the clearance of Aβ42–ApoJ complexes, via LRP2 [46–48]. Although the predominant species of Aβ in CAA is Aβ40, with progressive failure of perivascular clearance of interstitial fluid, there is also accumulation of Aβ42 [49]. Clusterin appears to be sequestered with Aβ species in the vascular amyloid deposits in sporadic CAA, as well as in the white matter abnormalities in cerebral autosomal dominant arteriopathy with subcortical infarcts and leukoencephalopathy (CADASIL) [50,51]. A recent study found a significant positive correlation between clusterin concentration and regional levels of insoluble Aβ42 [52]. It is therefore possible that the up-regulation of clusterin observed in the CAA arteries, is due to either entrapment of the Aβ–ApoJ complex in the perivascular drainage pathways, or a compensatory up-regulation of ApoJ to clear the excess Aβ42 that cannot be eliminated normally.

In this study, we demonstrated that the expression of TIMP3 in the brain is restricted to the walls of leptomeningeal arteries and increases in CAA. Homeostasis of the extracellular matrix in the brain is maintained by the balanced action of matrix metalloproteinases that degrade extracellular matrix and by tissue inhibitors of metalloproteinases (TIMP) proteins. Human TIMP3 is a 25-kDa protein that contains disulphide bonds and is expressed in normal central nervous system [53]. In a study by Hoe *et al.* [54], TIMP3 expression was found to increase in human brains affected by Alzheimer's disease (AD). Furthermore, this study showed that TIMP3 prevents α-

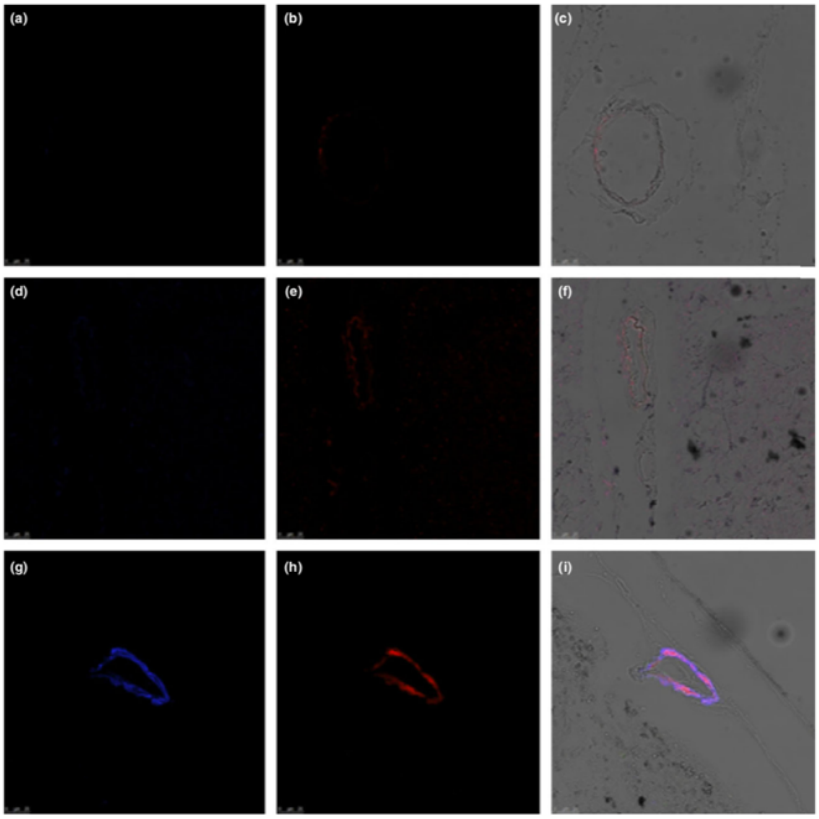

Figure 6. Confocal microscopy images showing distribution of tissue inhibitor of metalloproteinases 3 (TIMP3) (blue) and Aβ (red) in leptomeningeal arteries from young (**a–c**) and elderly females (**d–f**) and patients with cerebral amyloid angiopathy (CAA) (**g–i**). Co-localization of Aβ and TIMP3 is observed in CAA, on transmission merged images (**c–i**). Images obtained with ×20 objective. False colour applied to channels.

cleavage of amyloid precursor protein (APP), whereas it promotes β-cleavage of APP thus contributing to elevated Aβ levels in AD. TIMP3 preserves the integrity of extracellular matrix in arteries as the absence of TIMP3 in knock-out mice results in pathological arterial vasodilation [55]. Our results showed that expression of TIMP3 in the brain is restricted to the walls of leptomeningeal, thus antagonistically targeting TIMP-3 could also facilitate perivascular drainage of Aβ. Examining this hypothesis was beyond the scope of the present study and constitutes a future objective.

In conclusion, this proteomic study demonstrates the activation of inflammatory and extracellular matrix remodelling pathways in human leptomeningeal arteries from CAA patients compared to these from cognitively normal young and elderly controls. Furthermore, we observed increased levels of clusterin and TIMP3 in leptomeningeal arteries from CAA patients compared to young and elderly controls and co-localization of these two proteins with Aβ in the occipital cortex of the CAA cases. Future work will test the hypothesis that clusterin and TIMP3 could facilitate perivascular clearance and represent novel therapeutic targets for CAA.

Acknowledgements

We are indebted to Mr. Roger Allsopp, Mr. Derek Coates and Hope for Guernsey for their fund raising and vision in establishing a clinical mass spectrometry laboratory at the University of Southampton. This study was funded by the BBSRC, Rosetrees Trust and the Wessex Cancer Trust and Medical Research, UK. The authors are grateful to the support of King Saud University, Deanship of Scientific Research Chair, Prince Mutaib Bin Abdullah Chair for Biomarkers of Osteoporosis, College of Science, as well as the Visiting Professor Program of King Saud University, Riyadh, Saudi Arabia. Tissue for this study was provided by the Newcastle Brain Tissue Resource, which is funded in part by a grant from the UK Medical Research Council (grant number G0400074) and by Brains for Dementia Research, a joint venture between Alzheimer's Society and Alzheimer's Research UK.

Author contributions

AM performed the proteomic experiments, interpreted the results and wrote manuscript. MG performed the immunohistochemistry experiments and interpreted the results. CHW performed the bioinformatics analysis. CS and JARN interpreted the results and edited the manuscript. MJ, RK and JA provided the samples and edited the manuscript. SDG designed the proteomic experiments, supervised their execution, interpreted the results and wrote manuscript. ROC conceived the study, funded the study, designed the immunohistochemistry experiments, interpreted the results and wrote manuscript.

Conflicts of interest

None declared.

References

1 Attems J, Jellinger K, Thal DR, Van Nostrand W. Review: sporadic cerebral amyloid angiopathy. *Neuropathol Appl Neurobiol* 2011; **37**: 75–93
2 Love S, Chalmers K, Ince P, Esiri M, Attems J, Jellinger K, Yamada M, McCarron M, Minett T, Matthews F, Greenberg S, Mann D, Kehoe PG. Development, appraisal, validation and implementation of a consensus protocol for the assessment of cerebral amyloid angiopathy in post-mortem brain tissue. *Am J Neurodegen Dis* 2014; **3**: 19–32
3 Alafuzoff I, Thal DR, Arzberger T, Bogdanovic N, Al-Sarraj S, Bodi I, Boluda S, Bugiani O, Duyckaerts C, Gelpi E, Gentleman S, Giaccone G, Graeber M, Hortobagyi T, Höftberger R, Ince P, Ironside JW, Kavantzas N, King A, Korkolopoulou P, Kovács GG, Meyronet D, Monoranu C, Nilsson T, Parchi P, Patsouris E, Pikkarainen M, Revesz T, Rozemuller A, Seilhean D, Schulz-Schaeffer W, Streichenberger N, Wharton SB, Kretzschmar H. Assessment of beta-amyloid deposits in human brain: a study of the BrainNet Europe Consortium. *Acta Neuropathol* 2009; **117**: 309–20
4 Preston SD, Steart PV, Wilkinson A, Nicoll JA, Weller RO. Capillary and arterial cerebral amyloid angiopathy in Alzheimer's disease: defining the perivascular route for the elimination of amyloid beta from the human brain. *Neuropathol Appl Neurobiol* 2003; **29**: 106–17
5 Tian J, Shi J, Smallman R, Iwatsubo T, Mann DM. Relationships in Alzheimer's disease between the extent of Abeta deposition in cerebral blood vessel walls, as cerebral amyloid angiopathy, and the amount of cerebrovascular smooth muscle cells and collagen. *Neuropathology Appl Neurobiol* 2006; **32**: 332–40
6 Weller RO, Subash M, Preston SD, Mazanti I, Carare RO. Perivascular drainage of amyloid-beta peptides from the brain and its failure in cerebral amyloid angiopathy and Alzheimer's disease. *Brain Pathol* 2008; **18**: 253–66
7 Cirrito JR, Deane R, Fagan AM, Spinner ML, Parsadanian M, Finn MB, Jiang H, Prior JL, Sagare A, Bales KR, Paul SM, Zlokovic BV, Piwnica-Worms D, Holtzman DM. P-glycoprotein deficiency at the blood-brain barrier increases amyloid-beta deposition in an Alzheimer disease mouse model. *J Clin Invest* 2005; **115**: 3285–90
8 Deane R, Wu Z, Sagare A, Davis J, Du Yan S, Hamm K, Xu F, Parisi M, LaRue B, Hu HW, Spijkers P, Guo H, Song X, Lenting PJ, Van Nostrand WE, Zlokovic BV. LRP/amyloid beta-peptide interaction mediates

differential brain efflux of Abeta isoforms. *Neuron* 2004; **43**: 333–44
9 Miners JS, Baig S, Palmer J, Palmer LE, Kehoe PG, Love S. Abeta-degrading enzymes in Alzheimer's disease. *Brain Pathol* 2008; **18**: 240–52
10 Tarasoff-Conway JM, Carare RO, Osorio RS, Glodzik L, Butler T, Fieremans E, Axel L, Rusinek H, Nicholson C, Zlokovic BV, Frangione B, Blennow K, Ménard J, Zetterberg H, Wisniewski T, de Leon MJ. Clearance systems in the brain-implications for Alzheimer disease. *Nat Rev Neurol* 2015; **11**: 457–70
11 Carare RO, Bernardes-Silva M, Newman TA, Page AM, Nicoll JA, Perry VH, Weller RO. Solutes, but not cells, drain from the brain parenchyma along basement membranes of capillaries and arteries: significance for cerebral amyloid angiopathy and neuroimmunology. *Neuropathol Appl Neurobiol* 2008; **34**: 131–44
12 Hawkes CA, Gatherer M, Sharp MM, Dorr A, Yuen HM, Kalaria R, Weller RO, Carare RO. Regional differences in the morphological and functional effects of aging on cerebral basement membranes and perivascular drainage of amyloid-beta from the mouse brain. *Aging Cell* 2013; **12**: 224–36
13 Hawkes CA, Hartig W, Kacza J, Schliebs R, Weller RO, Nicoll JA, Carare RO. Perivascular drainage of solutes is impaired in the ageing mouse brain and in the presence of cerebral amyloid angiopathy. *Acta Neuropathol* 2011; **121**: 431–43
14 Hawkes CA, Sullivan PM, Hands S, Weller RO, Nicoll JA, Carare RO. Disruption of arterial perivascular drainage of amyloid-beta from the brains of mice expressing the human APOE epsilon4 allele. *PLoS ONE* 2012; **7**: e41636
15 Galanos P, Vougas K, Walter D, Polyzos A, Maya-Mendoza A, Haagensen EJ, Kokkalis A, Roumelioti FM, Gagos S, Tzetis M, Canovas B, Igea A, Ahuja AK, Zellweger R, Havaki S, Kanavakis E, Kletsas D, Roninson IB, Garbis SD, Lopes M, Nebreda A, Thanos D, Blow JJ, Townsend P, Sørensen CS, Bartek J, Gorgoulis VG. Chronic p53-independent p21 expression causes genomic instability by deregulating replication licensing. *Nat Cell Biol* 2016; **18**: 777–89. [Epub ahead of print]
16 Giannogonas P, Apostolou A, Manousopoulou A, Theocharis S, Macari SA, Psarras S, Garbis SD, Pothoulakis C, Karalis KP. Identification of a novel interaction between corticotropin releasing hormone (Crh) and macroautophagy. *Sci Rep* 2016; **6**: 23342
17 White CH, Johnston HE, Moesker B, Manousopoulou A, Margolis DM, Richman DD, Spina CA, Garbis SD, Woelk CH, Beliakova-Bethell N. Mixed effects of suberoylanilide hydroxamic acid (SAHA) on the host transcriptome and proteome and their implications for HIV reactivation from latency. *Antiviral Res* 2015; **123**: 78–85
18 Delehouzé C, Godl K, Loaëc N, Bruyère C, Desban N, Oumata N, Galons H, Roumeliotis TI, Giannopoulou EG, Grenet J, Twitchell D, Lahti J, Mouchet N, Galibert MD, Garbis SD, Meijer L. CDK/CK1 inhibitors roscovitine and CR8 downregulate amplified MYCN in neuroblastoma cells. *Oncogene* 2014; **33**: 5675–87
19 Manousopoulou A, Saito S, Yamamoto Y, Al-Daghri NM, Ihara M, Carare RO, Garbis SD. Hemisphere asymmetry of response to pharmacologic treatment in an Alzheimer's disease mouse model. *J Alz Dis* 2016; **51**: 333–8
20 Manousopoulou A, Koutmani Y, Karaliota S, Woelk CH, Manolakos ES, Karalis K, Garbis SD. Hypothalamus proteomics from mouse models with obesity and anorexia reveals therapeutic targets of appetite regulation. *Nutr Diabetes* 2016; **6**: e204
21 Al-Daghri NM, Al-Attas OS, Johnston HE, Singhania A, Alokail MS, Alkharfy KM, Abd-Alrahman SH, Sabico SL, Roumeliotis TI, Manousopoulou-Garbis A, Townsend PA, Woelk CH, Chrousos GP, Garbis SD. Whole serum 3D LC-nESI-FTMS quantitative proteomics reveals sexual dimorphism in the milieu intérieur of overweight and obese adults. *J Proteome Res* 2014; **13**: 5094–105
22 Hanley CJ, Noble F, Ward M, Bullock M, Drifka C, Mellone M, Manousopoulou A, Johnston HE, Hayden A, Thirdborough S, Liu Y, Smith DM, Mellows T, Kao WJ, Garbis SD, Mirnezami A, Underwood TJ, Eliceiri KW, Thomas GJ. A subset of myofibroblastic cancer-associated fibroblasts regulate collagen fiber elongation, which is prognostic in multiple cancers. *Oncotarget* 2016; **7**: 6159–74
23 Manousopoulou A, Woo J, Woelk CH, Johnston HE, Singhania A, Hawkes C, Garbis SD, Carare RO. Are you also what your mother eats? Distinct proteomic portrait as a result of maternal high-fat diet in the cerebral cortex of the adult mouse. *Int J Obes (Lond)* 2015; **39**: 1325–8
24 Braak H, Alafuzoff I, Arzberger T, Kretzschmar H, Del Tredici K. Staging of Alzheimer disease-associated neurofibrillary pathology using paraffin sections and immunocytochemistry. *Acta Neuropathol* 2006; **112**: 389–404
25 Thal DR, Rub U, Orantes M, Braak H. Phases of A beta-deposition in the human brain and its relevance for the development of AD. *Neurology* 2002; **58**: 1791–800
26 Mirra SS, Heyman A, McKeel D, Sumi SM, Crain BJ, Brownlee LM, Vogel FS, Hughes JP, van Belle G, Berg L. The Consortium to Establish a Registry for Alzheimer's Disease (CERAD). Part II. Standardization of the neuropathologic assessment of Alzheimer's disease. *Neurology* 1991; **41**: 479–86
27 Montine TJ, Phelps CH, Beach TG, Bigio EH, Cairns NJ, Dickson DW, Duyckaerts C, Frosch MP, Masliah E, Mirra SS, Nelson PT, Schneider JA, Thal DR, Trojanowski JQ, Vinters HV, Hyman BT, National Institute on Aging; Alzheimer's Association. National

Institute on Aging–Alzheimer's Association guidelines for the neuropathologic assessment of Alzheimer's disease: a practical approach. *Acta Neuropathol* 2012; **123**: 1–11

28 McKeith IG, Dickson DW, Lowe J, Emre M, O'Brien JT, Feldman H, Cummings J, Duda JE, Lippa C, Perry EK, Aarsland D, Arai H, Ballard CG, Boeve B, Burn DJ, Costa D, Del ST, Dubois B, Galasko D, Gauthier S, Goetz CG, Gomez-Tortosa E, Halliday G, Hansen LA, Hardy J, Iwatsubo T, Kalaria RN, Kaufer D, Kenny RA, Korczyn A, Kosaka K, Lee VM, Lees A, Litvan I, Londos E, Lopez OL, Minoshima S, Mizuno Y, Molina JA, Mukaetova-Ladinska EB, Pasquier F, Perry RH, Schulz JB, Trojanowski JQ, Yamada M. Consortium on DLB. Diagnosis and management of dementia with Lewy bodies: third report of the DLB Consortium. *Neurology* 2005; **65**: 1863–72

29 Barnes LL, Wilson RS, Bienias JL, Schneider JA, Evans DA, Bennett DA. Sex differences in the clinical manifestations of Alzheimer disease pathology. *Arch Gen Psychiatry* 2005; **62**: 685–91

30 Corder EH, Ghebremedhin E, Taylor MG, Thal DR, Ohm TG, Braak H. The biphasic relationship between regional brain senile plaque and neurofibrillary tangle distributions: modification by age, sex, and APOE polymorphism. *Ann N Y Acad Sci* 2004; **1019**: 24–8

31 Shinohara M, Murray ME, Frank RD, Shinohara M, DeTure M, Yamazaki Y, Tachibana M, Atagi Y, Davis MD, Liu CC, Zhao N, Painter MM, Petersen RC, Fryer JD, Crook JE, Dickson DW, Bu G, Kanekiyo T. Impact of sex and APOE4 on cerebral amyloid angiopathy in Alzheimer's disease. *Acta Neuropathol* 2016; **132**: 225–34. [Epub ahead of print]

32 Levin Y. The role of statistical power analysis in quantitative proteomics. *Proteomics* 2011; **11**: 2565–7

33 Heneka MT, Carson MJ, El Khoury J, Landreth GE, Brosseron F, Feinstein DL, Jacobs AH, Wyss-Coray T, Vitorica J, Ransohoff RM, Herrup K, Frautschy SA, Finsen B, Brown GC, Verkhratsky A, Yamanaka K, Koistinaho J, Latz E, Halle A, Petzold GC, Town T, Morgan D, Shinohara ML, Perry VH, Holmes C, Bazan NG, Brooks DJ, Hunot S, Joseph B, Deigendesch N, Garaschuk O, Boddeke E, Dinarello CA, Breitner JC, Cole GM, Golenbock DT, Kummer MP. Neuroinflammation in Alzheimer's disease. *Lancet Neurol* 2015; **14**: 388–405

34 Zotova E, Bharambe V, Cheaveau M, Morgan W, Holmes C, Harris S, Neal JW, Love S, Nicoll JA, Boche D. Inflammatory components in human Alzheimer's disease and after active amyloid-beta42 immunization. *Brain* 2013; **136**: 2677–96

35 Gasque P, Neal JW, Singhrao SK, McGreal EP, Dean YD, Van BJ, Morgan BP. Roles of the complement system in human neurodegenerative disorders: proinflammatory and tissue remodeling activities. *Mol Neurobiol* 2002; **25**: 1–17

36 van Beek J, Elward K, Gasque P. Activation of complement in the central nervous system: roles in neurodegeneration and neuroprotection. *Ann N Y Acad Sci* 2003; **992**: 56–71

37 Tanskanen M, Lindsberg PJ, Tienari PJ, Polvikoski T, Sulkava R, Verkkoniemi A, Rastas S, Paetau A, Kiuru-Enari S. Cerebral amyloid angiopathy in a 95 + cohort: complement activation and apolipoprotein E (ApoE) genotype. *Neuropathol Appl Neurobiol* 2005; **31**: 589–99

38 Ariga T, Miyatake T, Yu RK. Role of proteoglycans and glycosaminoglycans in the pathogenesis of Alzheimer's disease and related disorders: amyloidogenesis and therapeutic strategies–a review. *J Neurosci Res* 2010; **88**: 2303–15

39 Genedani S, Agnati LF, Leo G, Buzzega D, Maccari F, Carone C, Andreoli N, Filaferro M, Volpi N. beta-Amyloid fibrillation and/or hyperhomocysteinemia modify striatal patterns of hyaluronic acid and dermatan sulfate: possible role in the pathogenesis of Alzheimer's disease. *Curr Alzheimer Res* 2010; **7**: 150–7

40 Ajmo JM, Bailey LA, Howell MD, Cortez LK, Pennypacker KR, Mehta HN, Morgan D, Gordon MN, Gottschall PE. Abnormal post-translational and extracellular processing of brevican in plaque-bearing mice over-expressing APPsw. *J Neurochem* 2010; **113**: 784–95

41 Sykova E, Vorisek I, Antonova T, Mazel T, Meyer-Luehmann M, Jucker M, Hajek M, Ort M, Bures J. Changes in extracellular space size and geometry in APP23 transgenic mice: a model of Alzheimer's disease. *Proc Natl Acad Sci U S A* 2005; **102**: 479–84

42 Lepelletier FX, Mann DM, Robinson AC, Pinteaux E, Boutin H. Early changes in extracellular matrix in Alzheimer's disease. *Neuropathol Appl Neurobiol* 2015; doi: 10.1111/nan.12295. [Epub ahead of print]

43 Xie Z, Harris-White ME, Wals PA, Frautschy SA, Finch CE, Morgan TE. Apolipoprotein J (clusterin) activates rodent microglia *in vivo* and *in vitro* 1. *J Neurochem* 2005; **93**: 1038–46

44 Harold D, Abraham R, Hollingworth P, Sims R, Gerrish A, Hamshere ML, Pahwa JS, Moskvina V, Dowzell K, Williams A, Jones N, Thomas C, Stretton A, Morgan AR, Lovestone S, Powell J, Proitsi P, Lupton MK, Brayne C, Rubinsztein DC, Gill M, Lawlor B, Lynch A, Morgan K, Brown KS, Passmore PA, Craig D, McGuinness B, Todd S, Holmes C, Mann D, Smith AD, Love S, Kehoe PG, Hardy J, Mead S, Fox N, Rossor M, Collinge J, Maier W, Jessen F, Schürmann B, Heun R, van den Bussche H, Heuser I, Kornhuber J, Wiltfang J, Dichgans M, Frölich L, Hampel H, Hüll M, Rujescu D, Goate AM, Kauwe JS, Cruchaga C, Nowotny P, Morris JC, Mayo K, Sleegers K, Bettens K, Engelborghs S, De Deyn PP, Van Broeckhoven C, Livingston G, Bass NJ, Gurling H, McQuillin A, Gwilliam R, Deloukas P, Al-Chalabi A, Shaw CE, Tsolaki M, Singleton AB,

Guerreiro R, Mühleisen TW, Nöthen MM, Moebus S, Jöckel KH, Klopp N, Wichmann HE, Carrasquillo MM, Pankratz VS, Younkin SG, Holmans PA, O'Donovan M, Owen MJ, Williams J. Genome-wide association study identifies variants at CLU and PICALM associated with Alzheimer's disease. *Nat Genet* 2009; **41**: 1088–93

45 Yu JT, Tan L. The role of clusterin in Alzheimer's disease: pathways, pathogenesis, and therapy. *Mol Neurobiol* 2012; **45**: 314–26

46 Bell RD, Sagare AP, Friedman AE, Bedi GS, Holtzman DM, Deane R, Zlokovic BV. Transport pathways for clearance of human Alzheimer's amyloid beta-peptide and apolipoproteins E and J in the mouse central nervous system. *J Cereb Blood Flow Metab* 2007; **27**: 909–18

47 Calero M, Rostagno A, Matsubara E, Zlokovic B, Frangione B, Ghiso J. Apolipoprotein J (clusterin) and Alzheimer's disease. *Microsc Res Tech* 2000; **50**: 305–15

48 Ladu MJ, Reardon C, Van Eldik L, Fagan AM, Bu G, Holtzman D, Getz GS. Lipoproteins in the central nervous system. *An N Y Acad Sci* 2000; **903**: 167–75

49 Soontornniyomkij V, Choi C, Pomakian J, Vinters HV. High-definition characterization of cerebral beta-amyloid angiopathy in Alzheimer's disease. *Hum Pathol* 2010; **41**: 1601–8

50 Craggs L, Taylor J, Slade JY, Chen A, Hagel C, Kuhlenbaeumer G, Borjesson-Hanson A, Viitanen M, Kalimo H, Deramecourt V, Oakley AE, Kalaria RN. Clusterin/Apolipoprotein J immunoreactivity is associated with white matter damage in cerebral small vessel diseases. *Neuropathol Appl Neurobiol* 2016; **42**: 194–209

51 Howlett DR, Hortobagyi T, Francis PT. Clusterin associates specifically with Abeta40 in Alzheimer's disease brain tissue. *Brain Pathol* 2013; **23**: 623–32

52 Miners JS, Clarke P, Love S. Clusterin levels are increased in Alzheimer's disease and influence the regional distribution of Aβ. *Brain Pathol* 2016; doi: 10.1111/bpa.12392. [Epub ahead of print]

53 Kishnani NS, Staskus PW, Yang TT, Masiarz FR, Hawkes SP. Identification and characterization of human tissue inhibitor of metalloproteinase-3 and detection of three additional metalloproteinase inhibitor activities in extracellular matrix. *Matrix Biol* 1995; **14**: 479–88

54 Hoe HS, Cooper MJ, Burns MP, Lewis PA, van der Brug M, Chakraborty G, Cartagena CM, Pak DT, Cookson MR, Rebeck GW. The metalloprotease inhibitor TIMP-3 regulates amyloid precursor protein and apolipoprotein E receptor proteolysis. *J Neurosci* 2007; **27**: 10895–905

55 Basu R, Lee J, Morton JS, Takawale A, Fan D, Kandalam V, Wang X, Davidge ST, Kassiri Z. TIMP3 is the primary TIMP to regulate agonist-induced vascular remodelling and hypertension. *Cardiovasc Res* 2013; **98**: 360–71

Supporting information

Additional Supporting Information may be found in the online version of this article at the publisher's web-site:

Table S1. Total proteome (peptide FDR confidence > 99%) (log2 ratio).

Table S2. Differentially expressed proteins in leptomeningeal arteries from elderly *vs.* young controls (log2 ratio).

Table S3. Differentially expressed proteins in leptomeningeal arteries from CAA patients *vs.* young controls (log2 ratio).

Table S4. Differentially expressed proteins in leptomeningeal arteries from CAA patients *vs.* age-matched controls (log2 ratio).

Received 23 February 2016
Accepted after revision 16 August 2016
Published online Article Accepted on 20 August 2016

1.14 Commentary on fourth publication

The main finding of the fourth publication is that leptomeningeal arteries affected by cerebral amyloid angiopathy have a distinct proteomic profile compared to unaffected from CAA leptomeningeal arteries from young and elderly controls. Immune response/classical complement activation and extracellular matrix remodelling pathways were significantly enriched the differentially expressed proteins between CAA and both young and elderly controls. Furthermore, clusterin (apoJ) and tissue inhibitor of metalloproteinases 3 (TIMP-3) analysed with proteomics to be expressed at higher levels in CAA vs. young and elderly controls, were found with immunohistochemistry to co-localise with Aβ in the walls of leptomeningeal arteries.

The present study was performed among female participants only. Since the publication of this paper, we have also performed the proteomic analysis of leptomeningeal arteries, using the same experimental design as in the present study, for male participants. We are currently examining the sex-specific effects of CAA on leptomeningeal arteries. Furthermore, it would be interesting to examine whether targeting clusterin and TIMP3 can improve perivascular drainage of amyloid-β fibrils and thus improve cognitive function using wild-type and transgenic mouse models.

One important study limitation is that the *post mortem* delay prior to sample collection varied from 9 to 114 hours in the analysed cohort. This could have adversely affected the integrity of proteins in the analysed tissue due to the action of proteases that are activated as part of the body decomposition process initiated by death. At least, *post mortem* delay was not significantly different between groups ($p = 0.33$ in young vs. old controls; $p = 0.30$ in young controls vs. CAA cases; $p = 0.77$ in elderly controls vs. CAA cases), therefore minimising the possibility that the differences in protein expression levels are due to discrepancies in the timing of sample collection and not due to the disease itself.

1.15 Oesophageal cancer and the tumour microenvironment

Following the proteomic studies in obesity and Alzheimer's disease, I decided to also apply our proteomics methodology in cancer, yet another common chronic disease, to assess its applicability in this type of samples. More specifically, I chose to study oesophageal adenocarcinoma because the UK has the highest incidence of this subtype of cancer in the world.

Oesophageal cancer ranks 8th among the most common types of cancer diagnosed and is the 6th leading cause of cancer-related deaths worldwide.[105,106] In 2012 approximately half a million new cases were diagnosed and an estimated 400,000 deaths occurred globally.[105] Oesophageal cancer is quite common because its main risk factors are lifestyle parameters, including smoking, alcohol consumption, obesity and a diet poor in fruit and vegetables (Cancer Research UK, Oesophageal cancer risk factors overview. Website: https://www.cancerresearchuk.org/health-professional/cancer-statistics/statistics-by-cancer-type/oesophageal-cancer/risk-factors#heading-Zero; Accessed: 20 July 2018). Oesophageal cancer is associated with very poor prognosis, with less than 20% overall five-year survival rates in the developed countries.[107]

There are two histologic subtypes of oesophageal cancer: the oesophageal adenocarcinoma (OAC) and squamous cell carcinoma (OSCC).[108] In the developed world, a rapid increase in the incidence of OAC has been observed over the past 40 years, whereas incidence of OSCC has decreased over the same time period.[109,110] In Western populations, the main risk factors for OSCC are alcohol use and tobacco smoking[111] whereas for OAC the two main risk factors are gastro-oesophageal reflux and obesity.[109]

The tumour microenvironment (TME) refers to the non-cancerous cells that are present in a tumour, including immune cells, fibroblasts and endothelial cells, but also the proteins surrounding the tumour, produced by cancerous and non-cancerous cells, and supporting the growth and metastasis of the cancer cells.[112]

Stephen Paget first suggested in 1889 that metastasis is non-random, as some tumour cells ("seed") preferentially grow in the microenvironment of

specific organs ("soil").[113] Paget's "seed and soil" hypothesis emphasized the importance of the microenvironment in regulating distant cancer dissemination. Emerging evidence suggests that the "cross-talk" between cells of the TME and the cancel cells supports tumour growth and progression. The cancer-associated fibroblasts (CAFs) are the major cellular component of the TME and their accumulation is a better predictor of poor patient prognosis in OAC compared to T, N or M stage.[114] Supporting research indicates that therapeutically targeting the TME, as adjuvant treatment, can improve patient outcomes. Lately much scientific interest has been drawn to the discovery of novel therapeutic targets in the TME. Therefore, the aim of the fifth publication was to examine the proteomic profile of primary cancer-associated fibroblasts derived from patients with oesophageal adenocarcinoma in order to identify novel therapeutic targets in the tumour microenvironment.

1.16 Fifth publication

BJC British Journal of Cancer

www.nature.com/bjc

ARTICLE

Molecular Diagnostics

Quantitative proteomic profiling of primary cancer-associated fibroblasts in oesophageal adenocarcinoma

Antigoni Manousopoulou[1], Annette Hayden[2], Massimiliano Mellone[2], Diana J. Garay-Baquero[3], Cory H. White[3,5], Fergus Noble[2], Monette Lopez[4], Gareth J. Thomas[2], Timothy J. Underwood[2] and Spiros D. Garbis[1,2]

BACKGROUND: Cancer-associated fibroblasts (CAFs) form the major stromal component of the tumour microenvironment (TME). The present study aimed to examine the proteomic profiles of CAFs vs. normal fibroblasts (NOFs) from patients with oesophageal adenocarcinoma to gain insight into their pro-oncogenic phenotype.
METHODS: CAFs/NOFs from four patients were sub-cultured and analysed using quantitative proteomics. Differentially expressed proteins (DEPs) were subjected to bioinformatics and compared with published proteomics and transcriptomics datasets.
RESULTS: Principal component analysis of all profiled proteins showed that CAFs had high heterogeneity and clustered separately from NOFs. Bioinformatics interrogation of the DEPs demonstrated inhibition of adhesion of epithelial cells, adhesion of connective tissue cells and cell death of fibroblast cell lines in CAFs vs. NOFs ($p < 0.0001$). KEGG pathway analysis showed a significant enrichment of the insulin-signalling pathway ($p = 0.03$). Gene ontology terms related with myofibroblast phenotype, metabolism, cell adhesion/migration, hypoxia/oxidative stress, angiogenesis, immune/inflammatory response were enriched in CAFs vs. NOFs. Nestin, a stem-cell marker up-regulated in CAFs vs. NOFs, was confirmed to be expressed in the TME with immunohistochemistry.
CONCLUSIONS: The identified pathways and participating proteins may provide novel insight on the tumour-promoting properties of CAFs and unravel novel adjuvant therapeutic targets in the TME.

British Journal of Cancer (2018) 118:1200–1207; https://doi.org/10.1038/s41416-018-0042-9

INTRODUCTION

Oesophageal cancer represents a significant global health burden with 395,000 deaths in 2010, an increase of nearly 15% from 1990.[1] Oesophageal adenocarcinoma (OAC) is the predominant histological subtype in western countries and age-standardised incidence rates are rising by 40% every 5 years.[2] The United Kingdom has the highest incidence of OAC in the world, and outcomes are poor because 60–70% of patients present with late-stage disease too advanced for treatment with curative intent.[3]

Using whole genome sequencing the OCCAMS consortium has identified new mutational signatures of OAC disease types that might be suitable for targeted treatments.[4–6] However, findings from the OCCAMS cohorts require pre-clinical validation prior to implementation in trials, and studies are needed to understand the extent to which the genomic distinction is maintained downstream, at the level of the transcriptome and proteome.[7] Moreover, although mutationally corrupted cancer cells are recognised as the driving force of tumour development and progression, a key knowledge gap hindering the prediction of which patients will benefit from treatment is that the contribution of the tumour microenvironment (TME) is not considered.[8]

Our group's work has focused on the relationship between tumour cells and cancer-associated fibroblasts (CAFs), which form the major cellular component of the TME.[9] The in vivo "education" or "reprogramming" of fibroblasts by tumour cells is an established mechanism by which cancer cells exploit the plastic nature of reactive cell populations to generate a tumour-supportive microenvironment.[10] The accumulation of CAFs in tumours correlates with poor prognosis across cancer types, including OAC, where we have shown that the presence of CAFs is more predictive of poor outcome than T, N or M stage.[11,12] CAFs are most commonly characterised by the acquisition of an "activated", alpha-smooth muscle actin (α-SMA) positive, myofibroblast phenotype,[11] which regulates a number of tumour promoting processes.[12,13] Additionally, CAFs may be implicated in the development of drug resistance during chemotherapy treatment of cancer patients.[14,15] Along these lines, anti-cancer drugs have been found to become ineffective against cancer cells co-cultured with various types of stromal cells.[16]

Shotgun proteomics, supported by recent technological advances in liquid chromatography with mass spectrometry (LC-MS), is gradually becoming an indispensible analytical tool in cancer research since the unbiased protein expression profiling of

[1]Institute for Life Sciences, University of Southampton, Southampton, UK; [2]Cancer Sciences Unit, Faculty of Medicine, University of Southampton, Southampton, UK; [3]Clinical and Experimental Sciences Unit, Faculty of Medicine, University of Southampton, Southampton, UK and [4]University Hospital Southampton NHS Foundation Trust, Southampton, UK
Correspondence: Timothy J. Underwood (T.J.Underwood@soton.ac.uk) or Spiros D. Garbis (S.D.Garbis@soton.ac.uk)
[5]Present address: Merck Exploratory Science Center, Cambridge, MA, USA
These authors contributed equally: Antigoni Manousopoulou and Annette Hayden.
These authors jointly supervised this work: Timothy J. Underwood and Spiros D. Garbis.

Received: 7 October 2017 Revised: 30 January 2018 Accepted: 30 January 2018
Published online: 29 March 2018

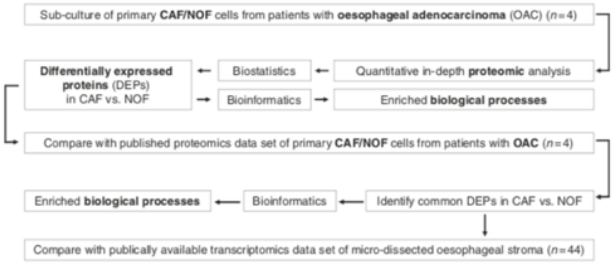

Fig. 1 Study workflow

tumours or their microenvironment can provide novel biological insight but also help identify novel diagnostic, prognostic and therapeutic targets that can eventually influence clinical practice.[13,17–20] There are only a limited number of studies that have examined the global proteomic portrait of primary CAFs derived from human cancer patients.[21–23]

We have previously reported the shotgun proteomic analysis of primary, patient-matched, CAF/NOF pairs ($n = 4$) from patients with OAC.[13] The focus of this study by Hanley et al. was to examine the relative expression levels of extracellular matrix proteins in primary patient-matched CAF/NOF pairs ($n = 4$). The LC-MS analysis resulted in the profiling of 3579 unique proteins, of which 172 were up- and 368 down-regulated in CAFs vs. NOFs.

The aim of the present study was to apply a more in-depth proteomics methodology in combination with comprehensive bioinformatics analysis to an additional cohort of primary patient-matched CAF/NOF pairs ($n = 4$) derived from patients with OAC in order to gain insight into the pro-oncogenic features of the myofibroblast phenotype. An additional aim was to identify novel therapeutic targets relevant to the TME. An overview of the study workflow is presented in Fig. 1.

MATERIALS AND METHODS

Primary cell culture

Experimental protocols received ethical approval by the Southampton and South West Hampshire Research Ethics Committee (09/H0504/66). All participants signed an informed consent form. Fibroblasts were derived from four patients with OAC and sub-cultured as previously described.[12] Normal fibroblasts (NOFs) were taken from the proximal resection margin (at least 10 cm distant from the cancer) of each patient. Cell culture passage number was consistently under four.

Quantitative proteomics sample processing

Cell pellets were snap frozen at −80 °C. These were dissolved in 0.5 M triethylammonium bicarbonate, 0.05% sodium dodecyl sulphate and subjected to pulsed probe sonication (Misonix, Farmingdale, NY, USA). Lysates were centrifuged (16,000*g*, 10 min, 4°C) and supernatants were measured for protein content using infrared spectroscopy (Merck Millipore, Darmstadt, Germany). Lysates were then reduced, alkylated and subjected to trypsin proteolysis. Peptides were labelled using the eight-plex iTRAQ reagent kit with the following reporter ion assignment: 113 = NOF patient 1, 114 = NOF patient 2, 115 = NOF patient 3, 116 = NOF patient 4, 117 = CAF patient 1, 118 = CAF patient 2, 119 = CAF patient 3, and 121 = CAF patient 4. The labelled peptides were then subjected to multi-dimensional liquid chromatography and tandem mass spectrometry as described below.

Two-dimensional LC-MS proteomic analysis

To enhance peptide separation efficiency and subsequent mass spectrometry analysis, the initial offline peptide fractionation was conducted with alkaline C4 Reverse Phase chromatography (Kromasil 150 × 2.1 mm, 3.5 µm particle, 100 Å pore size, Merck KGaA, Darmstadt, Germany) using gradient mobile phase conditions as previously reported by the authors.[24] All other method details were as reported by the authors.[24,25]

Database searching

Unprocessed raw files were submitted to Proteome Discoverer 1.4 for target decoy searching against the UniProtKB homo sapiens database comprised of 20,159 entries (release date January 2015), allowing for up to two missed cleavages, a precursor mass tolerance of 10ppm, a minimum peptide length of six and a maximum of two variable (one equal) modifications of; iTRAQ 8-plex (Y), oxidation (M), deamidation (N, Q), or phosphorylation (S, T, Y). Methylthio (C) and iTRAQ (K, Y and N-terminus) were set as fixed modifications. FDR at the peptide level was set at < 0.05. Percent co-isolation excluding peptides from quantitation was set at 50. Reporter ion ratios from unique peptides only were taken into consideration for the quantitation of the respective protein. Raw iTRAQ intensity values of unique peptides were median-normalised and $\log_2$ transformed. A Student's *T*-Test using the normalised raw iTRAQ intensity was performed to identify differentially expressed unique peptides between CAFs and NOFs. Significance was set at $p \leq 0.05$. A protein was considered to be differentially expressed in CAFs vs. NOFs when it had at least one differentially expressed unique peptide and a mean iTRAQ reporter ion $\log_2$ -ratio of ≥±0.2. In adherence to the Paris Publication Guidelines for the analysis and documentation of peptide and protein identifications (http://www.mcponline.org/site/misc/ParisReport_Final.xhtml), only proteins identified with at least two unique peptides were further subjected to bioinformatics. All mass spectrometry data have been deposited to the ProteomeXchange Consortium via PRIDE with the data set identifier PXD005444.

Bioinformatics analysis

Principal component analysis (PCA) using the $\log_2$ratio of each sample over the mean of all samples was performed using the online tool ClustVis (http://biit.cs.ut.ee/clustvis/). DAVID (https://david.ncifcrf.gov/) was applied to differentially expressed proteins in order to identify over-represented gene ontology terms and KEGG pathways. Fisher exact corrected *p*-values ≤ 0.05 were considered significant. Subcellular localisation of top up- and down-regulated proteins in CAF vs. NOF was manually assessed using ExPASy (www.expasy.org). The diseases and functions module of Ingenuity Pathway Analysis (IPA) (Qiagen, Hilden, Germany) was used to predict upstream biological processes

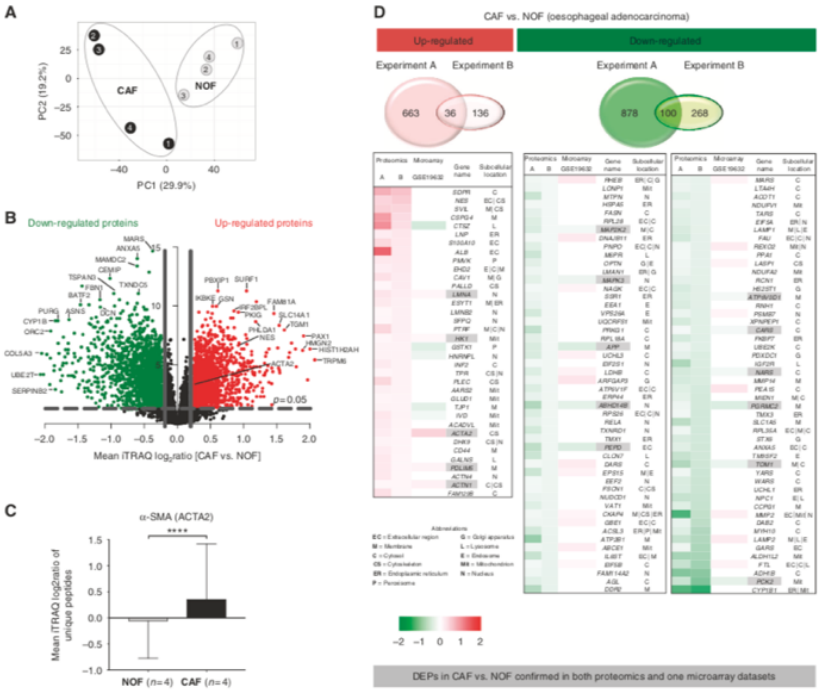

Fig. 2 **a** Principal component analysis using the reporter ion log_2ratios of all analysed proteins showed that CAFs had a distinct proteomic profile and higher heterogeneity compared to NOFs. **b** Volcano plot highlighting the differentially expressed proteins in CAFs vs. NOFs (red = up-regulated proteins; green = down-regulated proteins). **c** Alpha smooth muscle actin (*ACTA2*) was found to be significantly up-regulated in CAFs vs. NOFs (Mean log_2ratio (SD) = 0.2 (0.9); *p*-value <0.0001 at the peptide level) **d** In total, 136 DEPs were also analysed with the same trend of modulation in a previously published proteomics dataset of primary CAFs/NOFs from patients with OAC. Of these, five up-regulated and 11 down-regulated proteins were confirmed in the microarray dataset (highlighted in grey)

activated or inhibited based on a combination of up-regulated and down-regulated proteins observed. Biological processes with a Fisher's exact *p*-value <0.05 and a false discovery rate score (*z*-score) of ≥2 or ≤−2 were considered significantly activated or inhibited, respectively.[26,27]

Comparison of DEPs with published proteomics and transcriptomics data sets

DEPs were compared with our previously published proteomics dataset t of primary CAFs/NOFs from patients with OAC ($n = 4$).[13] To define DEPs in this previous dataset , the exact same criteria as described above for the present study were used. Common DEPs in the two proteomics experiments were compared with a publically available transcriptomics dataset of laser-capture micro-dissected oesophageal stroma ($n = 44$; 17 with intestinal metaplasia, 16 with dysplasia and 11 with adenocarcinoma) (NCBI/NIH; GEO; dataset ID: GSE19632).

In silico evaluation of the prognostic value of DEPs in OAC

Proteins identified to be differentially expressed in CAFs vs. NOFs in both proteomics experiments were *in silico* evaluated for their prognostic value in OAC using PrognoScan (http://www.abren.net/PrognoScan/), a database of published cancer microarray experiments linking gene expression to patient prognosis.[28]

Immunohistochemical validation of key findings

Immunohistochemical staining was performed in sections derived from a cohort of 183 OAC patients as previously described.[12] Briefly, sections of thickness 5μm were taken from the recipient paraffin block for IHC staining. Primary antibody dilution for polyclonal rabbit anti-human Nestin was 1:100 (DAKO no. M3515). Slides were de-paraffinised with xylene and rehydrated with alcohol. Incubation in 3% H_2O_2 (in deionised water) for 10 min was used to suppress endogenous peroxidase activity. Slides were incubated in 1 mM ethylenediaminetetraacetic acid for 15 min at

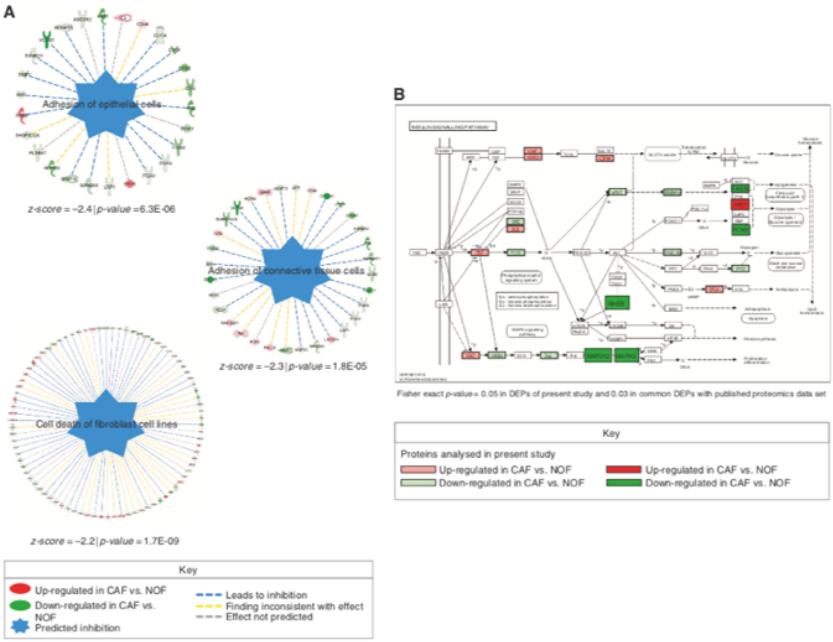

Fig. 3 **a** The diseases and functions module of IPA predicted the significant inhibition of adhesion of epithelial cells (*z*-score = −2.4 | $p = 6.3E-06$), adhesion of connective tissue cells (*z*-score = −2.3 | $p = 1.8E-05$) and cell death of fibroblast cell lines (*z*-score = −2.2 | $p = 1.7E-09$) in CAFs vs. NOFs. **b** KEGG pathway analysis using DAVID showed a significant enrichment of the insulin-signalling pathway (Fisher exact *p*-value = 0.03 for the common proteins between the two proteomics experiments and 0.05 for the DEPs analysed in the present study).

98 °C and pH 8.0, allowing antigen retrieval. Tissue was sequentially incubated in avidin, biotin, primary and biotinylated secondary antibody (at appropriate dilutions), streptabidin biotin-peroxidase complexes and DAB (3-3′-diaminobenzidine). Cores were counter-stained with Mayers Haematoxylin, dehydrated and mounted with DPX. The automated immunostainer DAKO® Autostainer Link 48 (Cambridge, UK) was used in a CPA-accredited cellular pathology department with the use of antibodies optimised to national diagnostic standards (NEQAS).

RESULTS

Proteomic profiling of primary oesophageal fibroblasts

We compared the global proteomic profiles of matched pairs of primary CAFs and NOFs taken from oesophageal resections of four OAC patients in order to identify proteins and pathways that may be responsible for the pro-oncogenic CAF phenotype and the poor patient prognosis associated with the accumulation of CAFs in OAC. Proteomic analysis resulted in the profiling of 7718 unique protein groups (peptide FDR *p*-value <0.05) (Supplementary Table 1), a substantial improvement of more than double the number of profiled unique proteins compared to our previously published proteomics dataset. PCA of all profiled proteins demonstrated that NOFs had a more homogeneous proteomic profile and clustered separately form the more heterogeneous CAFs. (Fig. 2a).

The differentially expressed proteome (DEP) comprised 699 up-regulated and 987 down-regulated proteins in CAFs compared to NOFs (Supplementary Table 2). A volcano plot representation of the mean iTRAQ reporter ion $\log_2$ -ratio of proteins in CAF vs. NOF plotted against the minus log10 (*p*-value) is presented in Fig. 2b. Alpha-SMA expression was found to be variable but with a mean $\log_2$ ratio of 0.2 ± 0.9 (*p*-value < 0.0001 at the peptide level) across all CAFs vs. NOFs examined (Fig. 2c).

Comparison of DEPs with published proteomics and transcriptomics data sets

Of the DEPs, 136 proteins were also identified with the same trend of modulation in our previously published proteomic analysis of primary CAF/NOF pairs from an independent cohort of patients with OAC[13] and the expression trend of five up-regulated and 11 down-regulated proteins was confirmed in the publically available microarray dataset of OAC micro-dissected stromal cells. These proteins are presented in heatmap format in Fig. 2d. Proteins identified in both proteomic experiments and confirmed with the same trend of modulation in the microarray data set are

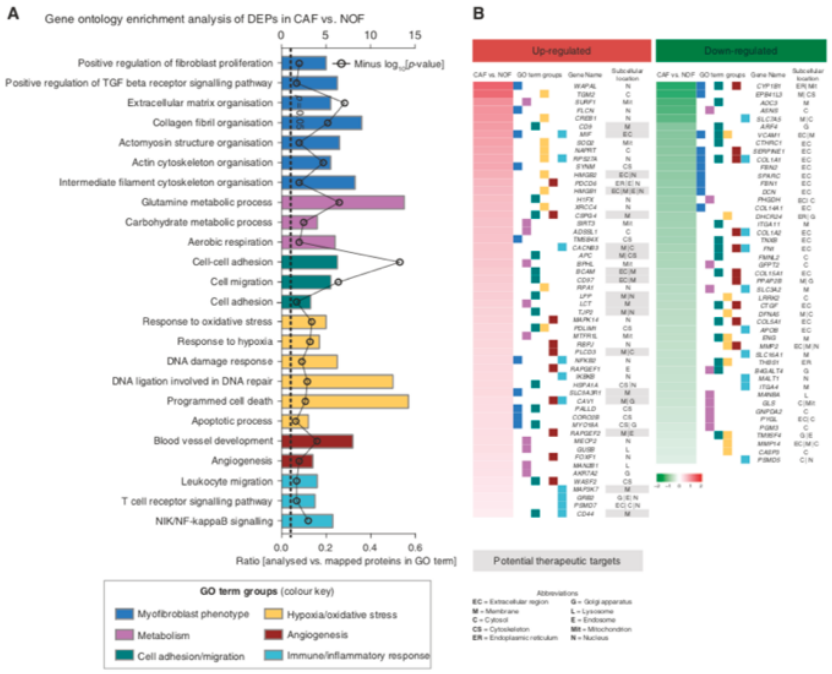

Fig. 4 **a** DAVID gene ontology analysis showed that gene ontology terms related with myofibroblast phenotype, metabolism, cell adhesion/migration, hypoxia/oxidative stress, angiogenesis, immune/inflammatory response were significantly over-represented in the DEPs. **b** Heatmap of top 10 up- and top 10 down-regulated proteins mapping to each gene ontology terms group . The subcellular location of each protein is also presented and up-regulated proteins that are either secreted or membrane are highlighted as potential therapeutic targets.

highlighted in grey (Fig. 2d). Among the proteins identified in both proteomics and confirmed at the transcriptomics data set to be up-regulated in CAFs vs. NOFs were α-SMA, lamin A (*LMNA*) and actin-1 (*ACTN1*).

Bioinformatics Analysis

The diseases and functions module of IPA predicted, based on the downstream up-regulated and down-regulated proteins, that adhesion of epithelial cells (z-score = −2.4 | p = 6.3E-06), adhesion of connective tissue cells (z-score = −2.3 | p = 1.8E−05) and cell death of fibroblast cell lines (z-score = −2.2 | p = 1.7E−09) were significantly inhibited in CAFs vs. NOFs (Fig. 3a). KEGG pathway analysis using DAVID showed a significant enrichment of the insulin-signalling pathway (Fisher exact p-value = 0.03 for the common proteins between the two proteomics experiments and 0.05 for the DEPs analysed in the present study) (Fig. 3b).

DAVID gene ontology analysis, accounting for both up-regulated and down-regulated proteins constituting the DEP, demonstrated that processes related with myofibroblast phenotype, metabolism, cell adhesion/migration, hypoxia/oxidative stress, angiogenesis, and immune/inflammatory response were over-represented (Fig. 4a). The top ten up-regulated and down-regulated proteins mapping to each GO term group are presented in heatmap format in Fig. 4b. The sub-cellular localisation of these proteins is also presented in the heatmap. Top up-regulated proteins that are either secreted or localised in the membrane are highlighted in the heatmap as potential therapeutic targets in CAFs (gene names of the respective proteins are: *CD9, MIF, HMGB2, HMGB1, CSPG4, CACNB3, APC, BCAM, CD97, LPP, LCT, TJP2, PLCD3, SLC9A3R1, CAV1, RAPGEF2, MAP3K7* and *CD44*) (Fig. 4b).

In silico evaluation of the prognostic value of Nestin in OAC

Using the *in silico* PrognoScan meta-analysis microarray database for the common DEPs in both proteomics experiments, increased levels of nestin was found to be associated with poor OAC patient prognosis [COX p-value = 0.003; HR (95% CI) = 78.0 (4.3 to 1409.8)] (Fig. 5a). Immunohistochemical staining of nestin was performed in a well-described cohort of 183 oesophageal tumours where the presence of α-SMA positive CAFs correlated strongly with poor overall survival.[12] The patient clinico-pathological characteristics of this cohort have been reported before.[12] Nestin showed a conserved expression pattern in the TME of OAC, being confined to CAFs, blood vessels and smooth muscle cells. Example staining is shown in Fig. 5b.

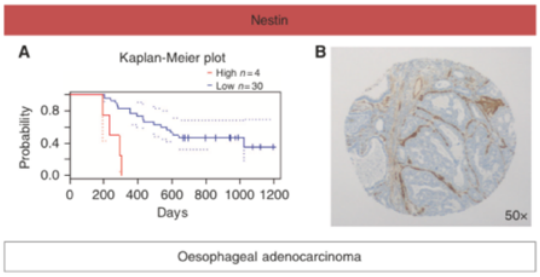

Fig. 5 **a** Using the *in silico* PrognoScan meta-analysis microarray database, higher expression levels of nestin were found to correlate with poor patient prognosis [COX *p*-value = 0.003; HR (95% CI) = 78.0 (4.3–1409.8)]. **b** Immunohistochemical staining of nestin in OAC showed a conserved expression pattern in the tumour microenvironment, with expression being confined to CAFs, blood vessels and smooth muscle cells.

DISCUSSION

The seminal work of Stephen Paget over a century ago proposed that cancer cells constitute the "seeds" that colonise a favourable stromal microenvironment as the receptive "soil".[29,30] A key "soil" constituent is the NOF that acquires a cancerous phenotype by the "seed" cancer cell to facilitate its proliferation, invasion, and metastasis.[31] However, the proteomic characterisation of such cancer fibroblasts remains limited.

To address this need, our study made use of a comprehensive quantitative proteomics approach (Fig. 1) and reports the most extensive proteome coverage to date of primary CAF/NOF pairs derived from patients with OAC. PCA against the reporter ion ratios of the 7718 unique protein analysed across all samples showed that CAFs had a distict proteomic profile relative to NOFs. (Fig. 2a). In keeping with previous findings,[12,32] PCA analysis showed marked heterogeneity in proteome expression between the CAFs relative to the more homogeneous proteome expression between the NOFs Significant differential expression was observed for 699 up-regulated and 987 down-regulated proteins across all CAFs relative to all NOFs, as highlighted in the volcano plot of Fig. 2b ($\log_2$ -ratio ≥ 0.2, $p \leq 0.05$, *t*-test). Alpha-SMA (*ACTA2*) was analysed to be marginally up-regulated in CAFs vs. NOFs (as illustrated in the volcano plot of Fig. 2b) ($\log_2$ratio = 0.2 ± 0.9; *p*-value <0.0001 at the peptide level) (Fig. 2c). By contrast, our quantitative proteome revealed a large spectrum of novel proteins exhibiting a higher and more consistent level of differential expression that may constitute more robust candidate markers of the CAF phenotype (Fig. 2b,c, Supplementary Table 2). Consistent protein differential expression of CAF canonical markers was observed between the current quantitative proteome, a proteomics dataset reported by the authors[13] and a publically available transcriptomics microarray dataset (Fig. 2d). Notable surrogate markers consistently observed in the CAF phenotype include the up-regulated proteins lamin A (*LMNA*) and actin-1 (*ACTN1*). *LMNA* has been implicated in the modulation of TGF-β1 on collagen production and mesenchymal differentiation,[13] and *ACTN1* up-regulation has been described in stromal fibroblasts derived from oral cancers.[34]

The diseases and functions module of IPA predicted the inhibition of adhesion of epithelial cells (*z*-score = −2.4 | *p* = 6.3E-06) and adhesion of connective tissue cells (*z*-score = −2.3 | *p* = 1.8E–05) (Fig. 3a). The inhibition of these processes suggests the involvement of CAFs on increasing the tumour's metastatic potential. These findings confirm and extend the current knowledge of the CAF phenotype also affecting cell adhesion/cell migration processes.[12,13]

Of relevance, given the endoergic character of increased cellular proliferation and pro-metastatic phenotypes observed, the insulin-signalling pathway was significantly enriched in the DEPs of the present study as well as the commonly observed proteins with our previously published proteomics dataset (Fig. 3b). Increased expression of the insulin-like growth factor 1 (IGF-I) and its receptor (IGF–IR) has been found to be associated with tumour progression and poor prognosis in different cancer types including gastrointestinal tumours.[35,36] The tumour promoting properties of the IGF–IR are interlinked with the activation of the down-stream insulin receptor substrates (IRS).[37,38] IGF-I also plays a key role in the autocrine and paracrine induction of CAF "activation".[14] A recent study showed that NT157, an inhibitor of the IGF–IR–IRS signalling pathway, resulted in inhibition of CAF "activation", as well as reduced expression of pro-oncogenic chemokines, cytokines and growth factors, including several interleukins (IL-6, IL-11, IL-23) and TGFβ.[39] The de-regulation of the insulin signalling pathway in CAFs could also be linked to the "Reverse Warburg effect", a model describing the metabolic coupling between stromal and cancer cells.[40] One interesting protein mapping to the insulin-signalling pathway was hexokinase-1 (HK1), which was consistently upregulated in both proteomic experiments and further confirmed at the microarray dataset (Figs. 2d and 3b). HK1 catalyses the first obligatory and rate-limiting step involving the phosphorylation of glucose to G6P.[41] Furthermore, HK1 has been suggested to regulate cell death, a process associated with abnormal proliferation and tumourigenesis.[42] HK1 has also been found to be upregulated in different cancer types, including kidney and breast carcinomas.[43,44] Additionally , a recent study showed that HK1 overexpression was associated with poor patient prognosis in colorectal cancer.[45] HK1 expression in CAFs and its implication with tumour aggressiveness warrants further investigation.

DAVID GO analysis identified terms related to the myofibroblast phenotype, metabolism, cell adhesion/migration, hypoxia/oxidative stress (including DNA damage response), angiogenesis, and immune/inflammatory response processes to be over-represented in the DEPs (Fig. 4a). The gene names of the top-10 differentially expressed proteins observed for each of these processes, including those classified as secreted or membrane associated, constitute novel observations and may reveal candidate therapeutic targets (Fig. 4b).

Hypoxia, oxidative stress and DNA damage response were significantly enriched GO terms. Oxidation–reduction is an established process in CAFs.[31,46] CAFs have been shown to overproduce reactive oxygen species (ROS), leading to oxidative stress, inflammation and significant cellular damage, which could

in turn affect DNA damage response.[31,47] The over-production of ROS by CAFs can induce oxidative stress in NOFs that further triggers CAF activation, thus leading to a positive feedback loop between ROS production and CAF activation.[48,49] Moreover , the cell death of fibroblasts was found to be inhibited (z-score = −2.2 | $p = 1.7E{-}09$), showing that CAFs may evade apoptosis possibly as a result of their enhanced DNA damage response.

Immune and inflammatory responses were also significantly over-represented terms in CAFs vs. NOFs (Fig. 4a). Previous studies have reported on the immunomodulatory effects of CAFs.[50–52] Specific pathways and their participatory proteins responsible for the interplay between CAFs and the host immune response may be of relevance to a number of current clinical trials using immune checkpoint inhibitors in unselected patients with OAC. The success rate of these therapies may not depend entirely on the immune system, but also implicate CAF-induced alterations of the TME in preventing immune cell entry. This may necessitate the combined use of immunotherapy and CAF permeability modifiers.[53] At the same token, CAFs have been reported to promote angiogenesis through different mechanisms, including ECM remodelling, recruitment of epithelial progenitor cells, and increased leucocyte infiltration through chemokine secretion, that in turn produce angiogenic factors.[54]

An up-regulated protein identified in both proteomic experiments was nestin. Nestin was further investigated as it was found to correlate with decreased overall survival in patients with oesophageal cancer when using the *in silico* microarray meta-analysis tool PrognoScan (Fig. 5a), suggesting its important role in OAC biology. Nestin is an intermediate filament protein originally detected in neuronal stem cells during development.[55] Nestin has been detected in various types of solid tumours, including mesenchymal tumours and cancers (e.g., breast, lung, ovarian and gastrointestinal).[56] Nestin has been suggested as a stem-cell marker indicating an undifferentiated and thus more invasive phenotype of transformed cells.[57] Immunohistochemical staining showed that nestin protein expression was confined to the TME of OAC (Fig. 5b). A recent study showed that nestin suppression reduced the metastatic potential of endometrial cancer cells by inhibiting the TGFβ signalling cascade,[58] the main pathway promoting aberrant CAF "activation".[59]

The main study limitation is that only four matched pairs of fibroblasts were used to generate the proteomic expression profiles. This is partly compensated, however, by the evaluation of the analysed proteins using our previously published proteomics dataset ($n = 4$) and an independent microarray dataset ($n = 44$).

In conclusion, this study reports the proteomic profiling of primary CAFs from patients with OAC, a cancer with a vast unmet clinical need. The biological pathways and networks observed for the primary CAFs examined were found to emulate all the intrinsic hallmarks of cancer, as expected given the strong functional cross-talk between fibroblasts and cancer cells. Consequently, the participating proteins to these biological processes may constitute novel adjuvant therapeutic targets for OAC in the TME as part of precision medicine protocols.

ACKNOWLEDGEMENTS

We are indebted to Mr. Roger Allsopp, Mr. Derek Coates and Hope for Guernsey for establishing the clinical mass spectrometry infrastructure at the University of Southampton. The authors are grateful to the support of King Saud University, Deanship of Scientific Research Chair, Prince Mutaib Bin Abdullah Chair for Biomarkers of Osteoporosis, College of Science, as well as the Visiting Professor Program of King Saud University, Riyadh, Saudi Arabia.

AUTHOR CONTRIBUTIONS

A.M. and A.H. designed study, performed experiments, interpreted results and wrote manuscript; M.M. interpreted results and edited manuscript; D.J.G.B., provided analytic tools; C.H.W. performed biostatistical analysis; F.N. and M.L. sample procurement; G.J.T. interpreted results and edited manuscript, T.J.U. and S.D.G. raised funding, designed study, interpreted results and wrote manuscript.

ADDITIONAL INFORMATION

Supplementary information is available for this paper at https://doi.org/10.1038/s41416-018-0042-9.

Competing interests: The authors declare no competing interests.

Funding: Wessex Cancer Trust, CRUK—Southampton Internal Pilot Grant, EU-FP7 Marie Curie (CANOMICS), Annual Adventures in Research—University of Southampton, EU-Excellence II—Systems Biology Framework FRA-SYS (Grant 4072), Cancer Research UK (Grants C34999/A13719 and RG84119), and MRC Clinician Scientist Fellowship (Grant G1002565).

REFERENCES

1. Lozano, R. et al. Global and regional mortality from 235 causes of death for 20 age groups in 1990 and 2010: a systematic analysis for the Global Burden of Disease Study 2010. *Lancet* **380**, 2095–2128 (2012).
2. Lepage, C., Rachet, B., Jooste, V., Faivre, J. & Coleman, M. P. Continuing rapid increase in esophageal adenocarcinoma in England and Wales. *Am. J. Gastroenterol.* **103**, 2694–2699 (2008).
3. Arnold, M., Soerjomataram, I., Ferlay, J. & Forman, D. Global incidence of oesophageal cancer by histological subtype in 2012. *Gut* **64**, 381–387 (2014).
4. Dulak, A. M. et al. Exome and whole-genome sequencing of esophageal adenocarcinoma identifies recurrent driver events and mutational complexity. *Nat. Genet.* **45**, 478–486 (2013).
5. Ross-Innes, C. S. et al. Whole-genome sequencing provides new insights into the clonal architecture of Barrett's esophagus and esophageal adenocarcinoma. *Nat. Genet.* **47**, 1038–1046 (2015).
6. Weaver, J. M. J. et al. Ordering of mutations in preinvasive disease stages of esophageal carcinogenesis. *Nat. Genet.* **46**, 837–843 (2014).
7. Secrier, M. et al. Mutational signatures in esophageal adenocarcinoma reveal etiologically distinct subgroups with therapeutic relevance. *Nat. Genet.* **48**, 1131–1141 (2016).
8. Hanahan, D. & Coussens, L. M. Accessories to the crime: functions of cells recruited to the tumor microenvironment. *Cancer Cell* **21**, 309–322 (2012).
9. De Wever, O., Demetter, P., Mareel, M. & Bracke, M. Stromal myofibroblasts are drivers of invasive cancer growth. *Int. J. Cancer* **123**, 2229–2238 (2008).
10. Erez, N., Truitt, M., Olson, P., Arron, S. T. & Hanahan, D. Cancer-associated fibroblasts are activated in incipient neoplasia to orchestrate tumor-promoting inflammation in an NF-kappaB-dependent manner. *Cancer Cell* **17**, 135–147 (2010).
11. Marsh, D. et al. Stromal features are predictive of disease mortality in oral cancer patients. *J. Pathol.* **223**, 470–481 (2011).
12. Underwood, T. J. et al. Cancer-associated fibroblasts predict poor outcome and promote periostin-dependent invasion in oesophageal adenocarcinoma. *J. Pathol.* **235**, 466–477 (2015).
13. Hanley, C. J. et al. A subset of myofibroblastic cancer-associated fibroblasts regulate collagen fiber elongation, which is prognostic in multiple cancers. *Oncotarget* **7**, 6159–6174 (2016).
14. Kalluri, R. & Zeisberg, M. Fibroblasts in cancer. *Nat. Rev. Cancer* **6**, 392–401 (2006).
15. Wang, C. et al. Metronomic chemotherapy remodel cancer-associated fibroblasts to decrease chemoresistance of gastric cancer in nude mice. *Oncol. Lett.* **14**, 7903–7909 (2017).
16. Straussman, R. et al. Tumour micro-environment elicits innate resistance to RAF inhibitors through HGF secretion. *Nature* **487**, 500–504 (2012).
17. Galanos, P. et al. Chronic p53-independent p21 expression causes genomic instability by deregulating replication licensing. *Nat. Cell Biol.* **18**, 777–789 (2016).
18. Larkin, S. E. et al. Detection of candidate biomarkers of prostate cancer progression in serum: a depletion-free 3D LC/MS quantitative proteomics pilot study. *Br. J. Cancer* **115**, 1078–1086 (2016).
19. Zeidan, B. et al. Annexin A3 is a mammary marker and a potential neoplastic breast cell therapeutic target. *Oncotarget* **6**, 21421–21427 (2015).
20. Bouchal, P. et al. Combined Proteomics and Transcriptomics Identifies Carboxypeptidase B1 and Nuclear Factor κB (NF-κB) Associated Proteins as Putative Biomarkers of Metastasis in Low Grade Breast Cancer. *Mol. Cell Proteom.* **14**, 1814–1830 (2015).
21. Fu, Z. et al. Cancer-associated fibroblasts from invasive breast cancer have an attenuated capacity to secrete collagens. *Int. J. Oncol.* **45**, 1479–1488 (2014).

22. Groessl, M. et al. Proteome profiling of breast cancer biopsies reveals a wound healing signature of cancer-associated fibroblasts. *J. Proteome Res.* **13**, 4773–4782 (2014).
23. Torres, S. et al. Proteome profiling of cancer-associated fibroblasts identifies novel proinflammatory signatures and prognostic markers for colorectal cancer. *Clin. Cancer Res.* **19**, 6006–6019 (*2013*).
24. Manousopoulou, A. et al. Systems proteomic analysis reveals that clusterin and tissue inhibitor of metalloproteinases 3 increase in leptomeningeal arteries affected by cerebral amyloid angiopathy. *Neuropathol. Appl. Neurobiol.* **43**, 492–504 (2017).
25. Manousopoulou, A. et al. Hypothalamus proteomics from mouse models with obesity and anorexia reveals therapeutic targets of appetite regulation. *Nutr. Diabetes* **6**, e204 (2016).
26. Al-Daghri, N. M. et al. Whole serum 3D LC-nESI-FTMS quantitative proteomics reveals sexual dimorphism in the milieu intérieur of overweight and obese adults. *J. Proteome Res.* **13**, 5094–5105 (2014).
27. Krämer, A., Green, J., Pollard, J. Jr & Tugendreich, S. Causal analysis approaches in ingenuity pathway analysis. *Bioinformatics* **30**, 523–530 (2014).
28. Mizuno, H., Kitada, K., Nakai, K. & Sarai, A. PrognoScan: a new database for meta-analysis of the prognostic value of genes. *BMC Med. Genom.* **2**, 18 (2009).
29. Han, Y., Zhang, Y., Jia, T. & Sun, Y. Molecular mechanisms underlying the tumor-promoting functions of carcinoma-associated fibroblasts. *Tumor Biol.* **36**, 1385–1394 (2015).
30. Baulida, J. Epithelial-to-mesenchymal transition transcription factors in cancer-associated fibroblasts. *Mol. Oncol.* **11**, 847–859 (2017).
31. Martin, O. A. et al. Systemic DNA damage related to cancer. *Cancer Res.* **71**, 3437–3441 (2011).
32. Ishii, G., Ochiai, A. & Neri, S. Phenotypic and functional heterogeneity of cancer-associated fibroblast within the tumor microenvironment. *Adv. Drug. Deliv. Rev.* **99**, 186–196 (2016).
33. Van Berlo, J. H. et al. A-type lamins are essential for TGF-beta1 induced PP2A to dephosphorylate transcription factors. *Hum. Mol. Genet.* **14**, 2839–2849 (2005).
34. Chatzistamou, I. et al. p21/waf1 and smooth-muscle actin α expression in stromal fibroblasts of oral cancers. *Cell Oncol. (Dordr.)* **34**, 483–488 (2011).
35. Giovannucci, E. Insulin, insulin-like growth factors and colon cancer: a review of the evidence. *J. Nutr.* **131**, 3109S–3120S (2001).
36. Woodson, K. et al. Loss of insulin-like growth factor-II imprinting and the presence of screen-detected colorectal adenomas in women. *J. Natl. Cancer Inst.* **96**, 407–410 (2004).
37. Ramocki, N. M. et al. Insulin receptor substrate-1 deficiency promotes apoptosis in the putative intestinal crypt stem cell region, limits Apcmin/+ tumors, and regulates Sox9. *Endocrinology* **149**, 261–267 (*2008*).
38. Chan, B. T. & Lee, A. V. Insulin receptor substrates (IRSs) and breast tumorigenesis. *J. Mammary Gland. Biol. Neoplasia.* **13**, 415–422 (2008).
39. Sanchez-Lopez, E. et al. Targeting colorectal cancer via its microenvironment by inhibiting IGF-1 receptor-insulin receptor substrate and STAT3 signaling. *Oncogene* **35**, 2634–2644 (2016).
40. Pavlides, S. et al. The reverse Warburg effect: aerobic glycolysis in cancer associated fibroblasts and the tumor stroma. *Cell Cycle* **8**, 3984–4001 (2009).
41. Smith, T. A. Mammalian hexokinases and their abnormal expression in cancer. *Br. J. Biomed. Sci.* **57**, 170–178 (2000).
42. Pastorino, J. G. & Howek, J. B. Hexokinase II: the integration of energy metabolism and control of apoptosis. *Curr. Med. Chem.* **10**, 1535–1551 (2003).
43. Hooft, L. et al. [18F]fluorodeoxyglucose uptake in recurrent thyroid cancer is related to hexokinase i expression in the primary tumor. *J. Clin. Endocrinol. Metab.* **90**, 328–334 (2005).
44. Millon, S. R. et al. Uptake of 2-NBDG as a method to monitor therapy response in breast cancer cell lines. *Breast Cancer Res. Treat.* **126**, 55–62 (2011).
45. He, X. et al. Overexpression of Hexokinase 1 as a poor prognosticator in human colorectal cancer. *Tumour Biol.* **37**, 3887–3895 (2016).
46. Balliet, R. M. et al. Mitochondrial oxidative stress in cancer-associated fibroblasts drives lactate production, promoting breast cancer tumor growth: understanding the aging and cancer connection. *Cell Cycle* **10**, 4065–4073 (2011).
47. Trinchieri, G. Cancer and inflammation: an old intuition with rapidly evolving new concepts. *Annu. Rev. Immunol.* **30**, 677–706 (2012).
48. Jezierska-Drutel, A., Rosenzweig, S. A. & Neumann, C. A. Role of oxidative stress and the microenvironment in breast cancer development and progression. *Adv. Cancer Res.* **119**, 107–125 (2013).
49. Chan, J. S. et al. Cancer-associated fibroblasts enact field cancerization by promoting extratumoral oxidative stress. *Cell Death Dis.* **8**, e2562 (2017).
50. Takahashi, H. et al. Cancer-associated fibroblasts promote an immunosuppressive microenvironment through the induction and accumulation of protumoral macrophages. *Oncotarget* **8**, 8633–8647 (*2017*).
51. Wen, X. et al. Fibroblast activation protein-α-positive fibroblasts promote gastric cancer progression and resistance to immune checkpoint blockade. *Oncol. Res.* **25**, 629–640 (2017).
52. Yeh, C. R. et al. Estrogen receptor α in cancer associated fibroblasts suppresses prostate cancerinvasion via reducing CCL5, IL6 and macrophage infiltration in the tumor microenvironment. *Mol. Cancer* **15**, 7 (2016).
53. Hanley C. J. et al. Targeting the Myofibroblastic Cancer-Associated Fibroblast Phenotype Through Inhibition of NOX4. *J. Natl. Cancer Inst.* https://doi.org/10.1093/jnci/djx121 (2018).
54. Tao, L., Huang, G., Song, H., Chen, Y. & Chen, L. Cancer associated fibroblasts: an essential role in the tumor microenvironment. *Oncol. Lett.* **14**, 2611–2620 (2017).
55. Lendahl, U., Zimmerman, L. B. & McKay, R. D. CNS stem cells express a new class of intermediate filament protein. *Cell* **60**, 585–595 (1990).
56. Ishiwata, T., Matsuda, Y. & Naito, Z. Nestin in gastrointestinal and other cancers: effects on cells and tumor angiogenesis. *World J. Gastroenterol.* **17**, 409–418 (2011).
57. Neradil, J. & Veselska, R. Nestin as a marker of cancer stem cells. *Cancer Sci.* **106**, 803–811 (2015).
58. Bokhari, A. A. et al. Nestin suppression attenuates invasive potential of endometrial cancer cells by downregulating TGF-β signaling pathway. *Oncotarget* **7**, 69733–69748 (2016).
59. Hawinkels, L. J. et al. Interaction with colon cancer cells hyperactivates TGF-beta signaling in cancer-associated fibroblasts. *Oncogene* **33**, 97–107 (2014).

1.17 Commentary on fifth publication

The main finding of the fifth publication is that cancer-associated fibroblasts (CAFs) affect a multitude of cancer-promoting processes. CAFs were found to be associated with decreased cell adhesion, suggesting that CAFs could directly promote cancer metastasis. Furthermore, key proteins participating in the insulin signalling pathway were found to be induced in CAFs. Induction of the insulin signalling pathway plays a key role in CAF activation. Furthermore, this de-regulation could also be related to the "Reverse Warburg effect", that refers to the production of energy-rich compounds (such as ketone bodies, fatty acids, lactate and pyruvate) by CAFs that can be used by the cancer cells for energy production.

A future perspective is to examine the participation of insulin signalling pathway in the pro-oncogenic phenotype of CAFs but also examine whether targeting the insulin signalling pathway, either through pharmacotherapy or through dietary and physical activity interventions, could improve the disease outcome in cancer patients with CAF accumulation in their tumour. Another future study could examine whether nestin can be used as an immunohistochemical marker of CAFs that also correlates with OAC patient prognosis, at the tissue and serum level.

An innovative feature of the bioinformatics analysis of this publication is that a publicly available microarray database of prognosis in patient with different caner types, PrognoScan, was used to assess which differentially expressed proteins in CAFs vs. NOFs also correlate with OAC patient prognosis at the mRNA level.

One study limitation is that primary CAFs derived from patients with oesophageal adenocarcinoma were first sub-cultured prior to their proteomic analysis. This *in vitro* sub-culturing of CAFs could have changed their proteomic profile. To minimise the introduction of any further bias, cell culture passage number was kept consistent among all samples (P3).

Section 2. Discussion

The present research describes the development of a novel, global quantitative proteomics methodology for the in-depth analysis of tissue and cell line specimens. This innovative methodology was applied in mouse model and human samples from biomedical studies of three different chronic diseases, namely obesity, Alzheimer's disease and cancer, in order to assess its suitability for the analysis of a wide array of sample types in different settings of biomedical research projects. An overview of the proteomics methodology presented in the present thesis is provided in **Appendix F**.

The first publication describes the development of an untargeted proteomics methodology for the study of brain samples from a wild-type mouse model.[115] Following protein reduction, alkylation and trypsin proteolysis, peptides from eight sample groups were labelled using the iTRAQ isobaric reagent kit. Labelled peptides were mixed and fractionated using reversed-phase chromatography. Resulting peptide fractions were analysed using the Orbitrap Elite mass spectrometry system.

The proteomics methodology contained the following novel features: 1. Brain tissue was homogenised using a benchtop homogenizing system. Samples were dissolved in 0.5 M triethylammonium biocarbomnate and 0.05% SDS using sample tubes filled with ceramic beads. Supernatants were transferred to a fresh tube and subjected further to probe sonication. 2. Offline fractionation was performed using C8 reversed-phase chromatography in alkaline conditions (Buffer A: Water with 0.1% NH_4OH; Buffer B: Acetonitrile with 0.1% NH_4OH). A two-hour long gradient was used to allow for sufficient separation of the peptides. 3. A liquid chromatographic online gradient adjusted to the retention time of each fraction at the offline C8 RP chromatography was used. Fractions eluted at the initial part of the C8 RP chromatography were analysed with a more hydrophilic gradient, fractions eluting at the middle part of the C8 RP chromatography with a more amphoteric gradient whereas fractions eluting at the last part of the offline C8 RP chromatography with a more hydrophobic gradient. By matching the

offline retention time with the online gradient peptide separation was maximised. 4. A 50 cm long C18 reversed phase chromatographic column was used for the online separation of peptides. The online chromatography was performed under acidic conditions, to achieve orthogonality in peptide separation compared to the offline alkaline chromatography. 5. In the buffers of the online chromatographic separation 5% dimethyl sulfoxide (DMSO) was added to improve ionization efficiency of the peptides. 6. A combined HCD-CID MS method was used. Each peptide was fragmented using both HCD and CID fragmentation techniques, with the CID spectra providing information mainly on the amino acid sequence of a specific peptide whereas the HCD spectra providing information on both the amino acid sequence of the peptide but also the relative expression levels of the peptide between samples. The complementarity in the acquired data allowed for a more in-depth proteomic coverage.

The proteomics methodology developed for the analysis of brain tissue in the first publication was applied for the analysis of brain tissue in the following three publications.[115-118] A further methodological refinement applied to the last publication was that the offline peptide fractionation was conducted with a C4-based RP stationary phase under the same high-pH mobile phase conditions used in the previous four studies.[119] This approach imparted a higher degree of orthogonality with the acidic C18-based RP stationary phase used for the 2nd dimension in-line with the nanospray source-mass spectrometer system, as in the previous studies. This was deemed an essential refinement given the intrinsic heterogeneity of the primary CAF/NOF cells examined. The enhanced peptide separation using this more orthogonal two-dimensional approach aided in reducing peptide co-isolation phenomena.

The overarching principle dictating the specific quantitative proteomics described in the present studies, was the use of highly chemically orthogonal liquid chromatographic techniques in combination with optimized ultra-high resolution mass spectrometry and complementary peptide fragmentation techniques in generating the product ion spectra. As previously described,

combining the offline high-pH RP followed by the online low-pH nano-capillary RP as the two-dimesional LC-MS proteomics approach provided the necessary degree of peptide separation and analytical sensitivity to generate state-of-the-art in-depth proteome coverage. Furthermore, the mobile phase conditions made use of volatile pH-modifiers at sufficiently low concentration levels so as to minimise nano-spray ionization suppression further supporting a robust and sensitive LC-MS analytical process.

The collective analytical attributes to these proteomics approaches was to minimize the peptide co-isolation effect that would otherwise alter the accuracy and sensitivity of relative proteotypic peptide quantitative along with their surrogate proteins.[120] Peptide co-elution is a common burden with isobaric proteomics approaches that utilise poor chromatographic technique. Furthermore, the high resolution product ion spectra used to determine the amino acid sequence of protein-surrogate peptides exhibit the necessary signal-to-noise and signal-to-background ratios to warrant qualitative assessment of peptide identification with manual *de novo* spectral interpretation.[121] Such was the case for all proteins used to generate the biological pathways, networks and pharmacologic/therapeutic targets that form the basis of the publications presented in this thesis. In line with this criterion, all raw and fully annotated spectral files were deposited in the PRIDE public repository and can easily be cross-referenced and verified as needed.

An additional attribute to the proteomics methods used for this thesis was their ability to capture both hydrophilic and membrane intact or associated lipophilic proteins as required for the enrichment of the biological pathways and potential therapeutic targets identified. To further verify the utility of these proteomics approaches, the accuracy of relative quantitation was demonstrated by the targeted analysis of key proteomics findings with independent quantitative assays (i.e. IHC and qRT-PCR).

To summarize, the published body of work presented in this thesis was made possible by the application of an advanced and highly standardized proteomic pipeline. Briefly, the use of copious tissue homogenization and cell

lysis, the effective protein isolation, the high-capacity offline high-pH RP tryptic peptide peak-dependent pre-fractionation followed by the use of ultra-high performance nano-capillary columns for the online low-pH RP separation of the offline peptide fractions contributed to the analysis efficiency. The nano-capillary columns are highly compatible with nano-spray ionization sources, which further contributed to enhanced sensitivity by comparison to the standard electrospray sources.

Other characteristic features of the proteomics pipeline include the use of the dimethyl sulfoxide (DMSO) additive in the LC-MS mobile phase that enhanced both the chromatographic and nanospray ionization process. Additionally, the theoretical mass of DMSO served as an internal mass calibration standard. Furthermore, the mass spectrometry parameters were iteratively optimized so as to achieve high mass accuracy with sensitivity while using sufficiently high scan speeds to effectively sample the transiently eluting peptides from the capillary column.[122] The effective use of multi-dimensional liquid chromatography aimed to reduce peptide co-isolation and thus enhance the accuracy of relative quantitation using isobaric tags. Another contributing factor to the extensive proteomes achieved was the thorough and frequent instrument tuning and mass calibration that ensure reproducibly high mass accuracy. The robust and reproducible performance of the LC-MS method was routinely verified by the analysis of comprehensive system suitability standards.

The increasing advancements made to liquid chromatography and mass spectrometry technologies will surely increase both analysis throughput and performance thus allowing the generation of yet higher quantitative proteome coverage with extensive peptide sequence coverage at a fraction of the turn-around times currently available. The degree of hyperplexing amenable to isobaric proteomics pipelines in combination to the increased resolution and capacity of the next generation mass spectrometers stands to double or triple the number of samples analysed in each run thus allowing more biological or clinical replicates being analysed under identical experimental conditions. Collectively, this will significantly

reduce the cost of analysis. Also, the advancements made to biostatistical and bioinformatics algorithms, the development of more comprehensive protein databases that will include more splice variants and post-translational features, improvement to machine learning approaches, and more effective integration of proteomes with other -omics based approaches will further contribute to the enhanced biological interpretation of large proteome datasets. A major limitation, however, stems from the lack of consensus between methodologies and their intra-laboratory validation. The use of suitable system suitability standards could aid to reducing this gap.

In conclusion, the innovative quantitative proteomics methodology we developed for the global, untargeted proteomic profiling of cell lines and tissue has wide applications in different subject areas of biomedical research. Depending on the samples analysed and experimental design, this methodological approach can provide novel insight into physiological processes, the pathophysiology of disease, as well as identify novel therapeutic targets of disease and disease markers.

Section 3. Future perspectives

Our methodological future perspectives include:

- The integrated multi-omic (genomic, transcriptomic, miRomic, metabolomic) analysis of tissue and cell lines for the more comprehensive understanding of physiological processes, pathophysiological mechanisms of disease, and systemic changes as a result of an intervention.
- The development of a targeted, antibody-independent absolute protein quantitation methodology for the large-scale validation of the findings from the initial untargeted quantitative proteomic profiling. Such a development will have far reaching effects to the low-cost adoption of targeted LC-MS techniques in a hospital or clinical setting.
- The development of a methodology for the untargeted analysis of phosphoproteins in cell lines and tissue, by combining offline C4 RP chromatography with phosphopeptide enrichment for each offline fraction using titanium dioxide tips, and subsequent LC-MS analysis using online HILIC chromatography.

References

1. Weston AD, Hood L. Systems biology, proteomics, and the future of health care: toward predictive, preventative, and personalized medicine. J Proteome Res 2004; 3: 179-96.

2. Cox J, Mann M. Quantitative, high-resolution proteomics for data-driven systems biology. Annu Rev Biochem 2011;80:273-99.

3. Tchourine K, Poultney CS, Wang L, Silva GM, Manohar S, Mueller CL et al. One third of dynamic protein expression profiles can be predicted by a simple rate equation. Mol Biosyst. 2014;10:2850-62

4. Gholami AM, Hahne H, Wu Z, Auer FJ, Meng C, Wilhelm M et al.Global proteome analysis of the NCI-60 cell line panel. Cell Rep 2013;4:609-20

5. Maier T, Güell M, Serrano L. Correlation of mRNA and protein in complex biological samples. FEBS Lett. 2009;583:3966-73

6. Ahn AC, Tewari M, Poon CS, Phillips RS. The limits of reductionism in medicine: could systems biology offer an alternative? PLoS Med 2006;3:e208.

7. Hasin Y, Seldin M, Lusis A. Multi-omics approaches to disease. Genome Biol 2017;18:83.

8. Bantscheff M, Lemeer S, Savitski MM, Kuster B. Quantitative mass spectrometry in proteomics: critical review update from 2007 to the present. Anal Bioanal Chem. 2012;404:939-65.

9. Scigelova M, Hornshaw M, Giannakopulos A, Makarov A. Fourier transform mass spectrometry. Mol Cell Proteomics. 2011;10:M111.009431.

10. Garbis S, Lubec G, Fountoulakis M. Limitations of current proteomics technologies. J Chromatogr A 2005;1077:1-18.

11. Spivak M, Weston J, Bottou L, Käll L, Noble WS. Improvements to the percolator algorithm for Peptide identification from shotgun proteomics data sets. J Proteome Res. 2009;8:3737-45.

12. Zhang Y, Fonslow BR, Shan B, Baek MC, Yates JR 3rd. Protein analysis by shotgun/bottom-up proteomics. Chem Rev 2013;113:2343-94.

13. Shabihkhani M, Lucey GM, Wei B, Mareninov S, Lou JJ, Vinters HV et al. The procurement, storage, and quality assurance of frozen blood and tissue biospecimens in pathology, biorepository, and biobank settings. Clin Biochem 2014;47:258-66.

14. Speers AE, Wu CC. Proteomics of integral membrane proteins-theory and application. Chem Rev 2007;107:3687-714.

15. Cañas B, Piñeiro C, Calvo E, López-Ferrer D, Gallardo JM. Trends in sample preparation for classical and second generation proteomics. J Chromatogr A 2007;1153:235-58.

16. Rodriguez J, Gupta N, Smith RD, Pevzner PA. Does trypsin cut before proline? J Proteome Res 2008;7:300-5.

17. Brownridge P, Beynon RJ. The importance of the digest: proteolysis and absolute quantification in proteomics. Methods 2011;54:351-60

18. Burkhart JM, Schumbrutzki C, Wortelkamp S, Sickmann A, Zahedi RP. Systematic and quantitative comparison of digest efficiency and specificity reveals the impact of trypsin quality on MS-based proteomics. J Proteomics 2012;75:1454-62

19. Wu Z, Huang J, Huang J, Li Q, Zhang X. Lys-C/Arg-C, a More Specific and Efficient Digestion Approach for Proteomics Studies. Anal Chem 2018;90:9700-7.

20. Glatter T, Ludwig C, Ahrné E, Aebersold R, Heck AJ, Schmidt A. Large-scale quantitative assessment of different in-solution protein digestion protocols reveals superior cleavage efficiency of tandem Lys-C/trypsin proteolysis over trypsin digestion. J Proteome Res 2012;11:5145-56.

21. Switzar L, Giera M, Niessen WM. Protein digestion: an overview of the available techniques and recent developments. J Proteome Res 2013;12:1067-77.

22. Srzentić K, Zhurov KO, Lobas AA, Nikitin G, Fornelli L, Gorshkov MV et al. Chemical-Mediated Digestion: An Alternative Realm for Middle-down Proteomics? J Proteome Res. 2018;17:2005-16.

23. Fornelli L, Parra J, Hartmer R, Stoermer C, Lubeck M, Tsybin YO. Top-down analysis of 30-80 kDa proteins by electron transfer dissociation time-of-flight mass spectrometry. Anal Bioanal Chem. 2013;405:8505-14.

24. Ting L, Rad R, Gygi SP, Haas W. MS3 eliminates ratio distortion in isobaric multiplexed quantitative proteomics. Nat Methods. 2011;8:937-40.

25. Wühr M, Güttler T, Peshkin L, McAlister GC, Sonnett M, Ishihara K et al. The Nuclear Proteome of a Vertebrate. Curr Biol. 2015;25:2663-71.

26. Rauniyar N, Yates JR 3rd. Isobaric labeling-based relative quantification in shotgun proteomics. J Proteome Res 2014;13:5293-309.

27. Wühr M, Haas W, McAlister GC, Peshkin L, Rad R, Kirschner MW et al. Accurate multiplexed proteomics at the MS2 level using the complement reporter ion cluster. Anal Chem 2012;84:9214-21.

28. Megger DA, Pott LL, Ahrens M, Padden J, Bracht T, Kuhlmann K et al. Comparison of label-free and label-based strategies for proteome analysis of hepatoma cell lines. Biochim Biophys Acta 2014;1844:967-76.

29. Sonnett M, Yeung E, Wühr M. Accurate, Sensitive, and Precise Multiplexed Proteomics Using the Complement Reporter Ion Cluster. Anal Chem 2018;90:5032-9.

30. Lambert JP, Ethier M, Smith JC, Figeys D. Proteomics: from gel based to gel free. Anal Chem 2005; 77: 3771-87.

31. Roe MR, Griffin TJ. Gel-free mass spectrometry-based high throughput proteomics: tools for studying biological response of proteins and proteomes. Proteomics 2006;6:4678-87.

32. Dugo P, Herrero M, Kumm T, Giuffrida D, Dugo G, Mondello L. Comprehensive normal-phase x reversed-phase liquid chromatography coupled to photodiode array and mass spectrometry detection for the analysis of free carotenoids and carotenoid esters from mandarin. J Chromatogr A 2008;1189:196-206.

33. Garbis SD, Roumeliotis TI, Tyritzis SI, Zorpas KM, Pavlakis K, Constantinides CA. A novel multidimensional protein identification technology approach combining protein size exclusion prefractionation, peptide zwitterion-ion hydrophilic interaction chromatography, and nano-ultraperformance RP chromatography/nESI-MS2 for the in-depth analysis of

the serum proteome and phosphoproteome: application to clinical sera derived from humans with benign prostate hyperplasia. Anal Chem 2011;83:708-18.

34. Gilar M, Olivova P, Daly AE, Gebler JC. Orthogonality of separation in two-dimensional liquid chromatography. Anal Chem 2005;77:6426-34.

35. Tsougeni K, Zerefos P, Tserepi A, Vlahou A, Garbis SD, Gogolides E. TiO2-ZrO2 affinity chromatography polymeric microchip for phosphopeptide enrichment and separation. Lab Chip 2011;11:3113-20.

36. Lavrik NV, Taylor LT, Sepaniak MJ. Nanotechnology and chip level systems for pressure driven liquid chromatography and emerging analytical separation techniques: a review. Anal Chim Acta 2011;694:6-20.

37. Huft J, Haynes CA, Hansen CL. Microfluidic integration of parallel solid-phase liquid chromatography. Anal Chem 2013;85:2999-3005.

38. Mellors JS, Black WA, Chambers AG, Starkey JA, Lacher NA, Ramsey JM. Hybrid capillary/microfluidic system for comprehensive online liquid chromatography-capillary electrophoresis-electrospray ionization-mass spectrometry. Anal Chem 2013;85:4100-6.

39. Tanaka K, Waki H, Ido Y, Akita S, Yoshida Y, Yoshida T et al. Protein and polymer analyses up to *m/z* 100 000 by laser ionization time-of-flight mass spectrometry. Rapid Comm Mass Spectrom 1988;2:151-60.

40. Bahr U, Deppe A, Karas M, Hillenkamp F, Giessmann U. Mass spectrometry of synthetic polymers by UV-matrix-assisted laser desorption/ionization. Anal Chem 1992;64:2866-9.

41. Whitehouse CM, Dreyer RN, Yamashita M, Fenn JB. Electrospray interface for liquid chromatographs and mass spectrometers. Anal Chem 1985;57:675-9.

42. Fenn JB, Mann M, Meng CK, Wong SF, Whitehouse CM. Electrospray ionization for mass spectrometry of large biomolecules. Science 1989;246:64-71.

43. Nadler WM, Waidelich D, Kerner A, Hanke S, Berg R, Trumpp A et al. MALDI versus ESI: The Impact of the Ion Source on Peptide Identification. J Proteome Res 2017;16:1207-15.

44. Papayannopoulos IA. The interpretation of collision-induced dissociation tandem mass spectra of peptides. Mass Spectrom Rev 1995;14:49-73.

45. Steen H, Mann M. The ABC's (and XYZ's) of peptide sequencing. Nat Rev Mol Cell Biol. 2004;5:699-711.

46. Davis RAH, Plaisance EP, Allison DB. Complementary Hypotheses on Contributors to the Obesity Epidemic. Obesity (Silver Spring) 2018;26:17-21.

47. Stenholm S, Head J, Kivimäki M, Kawachi I, Aalto V, Zins M et al. Smoking, physical inactivity and obesity as predictors of healthy and disease-free life expectancy between ages 50 and 75: a multicohort study. Int J Epidemiol 2016;45:1260-70.

48. Dhana K, Berghout MA, Peeters A, Ikram MA, Tiemeier H, Hofman A et al. Obesity in older adults and life expectancy with and without cardiovascular disease. Int J Obes (Lond) 2016;40:1535-40.

49. Keys A, Fidanza F, Karvonen MJ, Kimura N, Taylor HL. Indices of relative weight and obesity. J Chronic Dis 1972;25:329-43.

50. Global Health Observatory (GHO) data – Obesity. Website: http://www.who.int/gho/ncd/risk_factors/obesity_text/en/; Accessed: 10 June 2018.

51. Finucane MM, Stevens GA, Cowan MJ, Danaei G, Lin JK, Paciorek CJ et al. National, regional, and global trends in body-mass index since 1980: systematic analysis of health examination surveys and epidemiological studies with 960 country-years and 9·1 million participants. Lancet 2011;377:557-67.

52. Finkelstein EA, Khavjou OA, Thompson H, Trogdon JG, Pan L, Sherry B et al. Obesity and severe obesity forecasts through 2030. Am J Prev Med 2012;42:563-70.

53. WHO | World Health Organization. Prevalence of obesity among adults, ages 18+, 1975-2016 (age standardized estimate): Both sexes, 2016. Website:http://gamapserver.who.int/gho/interactive_charts/ncd/risk_factors/obesity/atlas.html; Accessed: 25 June 2018.

54. Scarborough P, Bhatnagar P, Wickramasinghe KK, Allender S, Foster C, Rayner M. The economic burden of ill health due to diet, physical inactivity, smoking, alcohol and obesity in the UK: an update to 2006-07 NHS costs. J Public Health (Oxf) 2011;33:527-35.

55. Berthoud HR, Klein S. Advances in Obesity: Causes, Consequences, and Therapy. Gastroenterology 2017;152:1635-7.

56. Meldrum DR, Morris MA, Gambone JC. Obesity pandemic: causes, consequences, and solutions-but do we have the will? Fertil Steril 2017;107:833-9.

57. Petrakis D, Vassilopoulou L, Mamoulakis C, Psycharakis C, Anifantaki A, Sifakis S et al. Endocrine Disruptors Leading to Obesity and Related Diseases. Int J Environ Res Public Health 2017;14:E1282.

58. Heindel JJ, Newbold R, Schug TT. Endocrine disruptors and obesity. Nat Rev Endocrinol 2015;11:653-61.

59. Herrera BM, Lindgren CM. The genetics of obesity. Curr Diab Rep 2010;10:498-505.

60. Sung KC, Lee MY, Kim YH, Huh JH, Kim JY, Wild SH et al. Obesity and incidence of diabetes: Effect of absence of metabolic syndrome, insulin resistance, inflammation and fatty liver. Atherosclerosis 2018;275:50-7.

61. Kotsis V, Tsioufis K, Antza C, Seravalle G, Coca A, Sierra C et al. Obesity and cardiovascular risk: a call for action from the European Society of Hypertension Working Group of Obesity, Diabetes and the High-risk Patient and European Association for the Study of Obesity: part B: obesity-induced cardiovascular disease, early prevention strategies and future research directions. J Hypertens 2018;36:1441-55.

62. Pedditizi E, Peters R, Beckett N. The risk of overweight/obesity in mid-life and late life for the development of dementia: a systematic review and meta-analysis of longitudinal studies. Age Ageing 2016;45:14-21.

63. Kiliaan AJ, Arnoldussen IA, Gustafson DR. Adipokines: a link between obesity and dementia? Lancet Neurol 2014;13:913-23.

64. Arnold M, Pandeya N, Byrnes G, Renehan PAG, Stevens GA, Ezzati PM et al. Global burden of cancer attributable to high body-mass index in 2012: a population-based study. Lancet Oncol 2015;16:36-46.

65. Arcidiacono B, Iiritano S, Nocera A, Possidente K, Nevolo MT, Ventura V et al. Insulin resistance and cancer risk: an overview of the pathogenetic mechanisms. Exp Diabetes Res 2012;2012:789174.

66. Kim SY, Dietz PM, England L, Morrow B, Callaghan WM. Trends in pre-pregnancy obesity in nine states, 1993-2003. Obesity (Silver Spring) 2007;15:986-93.

67. Lindberg S, Anderson C, Pillai P, Tandias A, Arndt B, Hanrahan L. Prevalence and Predictors of Unhealthy Weight Gain in Pregnancy. WMJ 2016;115:233-7.

68. Siega-Riz AM, Gray GL. Gestational weight gain recommendations in the context of the obesity epidemic. Nutr Rev 2013;71 Suppl 1:S26-30.

69. Moussa HN, Alrais MA, Leon MG, Abbas EL, Sibai BM. Obesity epidemic: impact from preconception to postpartum. Future Sci OA 2016;2:FSO137.

70. Huda SS, Brodie LE, Sattar N. Obesity in pregnancy: prevalence and metabolic consequences. Semin Fetal Neonatal Med 2010;15:70-6.

71. Barker DJ. The fetal origins of diseases of old age. Eur J Clin Nutr 1992;46 Suppl 3:S3-9.

72. Iozzo P, Holmes M, Schmidt MV, Cirulli F, Guzzardi MA, Berry A et al. Developmental ORIgins of Healthy and Unhealthy AgeiNg: the role of maternal obesity--introduction to DORIAN. Obes Facts 2014;7:130-51.

73. Sanchez CE, Barry C, Sabhlok A, Russell K, Majors A, Kollins SH et al. Maternal pre-pregnancy obesity and child neurodevelopmental outcomes: a meta-analysis. Obes Rev 2018;19:464-84.

74. Edlow AG. Maternal obesity and neurodevelopmental and psychiatric disorders in offspring. Prenat Diagn 2017;37:95-110.

75. Lechan RM and Toni R. Functional Anatomy of the Hypothalamus and Pituitary. In: De Groot LJ, Chrousos G, Dungan K, Feingold KR, Grossman A, Hershman JM, Koch C,Korbonits M, McLachlan R, New M, Purnell J, Rebar R, Singer F, Vinik A, editors. Endotext [Internet]. South Dartmouth (MA): MDText.com, Inc.; 2000-2016 Nov 28.

76. Loes DJ, Barloon TJ, Yuh WT, DeLaPaz RL, Sato Y. MR anatomy and pathology of the hypothalamus. AJR Am J Roentgenol 1991;156:579-85.

77. Brobeck JR. Mechanism of the development of obesity in animals with hypothalamic lewsions. Physiol Rev 1946;26:541-59.

78. Strominger JL, Brobeck JR. A mechanism of regulation of food intake. Yale J Biol Med 1953;25:383-90.

79. Elmquist JK, Elias CF, Saper CB. From lesions to leptin: hypothalamic control of food intake and body weight. Neuron 1999;22:221-32.

80. Myers MG, Jr., Olson DP. Central nervous system control of metabolism. Nature 2012;491:357-63.

81. Brobeck JR. Mechanism of the development of obesity in animals with hypothalamic lewsions. Physiol Rev 1946;26:541-59.

82. Hetherington AW, Ranson SW. The relation of various hypothalamic lesions to adiposity in the rat. J Comp Neurol 1942;76:475-99.

83. Hetherington AW. Non-production of hypothalamic obesity in the rat by lesions rostral or dorsal to the ventromedial hypothalamic nuclei. J Comp Neurol 1944;80:33-45.

84. Anand BK, Brobeck JR. Hypothalamic control of food intake in rats and cats. Yale J Biol Med 1951;24:123-40.

85. Hetherington AW. The relation of various hypothalamic lesions to adiposity and other phenomena in the rat. Am J Physiol 1941;133:326.

86. Zhang Y, Proenca R, Maffei M, Barone M, Leopold L, Friedman JM. Positional cloning of the mouse obese gene and its human homologue. Nature 1994;372:425-32.

87. Mercer JG, Hoggard N, Williams LM, Lawrence CB, Hannah LT, Trayhurn P. Localization of leptin receptor mRNA and the long form splice variant (Ob-Rb) in mouse hypothalamus and adjacent brain regions by in situ hybridization. FEBS Lett 1996;387:113-6.

88. Schwartz MW, Seeley RJ, Campfield LA, Burn P, Baskin DG. Identification of targets of leptin action in rat hypothalamus. J Clin Invest 1996;98:1101-6.

89. Elias CF, Aschkenasi C, Lee C, Kelly J, Ahima RS, Bjorbaek C et al. Leptin differentially regulates NPY and POMC neurons projecting to the lateral hypothalamic area. Neuron 1999;23:775-86.

90. Kumar A, Tsao JW. Alzheimer Disease StatPearls [Internet]. Treasure Island (FL): StatPearls Publishing; 2018.

91. World Alzheimer Report 2015: The Global Impact of Dementia. Website: https://www.alz.co.uk/research/world-report-2015; Accessed: 29 May 2018

92. Alzheimer's Society. Dementia UK report. Website: https://www.alzheimers.org.uk/about-us/policy-and-influencing/dementia-uk-report; Accessed 24 June 2018.

93. Knopman DS. β-Amyloidosis and neurodegeneration in Alzheimer disease: who's on fist? Neurology 2014;82:1756-7.

94. Douaud G, Menke RA, Gass A, Monsch AU, Rao A, Whitcher B et al. Brain microstructure reveals early abnormalities more than two years prior to clinical progression from mild cognitive impairment to Alzheimer's disease. J Neurosci 2013;33:2147-55.

95. Singh V, Chertkow H, Lerch JP, Evans AC, Dorr AE, Kabani NJ. Spatial patterns of cortical thinning in mild cognitive impairment and Alzheimer's disease. Brain 2006;129:2885-93.

96. Thompson PM, Hayashi KM, de Zubicaray G, Janke AL, Rose SE, Semple J et al. Dynamics of gray matter loss in Alzheimer's disease. J Neurosci. 2003;23:994-1005.

97. Neves-Zaph SR. Phosphodiesterase Diversity and Signal Processing Within cAMP Signaling Networks. Adv Neurobiol. 2017;17:3-14.

98. Motte E, Le Stunff C, Briet C, Dumaz N, Silve C. Modulation of signaling through GPCR-cAMP-PKA pathways by PDE4 depends on stimulus intensity: Possible implications for the pathogenesis of acrodysostosis without hormone resistance. Mol Cell Endocrinol. 2017;442:1-11.

99. Esiri MM, Lee VMY, Trojanowski JQ (eds) (2004) The Neuropathology of Dementia, 2nd edn. Cambridge University Press: Cambridge.

100. Walsh DM, Minogue AM, Sala Frigerio C, Fadeeva JV, Wasco W, Selcoe DJ. The APP family of proteins: similarities and differences. Biochem Soc Trans 2007;35:416-20

101. Revesz T, Ghiso J, LashleyT, Plant G, Rostagno A, Frangione B, Holton JL. Cerebral amyloid angiopathies: a Pathologic, Biochemical, and Genetic View. J Neuropathol Exp Neurol 2003;62:885-98

102. Braak H, Alafuzoff I, Arzberger T, Kretzschmar H, Del Tredici K. Staging of Alzheimer disease-associated neurofibrillary pathology using paraffin sections and immunohistochemistry. Acta Neuropathol (Berl) 2006;112:389-404

103. Mira SS, Heyman A, McKeel D, Sumi SM, Crain BJ, Brownlee LM et al. The Consortium to Establish a Registry for Alzheimer's Disease (CERAD). Part II. Standardisation for the neuropathologic assessment of Alzheimer's disease. Neurology 1991;41:479-86

104. Weller RO, Subash M, Preston SD, Mazanti I, Carare RO. Perivascular drainage of amyloid-beta peptides from the brain and its failure in cerebral amyloid angiopathy and Alzheimer's disease. Brain Pathol. 2008;18:253-66.

105. Ferlay, J., Soerjomataram, I. & Ervik, M. *et al*. GLOBOCAN 2012v1.0, Cancer Incidence and Mortality Worldwide. IARC Cancer Base No. 11. Lyon, France: International Agency for Research on Cancer (2013).

106. Oesophageal cancer, in: Stewart B, Wild C (Eds.), World cancer report 2014. Lyon, France: International Agency for Research on Cancer, 2014.

107. Lagergren J, Smyth E, Cunningham D, Lagergren P. Oesophageal cancer. Lancet 2017;390:2383-96.

108. Trivers KF, Sabatino SA, Stewart SL. Trends in esophageal cancer incidence by histology, United States, 1998-2003. Int J Cancer 2008;123:1422-8.

109. Coleman HG, Xie SH, Lagergren J. The Epidemiology of Esophageal Adenocarcinoma. Gastroenterology 2018;154:390-405.

110. Xie SH, Rabbani S, Petrick JL, Cook MB, Lagergren J. Racial and Ethnic Disparities in the Incidence of Esophageal Cancer in the United States, 1992-2013. Am J Epidemiol 2017;186:1341-51.

111. Abnet CC, Arnold M, Wei WQ. Epidemiology of Esophageal Squamous Cell Carcinoma. Gastroenterology 2018;154:360-73.

112. Whiteside TL. The tumor microenvironment and its role in promoting tumor growth. Oncogene 2008;27:5904-12.

113. Paget S. The distribution of secondary growths in cancer of the breast. 1889. Cancer Metastasis Rev 1989;8:98-101.

114. Underwood TJ, Hayden AL, Derouet M, Garcia E, Noble F, White MJ et al. Cancer-associated fibroblasts predict poor outcome and promote periostin-dependent invasion in oesophageal adenocarcinoma. J Pathol 2015;235:466-77.

115. Manousopoulou A, Woo J, Woelk CH, Johnston HE, Singhania A, Hawkes C et al. Are you also what your mother eats? Distinct proteomic portrait as a result of maternal high-fat diet in the cerebral cortex of the adult mouse. Int J Obes (Lond) 2015;39:1325-8.

116. Manousopoulou A, Koutmani Y, Karaliota S, Woelk CH, Manolakos ES, Karalis K et al. Hypothalamus proteomics from mouse models with obesity and anorexia reveals therapeutic targets of appetite regulation. Nutr Diabetes 2016;6:e204.

117. Manousopoulou A, Saito S, Yamamoto Y, Al-Daghri NM, Ihara M, Carare RO et al. Hemisphere Asymmetry of Response to Pharmacologic Treatment in an Alzheimer's Disease Mouse Model. J Alzheimers Dis 2016;51:333-8.

118. Manousopoulou A, Gatherer M, Smith C, Nicoll JAR, Woelk CH, Johnson M et al. Systems proteomic analysis reveals that clusterin and tissue inhibitor of metalloproteinases 3 increase in leptomeningeal arteries affected by cerebral amyloid angiopathy. Neuropathol Appl Neurobiol 2017;43:492-504.

119. Manousopoulou A, Hayden A, Mellone M, Garay-Baquero DJ, White CH, Noble F et al. Quantitative proteomic profiling of primary cancer-associated fibroblasts in oesophageal adenocarcinoma. Br J Cancer 2018;118:1200-7.

120. Wenger CD, Lee MV, Hebert AS, McAlister GC, Phanstiel DH, Westphall MS et al. Gas-phase purification enables accurate, multiplexed proteome quantification with isobaric tagging. Nat Methods 2011;8:933-5.

121. Papayannopoulos IA. The interprestation of collision-induced dissociation tandem mass spectra of peptides. Mass Spectrom Rev 1995;14:49-73.

122. Kalli A, Smith GT, Sweredoski MJ, Hess S. Evaluation and optimization of mass spectrometric settings during data-dependent acquisition mode: focus on LTQ-Orbitrap mass analyzers. J Proteome Res. 2013;12:3071-86.

Appendix A

Statement of first author's contribution in the publications included in the current PhD thesis:

"Antigoni Manousopoulou designed the proteomics experiments, developed the proteomics methodology, performed the proteomics experiments, analysed the proteomics data, interpreted the proteomics data, performed the bioinformatics analysis of the proteomics data and wrote the manuscript."

Co-author approval

Publication	Co-author name	Comment
Manousopoulou A et al. Int J Obes 2015	Woo J	"Yes! It was lovely working with you"
	Woelk CH	"I consent!"
	Johnston HE	"I consent"
	Singhania A	""I consent with this statement"
	Hawkes C	"Yes, that's fine."
	Garbis SD	"I consent"
	Carare RO	"Absolutely!"
Manousopoulou A et al. Nutr Diabetes 2016	Koutmani Y	"Congratulations! You have my consent on this statement and I hope you will continue your career in the academia! Thank you for everything, especially for your crucial, precious contribution on this paper."
	Karaliota S	"I consent"
	Woelk CH	"I consent!"
	Manolakos ES	"Congratulations on the completion of your degree. I consent with the statement."

	Karalis K	"This is fine Antigoni. Congratulations"
	Garbis SD	"I consent"
Manousopoulou A et al. J Alzheimers Dis 2016	Saito S	"I consent"
	Yamamoto Y	"I consent with the statement. Good luck with your thesis"
	Al-Daghri NM	"I consent to this statement and I wish you the best of luck in your PhD"
	Ihara M	"I consent to the statement"
	Carare RO	"Absolutely!"
	Garbis SD	"I consent"
Manousopoulou A et al. Neuropathol Appl Neurobiol 2017	Gatherer M	"Your statement is absolutely acceptable to me. Thank you for all your hard work and expertise"
	Smith C	"I'm happy with what you suggest."
	Nicoll JAR	"Fine with me. I hope all goes well."
	Woelk CH	"I consent!"
	Johnson M	"Hope all well with you, completely give my consent."
	Kalaria R	"This is perfectly acceptable by me. It was an important study."
	Attems J	"Fine by me!"
	Garbis SD	"I consent"
	Carare RO	"Absolutely!"
Manousopoulou A et al. Br J Cancer 2018	Hayden A	"I consent"
	Mellone M	"You have got my consent. You did all that you said."
	Garay-Baquero DJ	"I agree with the statement of authorship that you have described for your contribution"
	White CH	"Glad things are going well with your PhD., and the statement is fine."

	Noble F	“I consent with this statement”
	Lopez M	“I consent. Thank you for all your hard work”
	Thomas GJ	“I consent to this statement”
	Underwood TJ	“I consent”
	Garbis SD	“I consent”

Appendix B

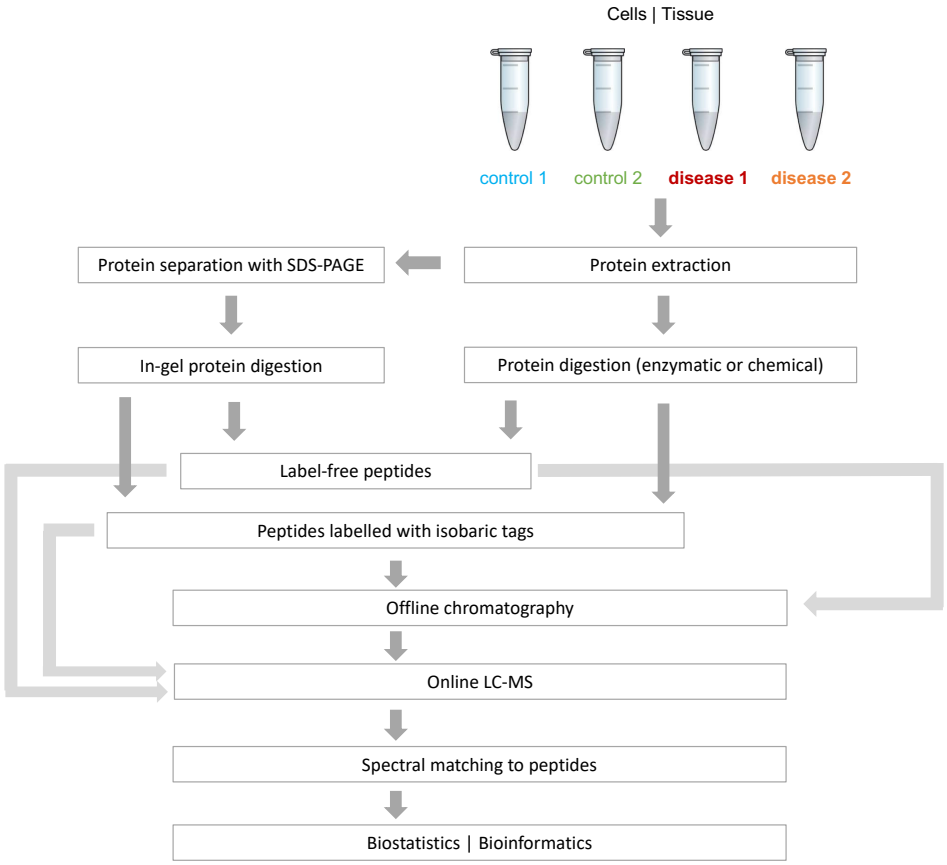
Cells | Tissue
control 1
control 2
disease 1
disease 2
Protein extraction
Protein separation with SDS-PAGE
Protein digestion (enzymatic or chemical)
In-gel protein digestion
Label-free peptides
Peptides labelled with isobaric tags
Offline chromatography
Online LC-MS
Spectral matching to peptides
Biostatistics | Bioinformatics

Appendix C

Annotated MS/MS spectrum

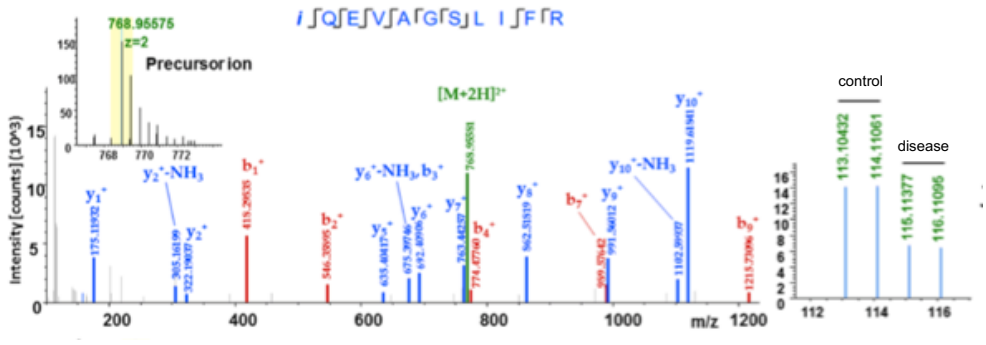

Appendix D

Overview of bioinformatics software tools

Name	Gene ontology analysis	Pathway | Processes analysis	Directionality of effect on process	Manually curated	Protein interaction networks
DAVID	✓	✓	×	×	×
BiNGO	✓	×	×	×	×
MetaCore	✓	✓	×	✓	✓
IPA	×	✓	✓	✓	✓
STRING	×	×	×	×	✓

Appendix E

Nuclei of the human hypothalamus

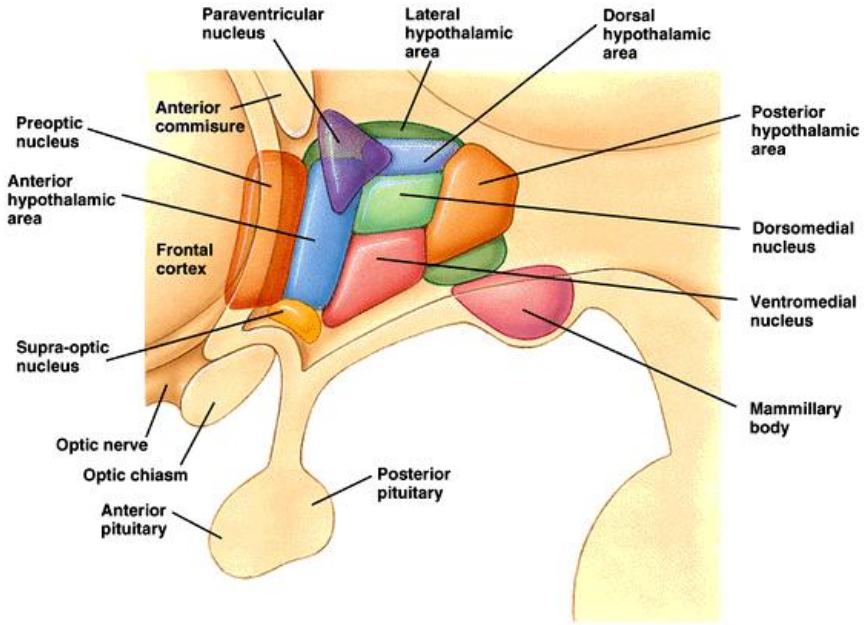

Appendix F

Hypothalamus dissection from mouse brain

1. Remove the brain from the skull and place ventral side up (Fig. 1).
2. Use curved forceps and push down the curved part of the forceps around the hypothalamus, lift and and pinch out the hypothalamus while pushing down with the forceps (Fig. 2).
3. Place tissue into a 1.5 mL falcon tube and snap freeze in liquid nitrogen or dry ice. Store in a -80^{o}C freezer.
4. There should be a visible depression on the brain at the position of the hypothalamus prior to its removal (Fig.3).

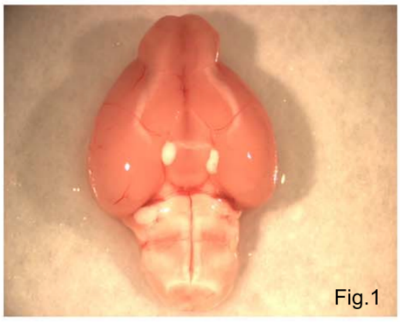
Fig.1

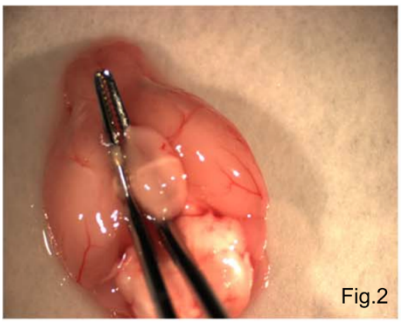
Fig.2

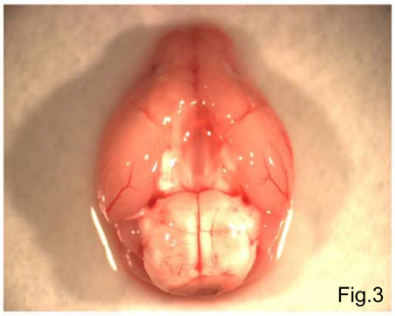
Fig.3

Appendix G

Overview of our proteomics methodology presented in the present thesis